



Fatigue strength Comparative study of knuckle joints in LNG carrier by different approaches of classification society's rules

Sacheendra Naik

Master Thesis

presented in partial fulfillment
of the requirements for the double degree:
"Advanced Master in Naval Architecture" conferred by University of Liege
"Master of Sciences in Applied Mechanics, specialization in Hydrodynamics,
Energetics and Propulsion" conferred by Ecole Centrale de Nantes

developed at West Pomeranian University of Technology, Szczecin
in the framework of the

"EMSHIP"
Erasmus Mundus Master Course
in "Integrated Advanced Ship Design"

Ref. 159652-1-2009-1-BE-ERA MUNDUS-EMMC

Supervisor: Prof. Maciej Taczala, West Pomeranian University of
Technology, Szczecin

Reviewer: Prof. Dario Boote, University of Genova

Szczecin, February 2017



CONTENTS

DECLARATION OF AUTHORSHIP	6
ABBREVIATIONS.....	7
ABSTRACT	8
1. INTRODUCTION.....	9
1.1. Overview	9
1.2. Objective	11
1.3. Methodology	12
1.4. Thesis Organisation.....	15
2. GAS CARRIERS: BRIEF DESCRIPTION.....	16
2.1. Types of gas carrier ships.....	16
2.1.1. Cargo tank types.....	17
2.1.2. Independent tank	17
2.1.3. Membrane tank.....	19
3. THEORETICAL BACKGROUND	20
3.1. General	20
3.2. Fatigue damage models	20
3.3. Different methods of fatigue load calculations	22
3.3.1. Simplified method.....	22
3.3.2. Equivalent design wave method	23
3.3.3. Spectral Method	23
3.3.4. Short-term response	25
3.3.5. Long-term response.....	26
3.4. Fatigue strength calculation based on S-N curve	27
3.5. Uncertainties in fatigue strength prediction	31
4. ANALYSIS METHODOLOGY AND SOFTWARE TOOLS USED	32
4.1. Analysis Methodology	32
4.2. Software Tools Used	33
4.2.1. Sesam Genie	33
4.2.2. Sestra.....	33
4.2.3. HydroD-Wasim.....	34
4.2.4. Xtract.....	34
4.2.5. Postresp.....	35
4.2.6. Cutres	35

4.2.7. <i>Submod</i>	35
4.2.8. <i>Stofat</i>	35
5. STRUCTURAL MODELLING.....	36
5.1. Co-ordinate and unit system.....	37
5.2. Geometrical Modelling	38
5.2.1. <i>Double Bottom</i>	38
5.2.2. <i>Double Side shell</i>	40
5.2.3. <i>Transverse Bulkhead</i>	40
5.2.4. <i>Foundation Deck and Cargo tank support</i>	41
5.2.5. <i>Upper Deck</i>	43
5.3. Boundary conditions	43
5.4. Structural Mesh Model.....	45
5.4.1. <i>Global Model</i>	45
5.4.2. <i>Sub Model</i>	46
6. GLOBAL RESPONSE ANALYSIS	48
6.1. Analysis Setup.....	48
6.1.1. <i>Load cases</i>	49
6.2. Global Motion Responses	51
7. GLOBAL STRUCTURAL ANALYSIS.....	54
7.1. Verification of load transfer	54
7.2. Stress Transfer function	56
8. FATIGUE ANALYSIS	58
9. CONCLUSIONS AND RECOMMENDATIONS.....	66
ACKNOWLEDGEMENTS	69
REFERENCES.....	70
APPENDICES.....	72
Appendix A: Summary of Element Fatigue damage Calculation	72
Appendix B: Summary of Hot Spot Fatigue damage Calculation	73
Appendix C : Fatigue Calculation Result.....	74

LIST OF FIGURES

Figure 1. LNG carrier structural model analysed.....	11
Figure 2. Flow chart spectral method approach.	13
Figure 3. Self-supporting prismatic Type 'A' tank [23].....	17
Figure 4. Self-supporting prismatic Type 'B' tank [23].....	18
Figure 5. Self-supporting prismatic Type 'C' tank [23].....	18
Figure 6. Membrane tank [23].....	19
Figure 7. Stress definition.	21
Figure 8. S-N curve in air –DNV GL[11].	29
Figure 9. Stress read out points and hot spot stress for 8-node shell elements [11].	30
Figure 10. Notch model [12].	31
Figure 11. LNG carrier FE model.	36
Figure 12. Co-ordinate system.	37
Figure 13. Midship section of LNG carrier.....	39
Figure 14. Double bottom view.....	39
Figure 15. Double sided hull- 3-dimensional view.	40
Figure 16. Seawater ballast tank and bulkhead.	41
Figure 17. Transverse bulkhead and foundation support side girder.	41
Figure 18. Foundation deck – sectional view just above the foundation.	42
Figure 19. Sectional view showing skirt orientation.....	42
Figure 20. Isometric views showing stiffened deck.....	43
Figure 21. Boundary condition [7].....	44
Figure 22. Midship FE mesh -Longitudinal section at the centre line.	45
Figure 23. Fore and Aft Ship FE mesh.....	45
Figure 24. Locations of knuckle joints.....	46
Figure 25. Sub model from the global FE model.....	47
Figure 26. Hydrodynamic model.	48
Figure 27. Wave heading direction for different load cases	49
Figure 28. Tank arrangement for full load case- Longitudinal view	49
Figure 29. Tank arrangement for full load case- Plan view	50
Figure 30. Tank arrangement for full ballast load case- Longitudinal view	50
Figure 31. Tank arrangement for ballast load case- Plan view	50
Figure 32. Wave heading direction for different load cases	51
Figure 33. Global motions response –Full load case	52

Figure 34. Global motions response – Ballast load case..... 53

Figure 35. Wave load pressure on global model transferred from the hydrodynamic analysis.
..... 54

Figure 36. Vertical Bending Moment – 1m wave amplitude for a 90⁰ heading wave with period 24s. 55

Figure 37. Vertical Shear Force – 1m wave amplitude for a 90⁰ heading wave with period 24s. 55

Figure 38. Maximum Principal stress-Ballast Load case 56

Figure 39. Principal Stress Transfer Function.-Ballast Load case 57

Figure 40. Wave spreading function for cosine power 2. 59

Figure 41. DNV-CN-30.7 2010 S-N curves [15]. 60

Figure 42. ABS S-N curves [8]. 60

Figure 43. Fatigue damage at different position of knuckle joints around tank2..... 63

Figure 44. Hotspot of Hopper knuckle joint. 64

Figure 45. Polar Plot of Total Fatigue Damage. 64

LIST OF TABLES

Table 1. Main characteristics of LNG carrier 36

Table 2. Material Properties 38

Table 3. Wave periods..... 49

Table 4. Mass Model – Full load case..... 50

Table 5. Mass Model – Ballast load case. 50

Table 6. S-N Curve Parameters. 58

Table 7. Wave Scatter Data - North Atlantic. 59

Table 8. Structural detail classification 61

Table 9. Total Fatigue Damage at knuckle joints for various S-N Curve. 62

Table 10. Fatigue Damage for various S-N Curve. 64

Table 11. Fatigue Damage at knuckle joints for various S-N Curve –Ballast Load case. 72

Table 12. Fatigue Damage at knuckle joints for various S-N Curve –Ballast Load case. 72

Table 13. Fatigue Damage for various S-N Curve –Ballast Load case..... 73

Table 14. Fatigue Damage for various S-N Curve –Full Load case. 73

DECLARATION OF AUTHORSHIP

I declare that this thesis and the work presented in it are my own and have been generated by me as the result of my own original research.

Where I have consulted the published work of others, this is always clearly attributed.

Where I have quoted from the work of others, the source is always given. With the exception of such quotations, this thesis is entirely my own work.

I have acknowledged all main sources of help.

Where the thesis is based on work done by myself jointly with others, I have made clear exactly what was done by others and what I have contributed myself.

This thesis contains no material that has been submitted previously, in whole or in part, for the award of any other academic degree or diploma.

I cede copyright of the thesis in favour of the University of West Pomeranian University of Technology, Poland.

Date:

Signature

ABBREVIATIONS

ABS	American Bureau of Shipping
HSE	Health Safety and Environment
AWS	American Welding standard
DNV	Det Norske Veritas
FE	Finite Element
LNG	Liquid Natural Gas
RAO	Response Amplitude Operator
SCF	Stress Concentration Factor
IGC	International Code of the Construction and Equipment of Ships Carrying Liquefied Gases in Bulk
IIW	International Institute of Welding

ABSTRACT

The cumulative damage due to fluctuating loads leads to fatigue fracture which is the main cause of the fracture of offshore vessels and structures. Knuckle joints are the most critical area due to its susceptibility to fatigue failure. This is mainly due to a high-stress concentration at knuckle joints. Also, the area is inaccessible for inspection and repair due to cargo tank containment arrangement. In this report, the spectral fatigue analysis is presented for 148k, Moss type spherical tank LNG carrier. The study is focused on the fatigue damage evaluation of hopper knuckle joint details by full spectral fatigue analysis.

The full spectral fatigue analysis involves the computations of hydrodynamic response, global structural analysis, local structural analysis and calculation of fatigue damage. The structural response is assessed by performing linear FE-analysis with a linear material response. In order to simulate structural response, a linear hydrodynamic analysis using unit wave amplitude is carried out to simulate the wave-induced loads on the LNG carrier, which is followed by a linear FE global analysis to assess stress transfer function. The wave loading is calculated by linear hydrodynamic analysis is based on 3D diffraction theory. The wave amplitude of 1.0m considering wave headings from 0 to 360 degrees with an increment of maximum 30 degrees is used to calculate the ship response. For each wave heading 25 wave frequencies are included to describe the shape of the transfer functions. The inertia loads, internal and external pressures are calculated in the hydrodynamic analysis and transferred directly to the global structural model. Direct wave load computations by the numerical method improve the accuracy of the calculated loads compared to the approach of using the classification society's formulae. Two type of loading cases i.e. full load and normal ballast condition are considered for the damage calculation. For each heading of sea state, fatigue damage is calculated by combing the hotspot transfer functions with stress cycle (S-N) curve data and wave scatter diagram.

Fatigue damage computations involve design variables such as S-N curve data, wave scatter data, wave spectrum, etc. Current rules of classification societies DNV GL and ABS are used to evaluate the fatigue damage of knuckle joint. In general, the spectral fatigue calculation is cumbersome due to time-consuming calculation process. However, the study also provides information about the procedures involved in the spectral fatigue calculation.

KEYWORDS: Spectral Fatigue, Fatigue damage, design variable

1. INTRODUCTION

1.1. Overview

In recent years the demand for environment-friendly clean energy is increasing due to growing environmental protection consciousness at the global level. Liquefied natural gas, LNG is considered as one of the clean energy source and its demand in the global market has opened up a new chapter in gas field development. Ship owners and gas suppliers are actively involved in negotiating on the construction and purchases of LNG carriers capable of sailing all around the world. The changes in the global LNG market lead to the relocation of typical shipping routes to new sea areas. Some of the new routes cross areas known for very rough conditions. As compared to a ship operating worldwide, shipping in North Sea, North Atlantic or at the Alaskan coast is much more challenging in regard to both strength and operational issues. Global Rise in the demand for natural gas has led to the increase in the size and capacity of LNG carriers used for marine transportation.

When the vessel operates in waves, the wave loads can force the ship to bend upwards and downwards. The hogging occurs when the wave crest is at amidships, while the sagging is caused due to wave trough at amidships. The alternative hogging and sagging due to wave loads lead to fatigue problems in a ship. When repeated cyclic load exceeds the material endurance limit, cracks initiate in welded joints or on metal surface weakening the structure. The crack growth continues with continued cyclic loading during the operation of the vessels, eventually, a crack will reach a critical size resulting failure of the structure. Fatigue crack initiation is a localized phenomenon which mainly depends on the structural geometrical details and stress concentrations. In welded structures, cracks initiate at stress concentrations which are due to faulty welding procedures, cut-outs and plate joints where abrupt geometrical transitions cause a rise in local stress intensity.

The fatigue damage is a continuous process during its operation lifetime. The damage depends on parameters such as sea state, loading condition, forward speed, heading angle etc. The major cause of damage is sea state which is a variable parameter characterized by the wave period and significant wave height. For strength reason, high strength steel is used in the construction of vessels using welding technology. Even though the high strength steel ensures the structures to withstand higher stress but it increases the stress amplitude of the response

resulting in lower fatigue life, so that fatigue failure likely to occur at a relatively faster rate in vessels built up of high strength steel compared to low strength steel. The safety of LNG carriers is equally as important as the economic aspect and vessel operator also concern the fatigue failure impact on vessel maintenance, repair cost and reputation. Fatigue strength assessment is considered as one of the important safety issues during design and service period.

Long-term variation of local stresses due to wave actions if handled properly at the design stage, then the failure phenomenon, probability of failure and reliability of structure can be addressed effectively. The fatigue strength evaluations of ship structural details during design stage or in the repair stage by classification societies rule require detailed consideration with an aim to ensure adequate structural strength in fatigue. Various classification societies such as ABS, DNV GL, Lloyd Register, Bureau veritas, Korean register of shipping etc. have published comprehensive rules and guidelines for the ship structure fatigue strength assessment. Depending on the type structural details, the fatigue assessment method varies from simple method to numerically intensive technique such as direct analysis. Over the past years, several studies have addressed the fatigue assessment of ship structural details either by rules or by direct calculations. Researchers have published literature on comparative fatigue strength study of structural details of either container ship or bulk carriers using different classification societies rule. Studies have shown that the fatigue damage depends on stress cycle curve, selection of stress approach, Weibull shape parameter. Even though IACAS-International Association of Classification Societies attempted to develop a common procedure for fatigue assessment, factors such as stress cycle curves and selection of stress approach are not harmonized and they are still dependent on classification societies rule.

The proposed thesis will be focused on fatigue strength sensitivity of hopper knuckle joints in a Moss type LNG carrier using spectral fatigue analysis. The effect of some of the parameters such as stress cycle curves studied and compared by using ABS and DNVGL classification rule approaches.

1.2. Objective

The main objective to make a comparative study on the fatigue strength hopper knuckle joints using classification societies DNV GL and ABS rules for the gas carrier. Design variables such as S-N curve data, wave scatter data, wave spectrum, etc. are the parameters involved in fatigue damage computations and these parameters are considered in this study. In order to accomplish the main objective, the following sub-targets to be completed.

- Prepare a 3D-model of the vessel for global FE analysis
- Perform the hydrodynamic analysis in the frequency domain with 1m wave amplitude considering different wave directions (heading angles). Transfer the calculated wave loads are to global FE model of the vessel.
- Identify fatigue-critical locations with respect to principal stress for each wave direction.
- Perform linear FE analysis of sub model at the critical location.
- Evaluate the fatigue damage

The LNG carrier studied in this report is represented by Figure 1. The vessel has an overall length of 289.5m, moulded depth of 27m and moulded breadth of 49m.

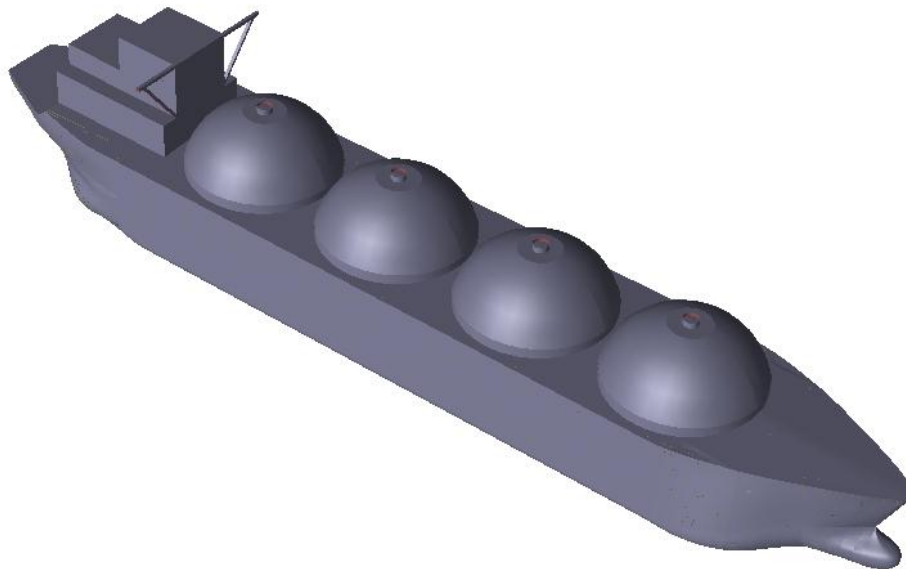


Figure 1. LNG carrier structural model analysed.

1.3. Methodology

To achieve the objective of fatigue evaluation by direct calculation, it is necessary to simulate numerically and analyze the structural response first and followed by the fatigue damage evaluation of hopper knuckle joints of LNG carrier. The fatigue damage is evaluated for both full load and ballast loading condition. The damages from full and ballast condition added together to obtain the final damage. The following three types of numerical analyses have been carried out:

Hydrodynamic response calculations.

Linear global structural analysis.

Local structural analysis.

Fatigue damage calculation.

Fatigue strength of welded ship can be evaluated stress based approach, strain based approach and fracture mechanics.

In stress based approach, the cyclic stresses including stress concentration factor (SCF) is assumed to be less than the yield stress of the material. The strain-based approach considers the localized plastic deformation that occurs in the local regions where the stresses are beyond material yield strength. The plastic deformation location is the probable location of fatigue crack initiation. In Fracture mechanics approach, the fatigue strength of welded joints is expressed in terms of the relationship between the stress intensity factor and the rate of crack growth.

In this study, stress based approach is employed for the fatigue evaluation. Welds are ignored in the FE-models, initial imperfection and the residual tensile stresses from the welding procedure are disregarded.

Figure 2 represents the flowchart of the methodology adopted in this thesis. Each of these parts will be described briefly in the subsequent chapters. Two levels of FE-models are used in the analysis for the fatigue evaluation; a full- vessel FE model with a relatively coarse mesh which represents the global model of the LNG carrier and a more detailed local sub-model with fine mesh.

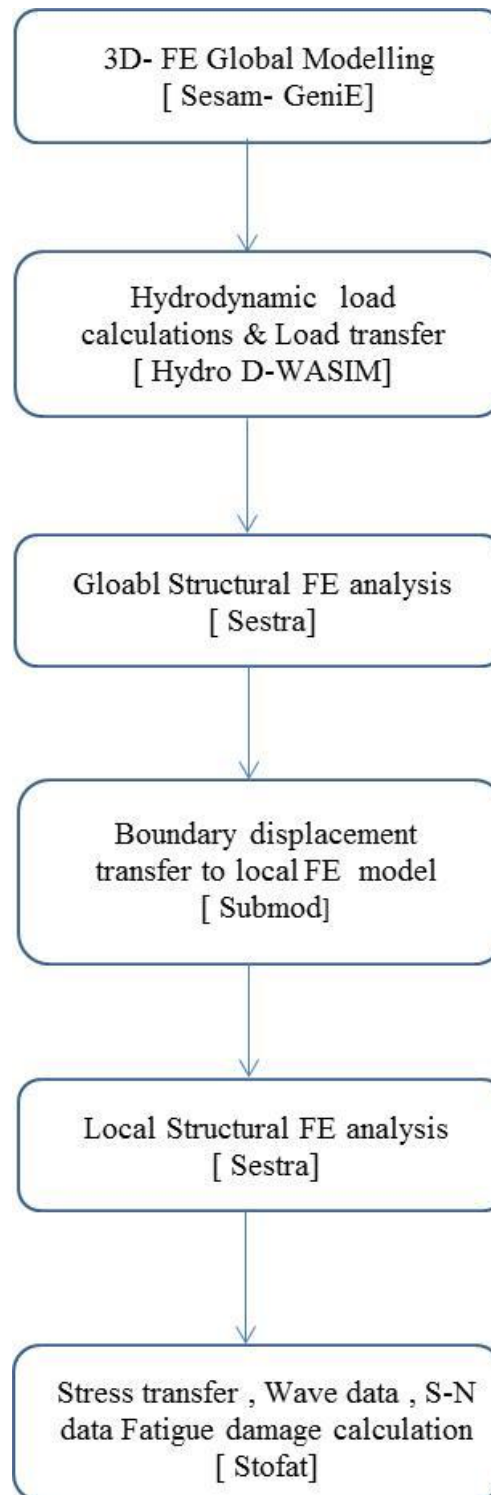


Figure 2. Flow chart spectral method approach.

Fatigue stress evaluations are carried out based on 3D finite element (FE) model using linear static analysis approach. A combination of beam and shell finite element model is used for the global structural analysis of LNG carrier to perform the required global response analysis of the structure. The software package SESAM developed by DNV, the Norwegian classification society has been used for the analysis in this thesis work. The SESAM software

package consists of several different modules which can be used depending on the type numerical simulation that is required to be carried out.

To perform the hydrodynamic response analysis, SESAM HydroD: Wasim has been used which is also a part SESAM software package. Wasim is a general purpose hydrodynamic analysis program based on 3D potential theory for calculation of wave loading and wave induced responses floating marine structures with forward speed.

The hydrodynamic simulations are performed using 1m wave amplitude, in the frequency domain with 25 frequencies and 12 wave directions (heading angles). The motion response of the LNG carrier extracted using a post-processing programme named Postresp.

For the structural concept modelling, a software programme SESAM GeniE has been used. The global structural analysis is carried out using software Sestra which is linear structural FE-analysis programme.

For the sub model analysis of a part of LNG carrier, Submod software is used to transfer the boundary displacements on local FE model from the result of the global structural analysis. The next step is to calculate of stress transfer function at the critical location. Fatigue damage is evaluated at the desired location using the stress transfer function, wave scatter data, wave energy spectrum, and S-N curve and calculation is performed in Stofat programme.

Using Xtract software, results are graphically presented. Chapter four describe shortly the software used in this thesis work.

1.4. Thesis Organisation

This master thesis report consists of nine sections and a reference section. After the introduction chapter, Chapter 2 presents a brief overview of the gas carrier.

In chapter 3 describe the theoretical background on fatigue calculation. It contains a brief overview, different fatigue analysis options are discussed from the simplified method to spectral method. The S-N curves and different parameters involved in the computation of cumulative damage are also presented.

Analysis methodology and the different software computation tools used in this thesis work are discussed in chapter 4.

Chapter 5 presents the global structural modelling of the LNG carrier studied in detail. FE modelling in 3 dimensions is discussed in detail with respect to material properties, meshing and boundary conditions.

Chapter 6 discusses the hydrodynamic analysis set up, mass model properties and load cases. Global motion response resulting from unit wave amplitude are presented in terms of RAOs

Chapter 7 has been used to present the calculation and results from the global response analysis in terms of the principal stress.

Fatigue analysis results are discussed in the eighth chapter with SN-curve and scatter data of the desired location. Furthermore, a variation of the fatigue damage for different S-N curves presented.

Chapter 9 discusses conclusion drawn from the current study performed and also presents recommendations for the future work.

Following chapter 9, all the references that are cited in this thesis work has been listed in the Reference. An additional chapter on appendix is compiled at the end summing up the output from fatigue analysis.

2. GAS CARRIERS: BRIEF DESCRIPTION

Liquefied natural gas, LNG is considered as one of the clean energy source and its demand in the global market has opened up a new chapter in gas field development. Due to growing environmental protection consciousness, the use of natural gas is increasing at the global level.

The seaborne transport of liquefied natural gas dating back to 1949 when a liquefied gas carrier was delivered with DNV class equipped with fully pressurised cargo tanks for transport of LPG/Ammonia [1]. To meet the growing demand for LNG around the globe, the construction of gas carrier transport vessel is increasing in recent years. The capacity of modern larger LNG carriers varies between 125,000 m³ and 267,000m³.

2.1. Types of gas carrier ships

The gas carrier is a special type of ship with a containment system holding the liquid cargo under pressure to prevent entrance of air into the cargo. The design, construction of gas carrier varies according to types cargoes carried and cargo containment system. In general, the gas carriers are grouped as below

- i.) **Fully pressurised:** These are first generation gas carrier types with small capacities up to 5000 to 6000 m³. They are fitted with horizontal or spherical tanks to transport liquefied petroleum gas to and from small gas terminals. The tanks are built without insulation.
- ii.) **Semi pressurised:** These carriers equipped with a reliquefaction plant and are built with tanks fabricated in special steels to accommodate the liquefied gas at low temperature. The tank either in cylindrical, spherical in shape with insulation.
- iii.) **Fully refrigerated:** The gas carriers in this group built with fully refrigerated storage tanks to transport liquefied gases at low temperature atmospheric. The cargo tanks are prismatic in shape fabricated from 3.5% nickel steel which allows the carriage of cargoes at temperatures as low as -48°C. The prismatic shape of tanks enables maximised the cargo holding capacity which enables fully refrigerated carrier suitable for carrying a large volume of cargo over a long distance.

iv.) **LNG carriers:** LNG ships are a special type of vessels built to transport natural gas in liquefied form at -161°C . These vessels fitted with independent tanks or membrane tanks for holding liquid cargo.

2.1.1. Cargo tank types

The total arrangement of cargo containment system includes

- Cargo tanks which acts as primary barrier
- Secondary barrier
- Thermal insulation
- Foundation structure to support the tanks

Type of cargo tanks divided into two categories as Independent tank and Membrane.

2.1.2. Independent tank

Independent tanks are self- supported and do not form ship's hull strength [6]. According to IGC code, independent tanks further classified as Types 'A', 'B' and 'C'.

Types 'A' tank

Type 'A' tanks are constructed with flat surfaces. The maximum allowable tank design pressure for this type of system is 0.7 barg. Cargoes require fully refrigerated condition at or near atmospheric pressure [2].

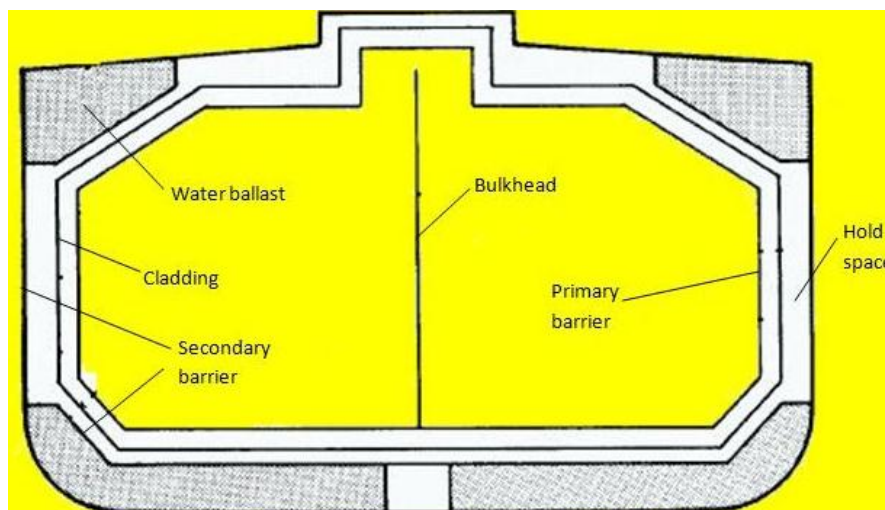


Figure 3. Self-supporting prismatic Type 'A' tank [23].

Types 'B' tank

These tanks can have either flat surfaces or of spherical type. The spherical tank is the most common type of B tank which is Kvaerner moss design [2]. This tank requires secondary barrier in the form of a drip tray. Type 'B' spherical tank is widely used in the vessel for transport of LNG.

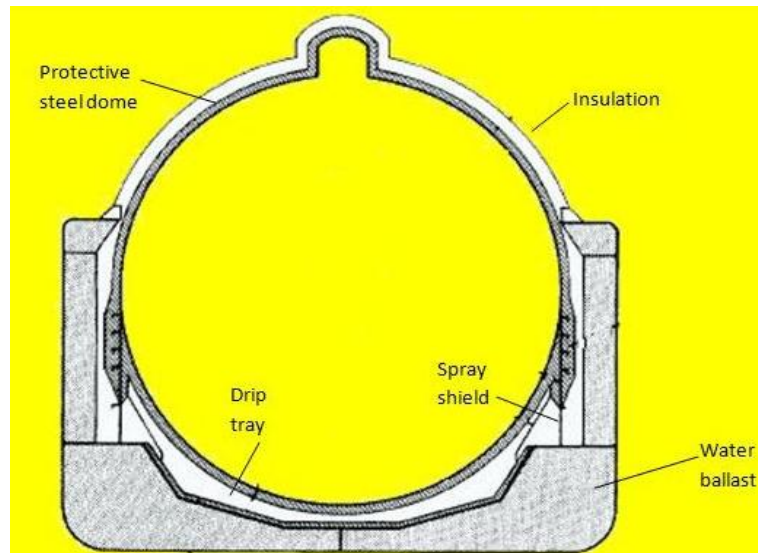


Figure 4. Self-supporting prismatic Type 'B' tank [23].

Types 'C' tank

Type 'C' tanks are of either spherical or cylindrical in shape. The cylindrical vessel is mounted either horizontally or vertically. The containment system with type C tank is used in fully pressurised or semi-pressurised gas carrier vessel.

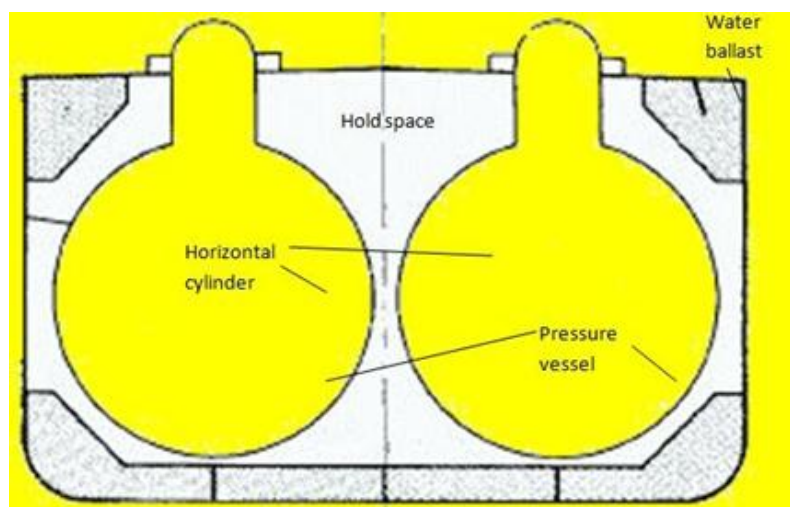


Figure 5. Self-supporting prismatic Type 'C' tank [23].

2.1.3. Membrane tank

In membrane tank, the containment system consists of a very thin primary barrier which is supported by the insulation. These tanks are not self-supported like an independent tank and an inner hull forms the loads bearing structure. Membrane containment system must always be provided with a secondary barrier to ensure the integrity of the total system [2]. The membrane is designed in such that thermal expansion or contraction is compensated without over stressing the membrane.

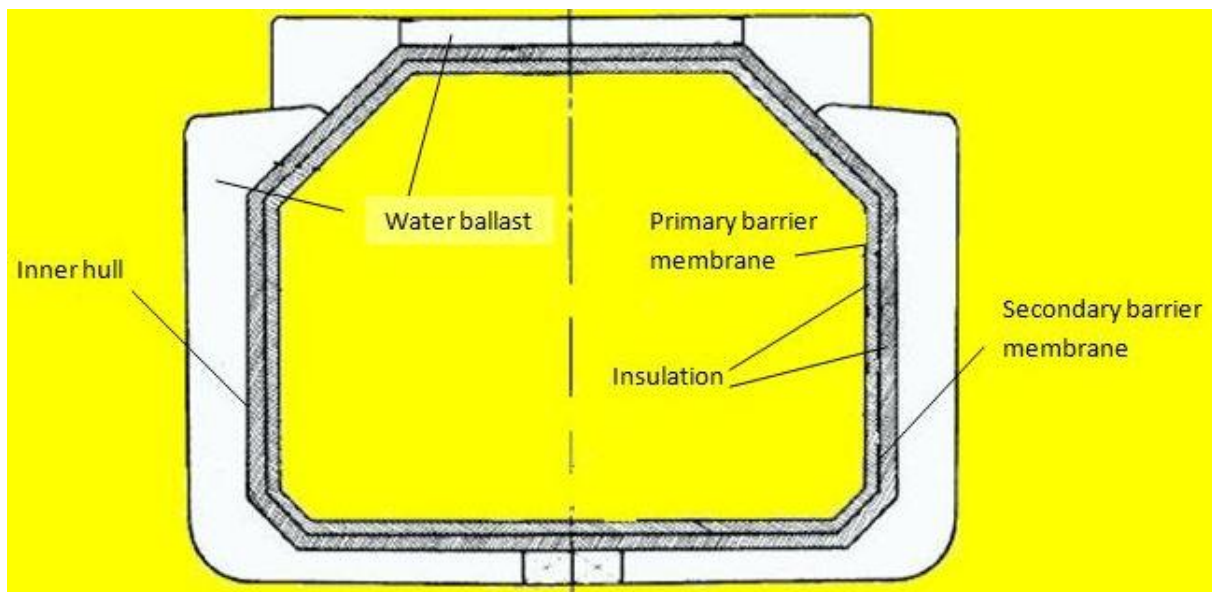


Figure 6. Membrane tank [23].

3. THEORETICAL BACKGROUND

3.1. General

Fatigue damage is the most common damage to offshore structures and vessels due to cyclic wave loads. Fluctuating stresses arising from wave loads can initiate fatigue cracks in the vicinity of joints which are inadequately designed, constructed and maintained. Though the load is not large enough to cause immediate failure, microscopic cracks gradually increase in size. Failure occurs after a certain number of cycles when the accumulated damage reaches threshold limit. Crack propagation may lead to the failure of primary members. The cost of inspection and repair of joints affected by fatigue cracks are high. Hence the fatigue design should be addressed properly at the early design stage.

3.2. Fatigue damage models

Approaches involved in the evaluation of fatigue damage are related to stress state at the crack. The stresses namely nominal stress, hotspot stress and notch stress are often used in fatigue strength calculation. The type of stresses used often depends on the problem to be solved and accuracy required.

Nominal stress: It is the stress that can be obtained from the section forces using general theories such as beam theory. It is a general stress in structural details without considering the effects due to structural discontinuities and presence of weld.

Hotspot stress: It is the structural or geometric stress at the hot spot that includes all stress raising effects from the geometry excluding the effect of the local profile of the weld.

Notch stress: It is the total stress that exists at the notch or at the weld toe due to stress concentration caused by the local notch SCF.

The three types of above stresses are shown in Figure 7.

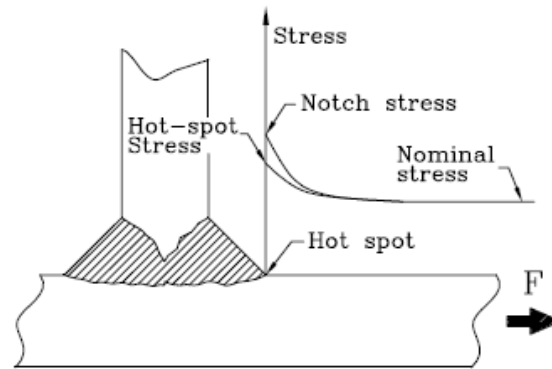


Figure 7. Stress definition.

The fatigue strength of welded ship can be evaluated using three types of approaches as given below.

Stress based approach: In this approach, the cyclic stresses including stress concentration factor (SCF) is assumed to be less than the yield stress of the material. SCF is defined as the ratio of hot spot stress to local nominal stress. The stress-based approach emphasizes nominal stresses and uses elastic stress concentration factors (SCF) instead of calculating the stresses and strains in local regions [4].

Strain based approach: This approach considers the localized plastic deformation that occurs in the local regions where the stresses are beyond material yield strength. The plastic deformation location is the probable location of fatigue crack initiation. In a strain-based approach, the strain range becomes more important than the stress range due to the plasticity of the material [4].

Fracture mechanics: In this approach, the fatigue strength of welded joints is expressed in terms of the relationship between the stress intensity factor and the rate of crack growth.

Mathematically [3] it is described as

$$\frac{da}{dN} = C(\Delta K)^m \quad (1)$$

Where da / dN represents the crack growth rate, ΔK is the stress intensity range, C and m are crack growth parameters.

In this study stress based approach is used to compute the cumulative fatigue damage. Fatigue strength assessment procedures vary among the different classifications societies but they include following common steps.

- i.) Load calculation
- ii.) Calculation of stress range
- iii.) Determination of fatigue capacity of welded joints
- iv.) Calculation of fatigue damage

3.3. Different methods of fatigue load calculations

Important methods of fatigue strength assessment of ship structures are Simplified Method, Equivalent Design Wave method (EDW), and Spectral Method [5], [8], [11]. Assessment of fatigue damage involves long-term load history which dictates the distribution of stress variation over a long period of time. The long term load history includes the following loads.

1. Still water loads
2. Wave-induced loads
3. Engine or propeller induced propeller loads
4. Impact loads such as slamming, sloshing and whipping

Wave-induced loads are the important contributing load to fatigue damage. The wave loads required for the structural FE analysis for a full load and ballast condition can be calculated in the following ways:

3.3.1. Simplified method

In this assessment technique, the calculation is performed limiting predicted stress range due to design loads below a permissible stress range. The simplified method is conservative, rapid and used for fatigue screening to identify the fatigue sensitive areas. The method employs two parameter shape and scale factors in Weibull distributions to predict the long-term distribution of stress due to sea states. Weibull shape parameter depends on the type of welding connection and different classification societies provide different values for shape factor.

3.3.2. Equivalent design wave method

Equivalent Design Wave (EDW) is a design wave which represents the long-term response of the load parameter. In this method, a rule based formulae used to calculate the wave induced load effects from an equivalent to design waves (EDW) effect. The main load wave induced load effects contributing to the fatigue damage are

- 1) Vertical wave bending moment
- 2) Horizontal bending moment
- 3) Wave torsional moment
- 4) External sea pressure
- 5) Internal liquid pressure.

Rules give the probability of exceedance of the maximum response for the (EDW). The vertical bending moment, horizontal bending moment, Torsional moment and shear force are calculated to simulate the dynamic effect of the wave. These loads are computed using ship parameters and coefficients according to classification rules. Loading from still water and dynamic waves are combined and stress responses are computed for the combined load effect using FE analysis. Compared to direct calculation or spectral method, a concept of EDW reduces the number of load cases to be considered in the design.

3.3.3. Spectral Method

In this method, fatigue assessment is based on directly calculated wave loads. Procedures described in classification society guidelines [4], [5] are briefly discussed in this section.

Wave loads are computed using 3D linear potential flow theory. The regular wave is analyzed in the frequency domain. Fatigue damages dominate due to moderate wave heights, hence non-linear effect due to large motion and waves can be neglected. The linear relationship between wave load and ship response is expressed in terms of a transfer function. Transfer functions are calculated for minimum 20 wave periods. Headings angles between 0 to 360° are covered with a maximum increment of 30° and for each heading minimum 20 wave frequencies should be included to describe the shape of the transfer functions [4], [5]. Transfer functions for the following are calculated considering wave frequency, heading angle and different ship speed.

1. Ship motions and accelerations.
2. Vertical bending moment.
3. Horizontal bending moment.
4. External sea pressures.
5. Internal ballast tank pressures.

Steps involved in spectral fatigue analysis are enumerated below.

- i.) Calculations of load transfer functions for a unit amplitude regular waves and for a range of heading angles θ , wave frequencies ω and ship speeds V .
- ii.) Calculation of stress transfer function $H_{\sigma}(\omega, \theta)$ for different heading angles, wave frequencies and ship speeds. This is obtained by load transfer function and performing global structural analysis using FE analysis. Hydrodynamic loads consist of panel pressure, inertia forces and internal tank pressure from wave analysis, directly transferred to the finite element structural model.
- iii.) From the global structural analysis, determine a short term structural response for different heading angles, wave frequencies and ship speeds.
- iv.) Using wave spectrum, wave scatter diagram and S-N data for various wave heading angles and ship speeds, determine the long-term stress range giving the probability of the stress range exceeding a specified maximum value.

For linear and harmonic responses, the stress transfer function at the desired location is obtained as a linear complex combination of the transfer functions for the various contributing load components [5].

$$H_{\sigma}(\omega, \theta, V) = \sum_{i=1}^n \sigma_{x_i} H_{x_i}(\omega, \theta, V) \quad (2)$$

where σ_{x_i} = calculated stress for a unit load component X_i
 $H_{\sigma}(\omega, \theta, V)$ = transfer function for the load component X_i

Ship's response to a random sea computed by the linear superposition of a large number of regular waves of various amplitudes, frequencies, phases, and directions. Stress energy spectrum $S_{\sigma}(T_Z, H_S, \theta)$ for any loading effect is generated by scaling the wave energy spectrum $S_m(T_Z, H_S, \omega)$ [5],

$$S_{\sigma}(T_Z, H_S, \theta) = |H_{\sigma}(\omega, \theta)|^2 S_m(T_Z, H_S, \omega) \quad (3)$$

where, T_Z = average zero up-crossing wave period, in seconds

H_S = significant wave height, in m

θ = wave heading angle

3.3.4. Short-term response

Calculation of the structural response of ship is based short-term response for a given sea state, which consists of the following assumptions [5].

- 1) A fully developed, wind-generated, mid-ocean sea state the wave spectrum is relatively narrow-banded. The ship acts as a filter such that the ship motions spectra and the resulting load effects are also narrow-banded. Like waves, ship responses follow Gaussian distribution and are stationary in the short term short for a given sea state. Since peak value wave height follow a Rayleigh distribution, the resulting ship responses also follow Rayleigh distribution.
- 2) Linear superposition is applicable.

With the above assumption, the stress range response $S = 2 \times$ mean stress, the probability density function of S is given by the Rayleigh distribution [5]:

$$P(S) = \frac{S}{4\mu^2} e^{-\frac{S^2}{8\mu^2}} \quad (4)$$

where the variance μ^2 is equal for a process with zero mean to the area under the stress response spectrum

$$\mu^2 = \int_0^{\infty} S_{\sigma}(\omega, \theta, V) d\omega = m_o \quad (5)$$

The probability of the stress range S exceeding a specified value S_0 for a given sea state is expressed as [5]:

$$P(S > S_0) = e^{-\frac{S^2}{8\mu^2}} \quad (6)$$

The cumulative probability distribution [5] is

$$P_s(S_0) = 1 - e^{-\frac{S^2}{8\mu^2}} \quad (7)$$

where $P_s(S_0)$ is the probability that a stress range of magnitude S_0 will not be exceeded for a given sea state.

3.3.5. Long-term response

During the lifetime of a ship a wide range of weather conditions, and hence different sea states will be encountered. This total time span considered as a large number of short intervals, each of a few hours duration, during which the sea state remains constant. Similarly, during the total lifetime response history of the ship may be considered of as a series of short-term intervals. Assuming that the short-term stress range response follows a Rayleigh distribution, the long-term probability $P_s(S > S_0)$ of the resultant stress range exceeding S_0 is computed [5] by considering:

1. The short-term stress range probability exceeding a specified value S_0 .
2. The probability $p(\bar{H}_s, T_m)$ of each sea state expressed by the mean period T_m and the average significant wave height H_s .
3. The probability $p(\theta)$ of occurrence of the heading angle θ .
4. The occurrence of the maximum speed or a reduced speed probability $p(V)$.

For a given loading condition the long-term probability of the stress range exceeding a specified value S_0 is given by [5]:

$$P(S > S_0) = \iiint e^{-\frac{S^2}{8\mu^2}} p(\bar{H}_s, T_m) p(\theta) p(V) d\theta dV dT d\bar{H} \quad (8)$$

The long-term distribution of the stress range is obtained by performing the above calculation for various values of S_0 .

3.4. Fatigue strength calculation based on S-N curve

The fatigue strength is expressed in term of the cumulative damage ratio D by Palmgren and Miner rule. According to this rule, if there are j number of different stress levels and the average number of cycles to failure is N_i , at the stress S_i then the damage D is expressed as

$$D = \sum_i^j \frac{n_i}{N_i} \quad (9)$$

where, n_i = number of cycles at stress range S_i ,

The structure is considered to be failed when damage ratio approaches unity. Considering factor safety γ , the maximum allowable damage ratio should be below unity.

$$D = \sum_i^j \frac{n_i}{N_i} \leq \frac{1}{\gamma} \quad (10)$$

Even though there are many different loading scenarios which occur during a ship's life, for the majority of cargo ships full load and ballast condition idealized as two standard conditions.

Total fatigue damage D , taking into the fatigue damage of full loading condition and ballast condition.

$$D = \alpha D_f + \beta D'_f \quad (11)$$

where, D_f = cumulative damage ratio in full load condition

D'_f = cumulative damage ratio in ballast condition

α = ship's life in full load condition

β = ship's life in ballast

Accumulated damage in full load or in ballast condition, D_f or D'_f is given by the following expression [11].

$$D_f \text{ or } D'_f = N_D \left[\frac{q^m}{K_2} \Gamma \left(1 + \frac{m}{\xi}; \left(\frac{\Delta\sigma_q}{q} \right)^\xi \right) + \frac{q^{m+\Delta m}}{K_3} \gamma \left(1 + \frac{m+\Delta m}{\xi}; \left(\frac{\Delta\sigma_q}{q} \right)^\xi \right) \right] \quad (12)$$

where:

$\Delta\sigma_q$ = Stress range in S-N curve, where the change of slope occurs

N_D = Total number of stress cycles experienced by ship during the design fatigue life

K_2, m = S-N fatigue parameters for $N < 10^7$ cycles

$K_{3,m+\Delta m}$ = S-N fatigue parameters for $N > 10^7$ cycles

$\Gamma (;)$ = Complementary Incomplete Gamma function, to be found in standard tables

$\gamma (;)$ = Incomplete Gamma function, to be found in standard tables

ξ = Weibull slope parameter

q = Weibull scale parameter

Number load cycles N to failure for a particular stress range can be obtained from S-N curve or stress Cycle curve. These curves are obtained by subjecting the material specimen to constant cyclic load until failure in laboratories. The curve represents a relation between the stress ranges against the stress cycle on logarithm scale. Figure 8 shows a set of typical S-N curves. Though there are various S-N curves available published by many institutions such as IIW, HSE UK, AWS available, only two of the following are used by the classification societies [5].

1) HSE S-N curves

2) IIW S-N curve

Using Miner's law and data from S-N curves fatigue life structure is assessed for various welded joints. The relationship between stress range $\Delta\sigma$ and the number of cycles to failure N can be represented by the following expression [11].

$$\log N = \log k_2 - m \log \Delta\sigma \quad (13)$$

where:

N = number of cycles to failure for stress range $\Delta\sigma$

$\Delta\sigma$ = stress range in N/mm^2

m = negative inverse slope of S-N curve

The intercept of $\log N$ -axis by S-N curve, $\log k_2$ is expressed as [11]:

$$\log k_2 = \log k_1 - 2\delta \quad (14)$$

where:

k_1 = Constant of mean S-N curve (50% probability of survival)

k_2 = Constant of design S-N curve (97.5% probability of survival)

δ = Standard deviation of $\log N$:

= 0.20

Depending on the level of refinement method used in FE analysis to calculate stresses, three types of stresses namely nominal stress, hotspot stress or notch stress are used in fatigue calculations.

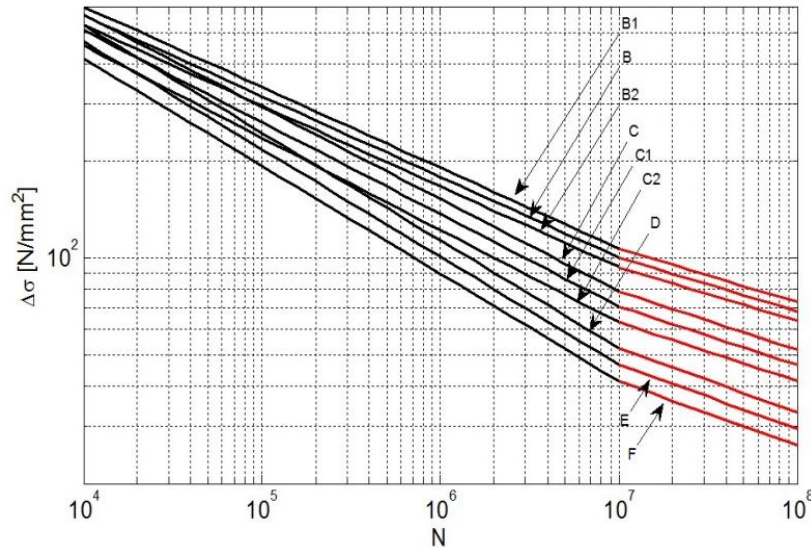


Figure 8. S-N curve in air –DNV GL[11].

With nominal Stress approach, stresses are assessed by structural mechanics or by coarse mesh FE analysis. If FE analysis employed, a uniform mesh shall be used with a smooth transition and abrupt changes in mesh size must be avoided. At the hot spot, the nominal stress is calculated by extrapolated stresses around the hotspot region. With nominal stress approach, the S-N curves can be used directly provided that the applicable S-N curve clearly identified for a welded joint detail under consideration. Due to the complexity of ship structural details, it is difficult to select the correct S-N curve and selection becomes a matter of judgment.

Hot spot stress approach considers the change in geometry of the structure. With this approach it is possible to handle fabrication imperfections such as linear or angular misalignments which introduce additional geometric stress concentrations. Hot spot stress contains additional stress increase due to geometrical discontinuity in addition to nominal stress. Stress arising from local weld geometry is excluded in stress calculation. At hot spot region, the stress distribution is highly dependent on the finite element mesh. For evaluation of hot spot stress by FE analysis, the shell element must be size $t \times t$, where t is the thickness of the plate where the hot spot is calculated. Stress evaluation points shall be at a distance of $0.5t$ and $1.5t$ from the weld toe or hot spot. The stresses values are determined by linear or

2nd order interpolation of the principal stresses at the centre of element faces in the region [11].

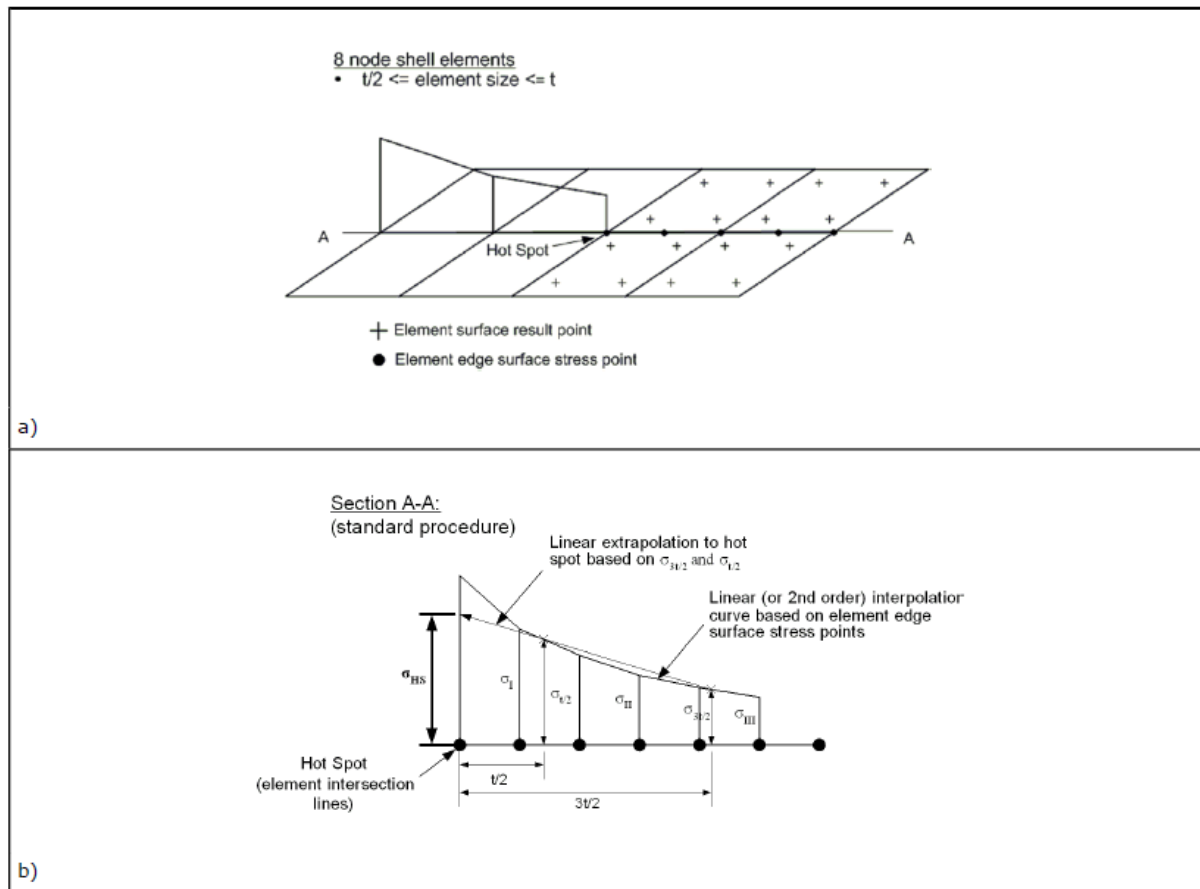


Figure 9. Stress read out points and hot spot stress for 8-node shell elements [11].

Notch stress approach includes the effects of welds. It is the total stress at the root of the notch which includes non-linear stress effect due to the notch at the weld toe. This method assessing stress is applicable to those welded joints which fail from the weld toe or weld root. Procedures described in classification society guideline [12] briefly discussed in the following paragraph.

The real weld is replaced by an effective one which takes into account of weld shape and non-linear material behaviour at the notch root as shown in Figure 10. Effective notch root radius of $r = 1.0$ mm has been verified and is recommended to use in notch stress evaluation using FE analysis of structural steels. Notch stress can be evaluated by parametric formulae or FE analysis with fine finite element mesh around the notch region. The effective notch radius is expressed such that the tip of the radius touches the root of the real notch. The maximum surface stress at the notch can be obtained directly from the surface nodal stress or from

extrapolation. The maximum surface stress calculated from FE analysis at the notch is the effective notch stress which shall be used together with the recommended S-N curve[12].

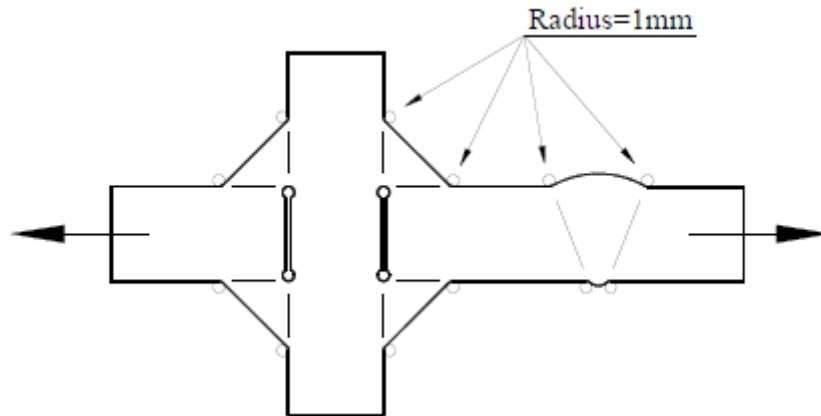


Figure 10. Notch model [12].

3.5. Uncertainties in fatigue strength prediction

There are a number of uncertainties associated with fatigue life prediction calculation. The main uncertainties associated with fatigue life calculations mainly due to wave loading, Stress calculations and S-N curves [3],[5], [11].

i.) Wave loading

Uncertainties related to wave load calculations due to random sea loads, the period length used for collection of environmental data, wave theories.

ii.) Stress calculations

Uncertainties associated with stress calculations dependent on FE modelling techniques, boundary conditions, mesh size, the method of combinations of various wave and quality of structural stress computation software tools. Since the fatigue damage is proportional to the inverse slope of the S-N curve, minor changes in stress lead to major changes in calculated fatigue life.

iii.) S-N curves

S-N curves are based on experimental results in the laboratory under free corrosion environment up to 10^7 cycles to failure. In ship structures, fatigue damage is significant when a number of cycles to failure $N > 10^7$. Therefore the method of extrapolation of S-N curves beyond 10^7 cycles is important for the assessment of fatigue life.

4. ANALYSIS METHODOLOGY AND SOFTWARE TOOLS USED

4.1. Analysis Methodology

The methodology adopted in this thesis project is described in Figure 2. For the fatigue damage, full spectral analysis wave loads are calculated by direct calculations. For fatigue damage evaluation it is assumed that the short return period wave loads contribute significantly to fatigue damage have short return periods. These waves are small in amplitude and frequently occur.

Wave loads are calculated using a 3D hydrodynamic program including the effect of forward speed. A vessel speed set to $2/3$ of the service speed in full load and ballast condition is applied in the hydrodynamic modelling. The hydrodynamic analysis in the linear frequency domain using 3-D potential theory is employed to calculate ship response. The wave amplitude of 1.0m considering wave headings from 0 to 360 degrees with an increment of maximum 30 degrees is used to calculate the ship response. For each wave heading 25 wave frequencies are included to describe the shape of the transfer functions.

In order to obtain balance in FE structural model and hydrodynamic model, mass has to be identical in FE and hydrodynamic model. Therefore mass model from global FE structural model is used in the hydrodynamic linear analysis. The mass in hydrodynamic analysis shall be represented correctly to obtain motion and sectional forces. The mass model shall include the following

- the total weight which includes light weight, ballast and liquid cargo
- longitudinal, vertical, transverse centre of gravity
- rotational mass in roll and pitch.

The weight of the cargo in spherical tanks of Moss type LNG carrier uniformly distributed along the skirt of the tank to the hull foundation. The panel pressures, inside tank pressure and inertia loads from the hydrodynamic analysis, are directly transferred to FE structural global model.

A linear FE structural analysis is performed for global ship model. Since the main purpose of the global analysis is to identify the critical locations, stress risers such as welds notches and

geometrical discontinuities are not modelled. A detailed local sub-model of details at the critical location is modelled with a fine mesh of size $t \times t$ where t is the thickness of the plate. The deformations from global FE analysis are applied on the border of the sub model. These deformations serve as boundary conditions for the local model. Wave loads from the hydrodynamic analysis are directly transferred to sub model.

For each heading of sea state, fatigue damage is calculated by combining the hotspot transfer functions with stress cycle (S-N) curve data and wave scatter diagram.

4.2. Software Tools Used

In order to execute the set of analysis defined in section 4.1, SESAM software package developed by DNV has been used. SESAM is a complete strength assessment programme for engineering of ships, offshore structures and risers based on the finite element methodology. This software package has various modules which can be used depending on the type numerical simulation that is required to be carried out. For the current study of LNG carrier the following modules used has been selected.

4.2.1. *Sesam Genie*

GeniE is the design analysis tool in SESAM used for designing and analyzing, the offshore and maritime structures made of beams/shells [16]. GeniE can be used as a stand-alone tool and user where the user can

- Model structure, equipment, environment and other loads
- Calculate hydrodynamic loads and run static structural analyses including non-linear pile soil analysis
- Visualize and post-process results
- Perform code checking based on recognized standards

4.2.2. *Sestra*

Sestra is a program for linear static and dynamic structural analysis within the SESAM program system **Error! Reference source not found.** It uses a displacement based finite element method. Sestra computes the local element matrices and load vectors, assembles them into global matrices and load vectors. The global matrices are used by algebraic numerical

algorithms to do the requested static, dynamic or linearized buckling analysis. It has interface with other program modules of SESAM

4.2.3. *HydroD-Wasim*

The Sesam HydroD capability of performing a hydrostatic and hydrodynamic analysis which includes a hydrodynamic model of the floating structure ships and offshore floating structures

Wasim is a program for computing global responses of and local loading on vessels moving at any forward speed. The simulations are carried out in the time domain, but results are also transformed to the frequency domain by using Fourier transform [18].

Rankine panel method is to solve the fully 3-dimensional radiation/diffraction problem by a Wasim. This method requires panels both on the hull and on the free surface. Based on the geometry of the hull supplied by the user, Wasim generates its own mesh. Analysis by Wasim include the following capabilities

- Global responses computation of
 - rigid body motions
 - sectional forces and moments
 - relative motion at specified points

- Computation of pressure on the vessel:
 - pressure at selected points on the hull
 - total pressure distribution on the whole hull

- Direct transfer of pressures to a finite element model for structural analysis

4.2.4. *Xtract*

Xtract software is post processing tool having features for selecting, further processing, displaying, tabulating and animating results from static and dynamic structural analysis as well as results from various types of hydrodynamic analysis [19]. With its high-performance 3D graphics enables easy and efficient interactive rotation, zooming and panning of the model for viewing and animation. Based on the FE analysis results with Xtract, it is possible to present the decomposed stress components into membrane and bending parts, principal stresses and Von Mises stresses. Furthermore, with Xtract, it is also possible to presents

deformed model, contour curves of stresses and displacement-Y graphs and tabulated data. In addition, the motion of vessel can be animated.

4.2.5. Postresp

The statistical post-processing of general responses of ship obtained from global hydrodynamic analysis in the frequency domain is obtained using Postresp software. These responses such as displacements, velocity etc. are represented as transfer function for FE structural analysis. The transfer functions are generated by the hydrodynamic program HydroD -Wasim. The displacement response variables such Surge, Sway, Heave, Roll, Pitch and Yaw motion are plotted as dimensionless quantities with respect to wave periods or frequencies at different wave headings. The graphs from the program and results are discussed in chapter 6.

4.2.6. Submod

The submod programme allows a part of a global model to be re-analyzed to produce more accurate results. For the local model separated from the global model, the displacements from global model analysis applied as prescribed displacements at the boundary[20].

4.2.7. Cutres

Cutres is a post-processor used for ship structures. With Cutres, cross-sections of ship structures can be created and combined into assemblies. Cutres calculate the force distribution across the cross section and can be presented graphically. With Cutres, force distribution in each cross section integrated to form the total axial force, shear forces and bending moment and torsional moment [21].

4.2.8. Stofat

The Stofat is software tool for fatigue design. Stofat performs stochastic fatigue analysis on structures modelled by 3D shell and solid elements and assesses whether the structure is likely to suffer failure due to the action of repeated loading [22] Stresses from the global or local FE analysis serves as stress transfer function for fatigue calculation. Accumulated damage is calculated using stress transfer function, S-N curve data, wave spectrum, weighted over sea states and wave.

5. STRUCTURAL MODELLING

The objective of the global structural modelling is to compute the stress transfer function from environmental wave loading by finite element method. The stresses required for the fatigue assessment is obtained from global FE analysis of the vessel. The global structural model represents the stiffness of the actual structure and comprises of shell finite elements in combination with beam elements. The structural FE model is further utilized in the hydrodynamic model to develop the panel and mass model. The panel model takes into account the finite elements exposed to the action of hydrodynamic wave loading and whole structural FE model represents the mass model. The use of FE structural model as a mass model in hydrodynamics analysis ensures the consistent load and response between hydrodynamic and structural analysis. The structural connections at key locations such as liquid cargo tanks with tank foundation deck and cargo tank with hull deck have been modelled with sufficient stiffness to ensure proper load distribution and to obtain correct global stress.

The main characteristic of the 148k LNG vessel that has been studied is shown in Table 1. The global FE model of the vessel is represented by Figure 11.

Table 1. Main characteristics of LNG carrier

Length Overall	289.50 m
Length between perpendiculars	277.00 m
Breadth moulded	49.00 m
Depth moulded	27.00 m
Design draught	11.90 m

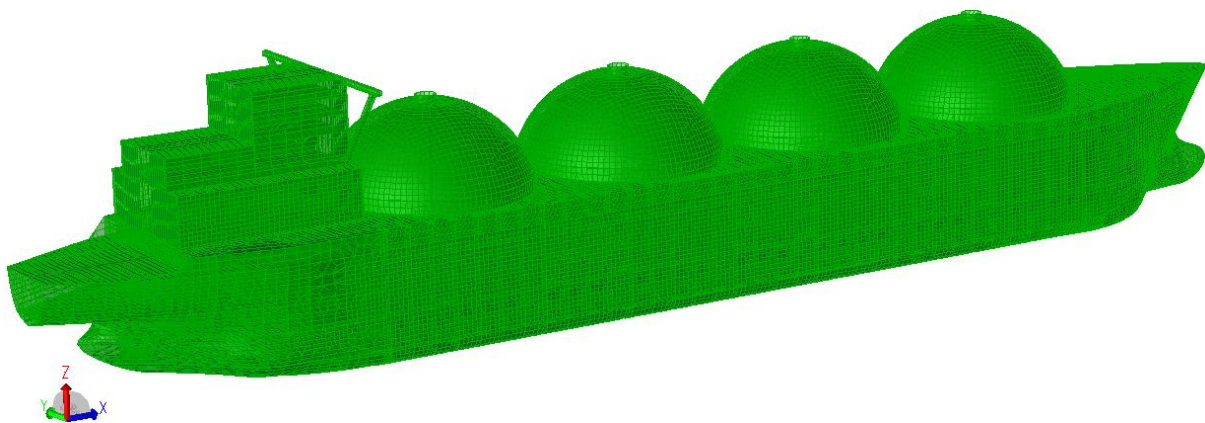


Figure 11. LNG carrier FE model.

5.1. Co-ordinate and unit system

The co-ordinate system adopted in the global model is as shown in Figure 12. The right-hand co-ordinate system is defined in accordance to the recommended practices with the

- positive x-axis pointing towards forward,
- positive y-axis towards port
- z-axis positive vertically from baseline to the deck.
- The origin is chosen at the intersection of baseline, aft perpendicular, and centreline.

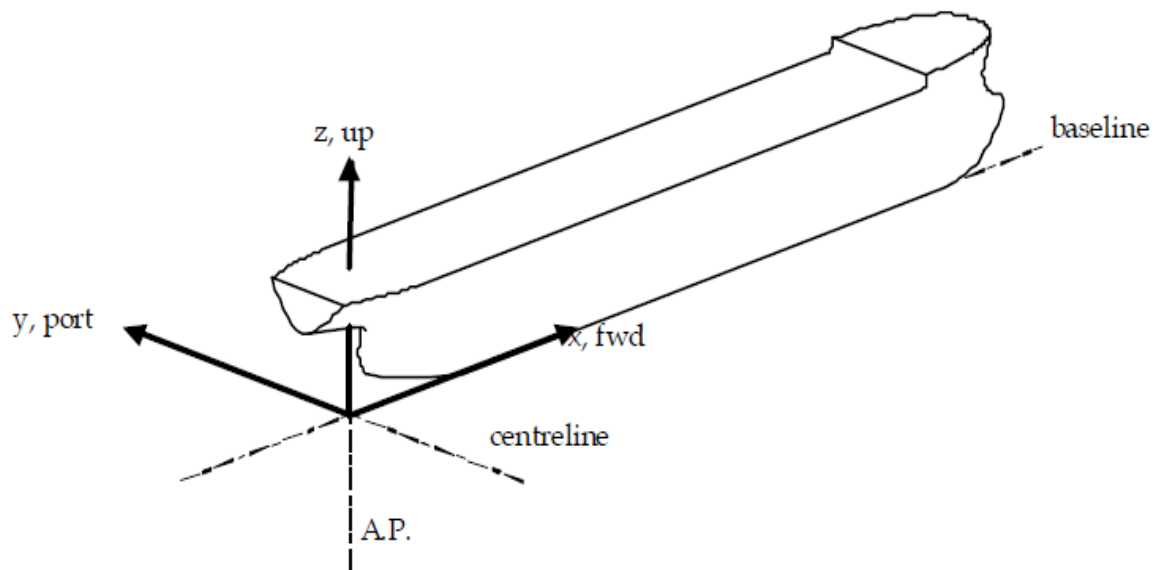


Figure 12. Co-ordinate system.

For structural modelling SI-units has been used with the following dimensional units :

- Mass = (kg)
- Length = (m)
- Time = (s)

Force and stress outputs from global structural analysis are evaluated in the following units:

- Force = (N)
- Stress = (Pa) or (MPa)

The material grades used for the structural modelling of the vessel is documented in Table 2.

Table 2. Material Properties

Material Property	Value		unit
Material grades and Yield stress	B,D	235 x10 ⁶	Pa
	A32,D32,E32	315 x10 ⁶	
	A36,D36,E36	355 x10 ⁶	
Density	7850		kg/m ³
Young's Modulus	2.1x10 ¹¹		Pa
Poisson's Ratio	0.3		-
Thermal Coefficient	1.2x10 ⁻⁵		W/(m.C-1)
Design draught	0.03		N.s/m

5.2. Geometrical Modelling

The finite element structural modelling package SESAM GeniE is used for the geometrical modelling of the vessel under study. The whole vessel is modelled taking into the effect of all structural elements. Plate and beam elements are used to simulate stiffened panels. The FE model deadweight is compared with the light weight of the vessel and additional mass elements are incorporated in the model to include the weight of equipment.

LNG carrier consists four spherical cargo tanks which are of independent tank type 'B'. The structural topology of the vessel which includes the main structural members such as double bottom, double-sided hull, foundation deck, watertight bulkheads and upper deck are presented in the following subsections. The typical midship section is shown in Figure 13.

5.2.1. Double Bottom

Double bottom provided with a minimum depth of 1.6 m at the centre line and the transverse girders in the double bottom are spaced at 2.52m centre to centre. The space inside the double bottom is void which facilitates the access during the fabrication inspection and repair. The space between the inner bottom and the spherical tank is free from obstruction and the sloped part of the inner bottom connected with the foundation deck.

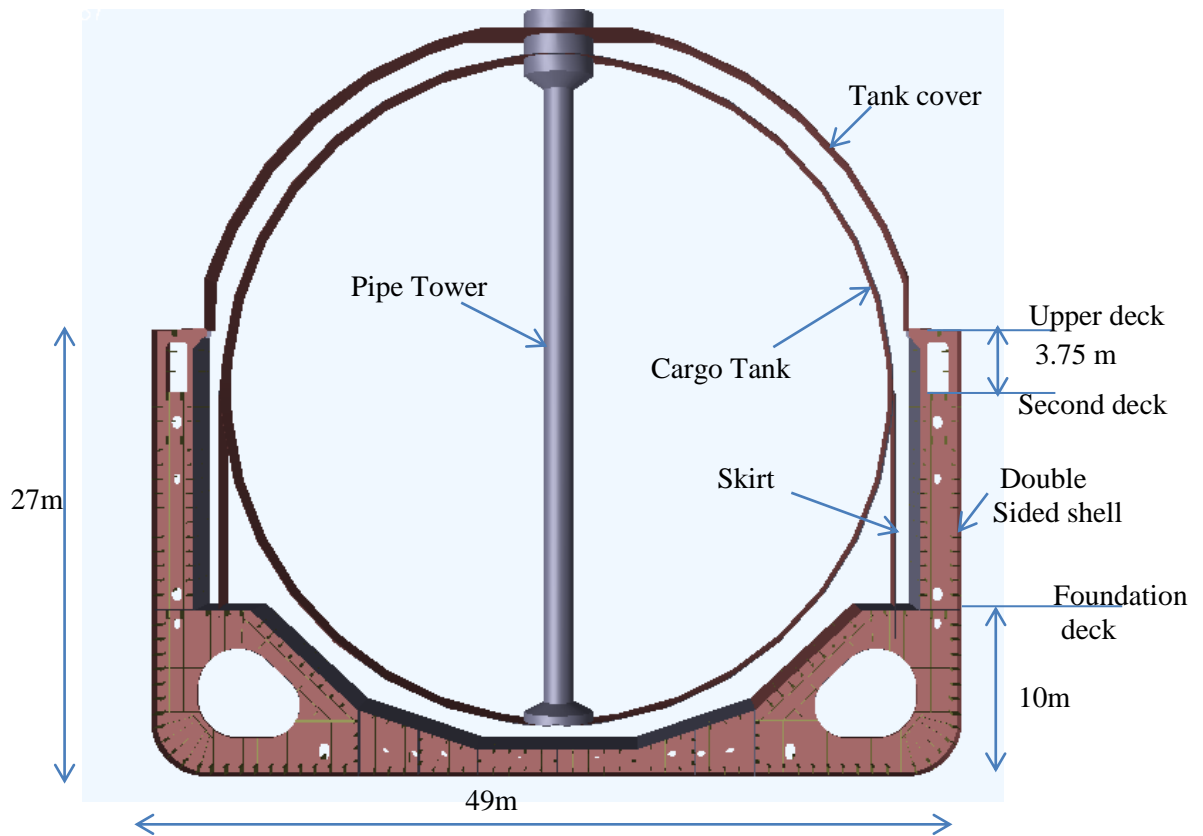


Figure 13. Midship section of LNG carrier.

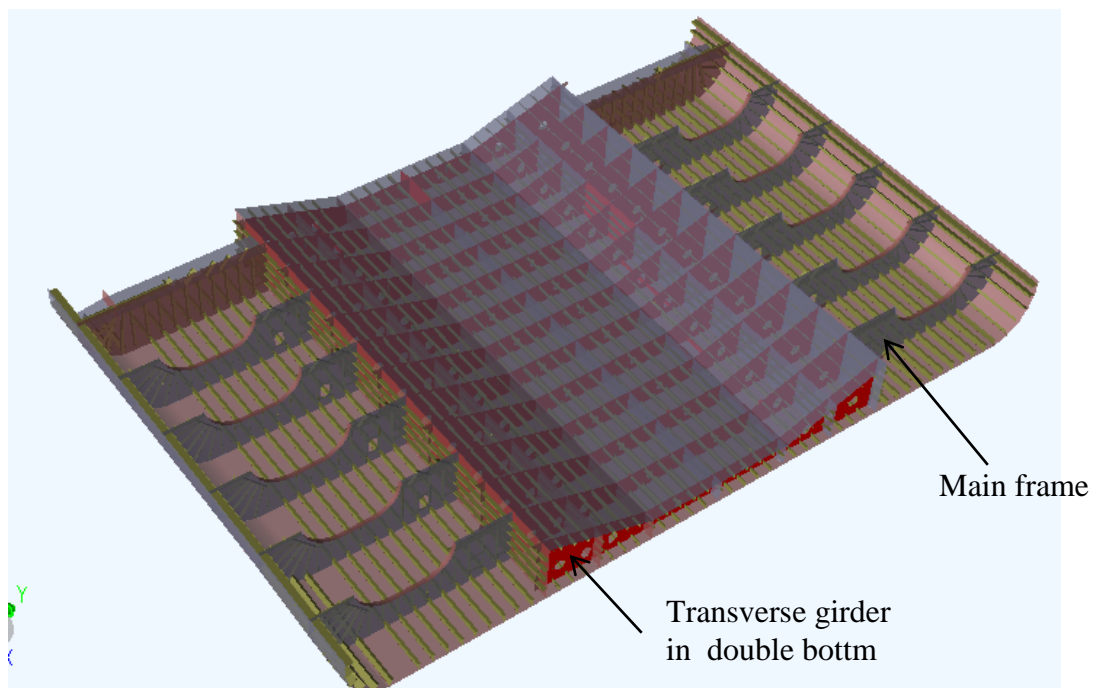


Figure 14. Double bottom view.

5.2.2. Double Side shell

The vessel has double side shell with a separation of 2.5m which provides sufficient space to the passageway. The main transverse web frames are spaced at 5.04m. Inner and outer shells are stiffened longitudinally with T girders

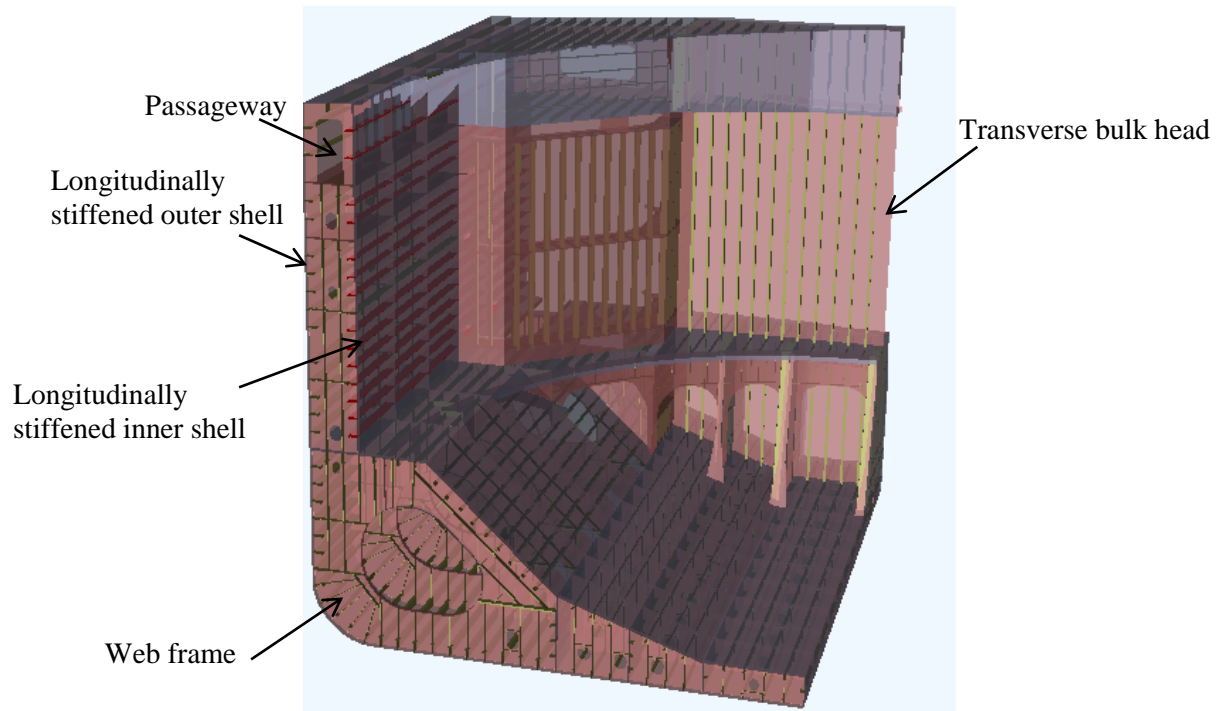


Figure 15. Double sided hull- 3-dimensional view.
(Cargo tanks and skirt foundation removed for clarity)

5.2.3. Transverse Bulkhead

Transverse bulkheads are spaced at 40.9 m centre to centre distance and situated in between the spherical cargo tanks. It imparts the additional structural rigidity to the vessel. These bulkheads are watertight and connected to the seawater ballast tanks. The bulkhead is stiffened with T girders. Figure 16 shows the transverse bulkhead and its connection to the adjacent structure.

The foundation deck supporting spherical cargo tanks, integrated with transverse bulkhead imparting further stiffness to the bulkhead. As shown in Figure 17, below the foundation deck, side girders highlighted in red color are provided with extended skirt plate to distribute cargo tank loads into the double bottom of the hull.

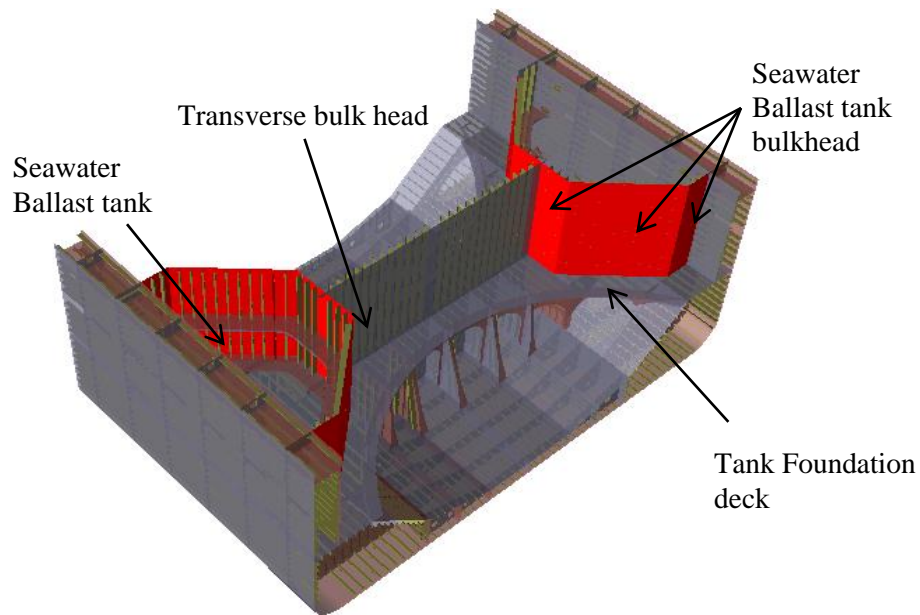


Figure 16. Seawater ballast tank and bulkhead.

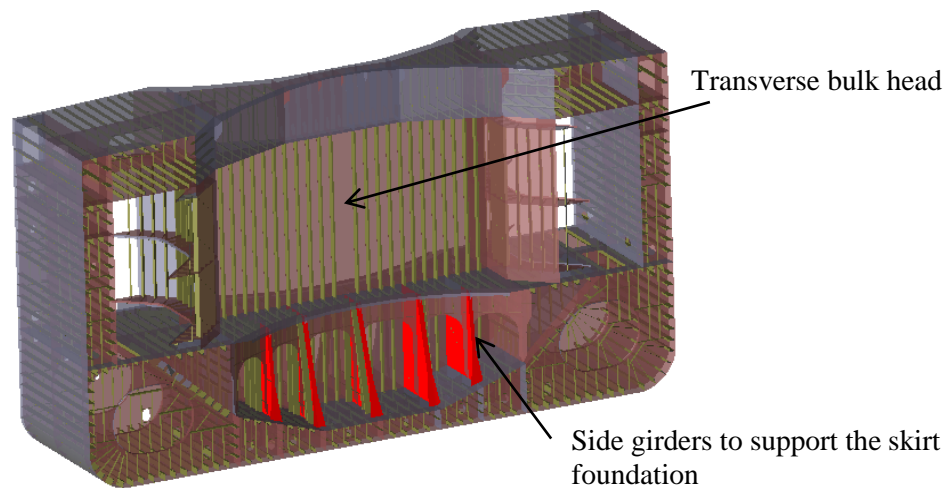


Figure 17. Transverse bulkhead and foundation support side girder.

5.2.4. Foundation Deck and Cargo tank support

The spherical cargo tanks holding liquid cargo are supported by the skirt. The upper edge of the skirt is connected to the bottom hemisphere of the cargo tank at the horizontal equator. The lower edge of the skirt is connected to the foundation deck. Skirt plate further extends into the foundation of the deck. The weight of the liquid cargo and dead weight of spherical tank are transferred to foundation deck by the skirt. Figure 18 and Figure 19 shows foundation deck and cargo tank support.

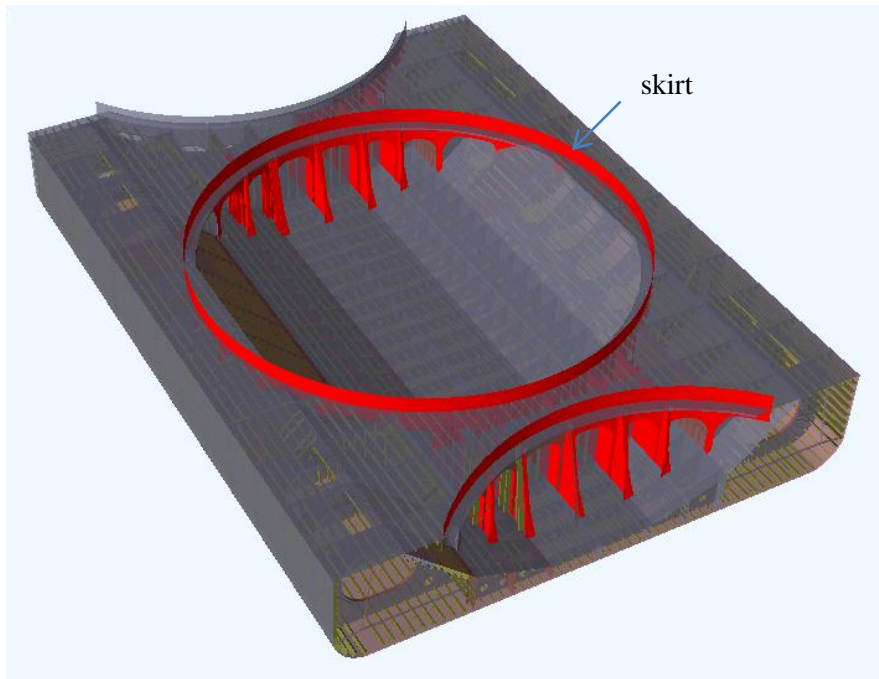


Figure 18. Foundation deck – sectional view just above the foundation.

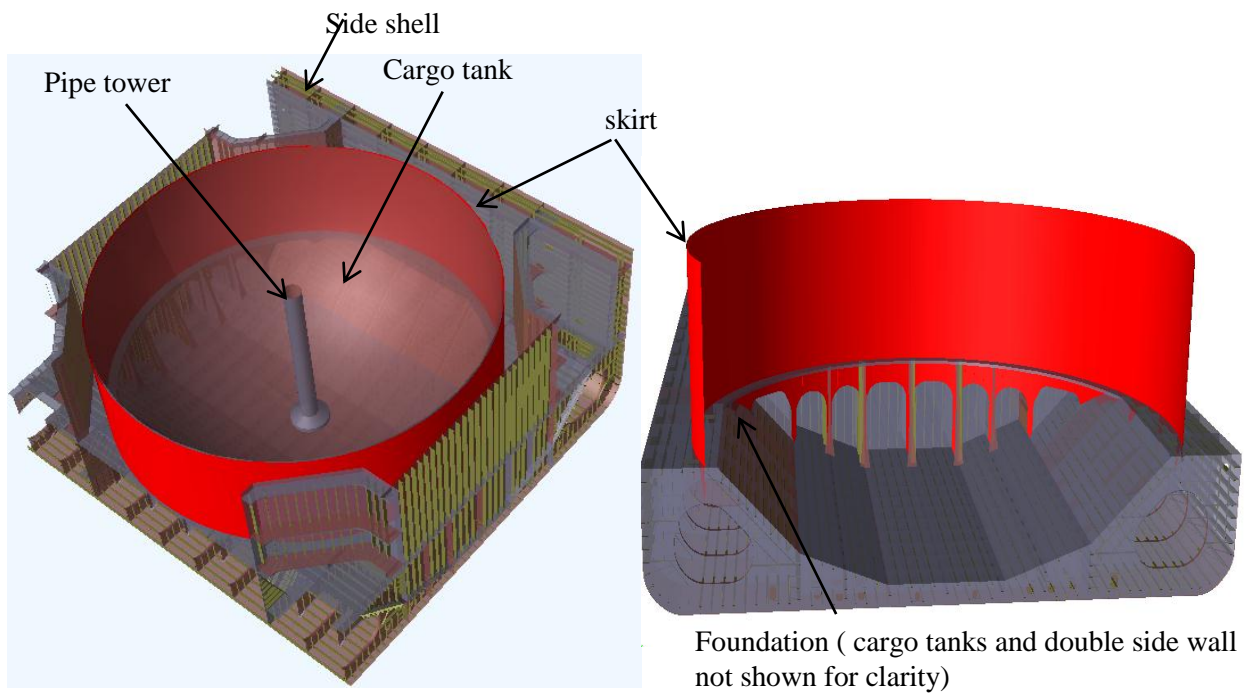


Figure 19. Sectional view showing skirt orientation.

5.2.5. Upper Deck

The deck plate thickness varies from 16mm to 30 mm. The thicker deck plate is provided due to high stress at the main deck level. The high stress arises due to the fact that the main deck is situated far away from the natural axis of the ship. The deck plate is stiffened longitudinally by T-section. Cargo tanks are protected by a weatherproof dome. The dome plate is supported on brackets which transfer the weight of the dome to the main deck. Figure 20 shows the main deck arrangement.

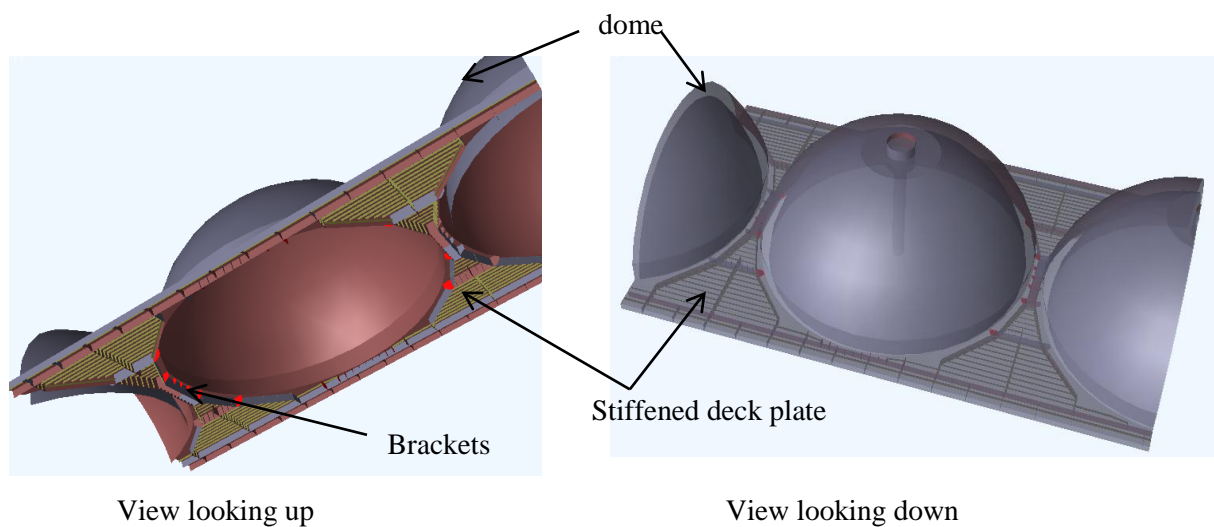


Figure 20. Isometric views showing stiffened deck.

5.3. Boundary conditions

The boundary condition used in the global analysis is illustrated in Figure 21. A three-two-one fixation is applied to the global model. In order to avoid the imbalance in the model due to the direct transfer of loads from the hydrodynamic load analysis, these fixation points are located away from the fatigue study points. The boundary condition points are applied along the centre line close to the forward and aft end of the vessel.

The boundary conditions are in the form of simple supports to avoid built-in stresses. The study of fatigue is centered around hopper knuckle located in the foundation supporting the spherical cargo tanks.

As can be seen from Figure 21, the global model is supported at three positions along the centerline of the vessel. These support condition of at these points are as follows

Point 'A' is located in a transverse bulkhead at the aft end of the ship and is along the centre line of the vessel in the waterline plane. At point 'A', pinned condition is applied i.e. the support is fixed for translation along three axes and free to rotate.

Point 'B' is located in a transverse bulkhead at the aft end of the ship and is along the centre line of the vessel but located at the upper continuous deck above the water plane. At point 'B' i.e. the support is fixed for translation along the transverse direction only. The point B is free to translate along x, z-direction and free to rotate about three axes.

Point C is located in a collision bulkhead at the forward end of the ship and is along the centre line of the vessel in the waterline plane. At point 'C' pinned condition applied i.e. the support is fixed for translation along the transverse direction and vertical direction only. The support is free to rotate about three axes.

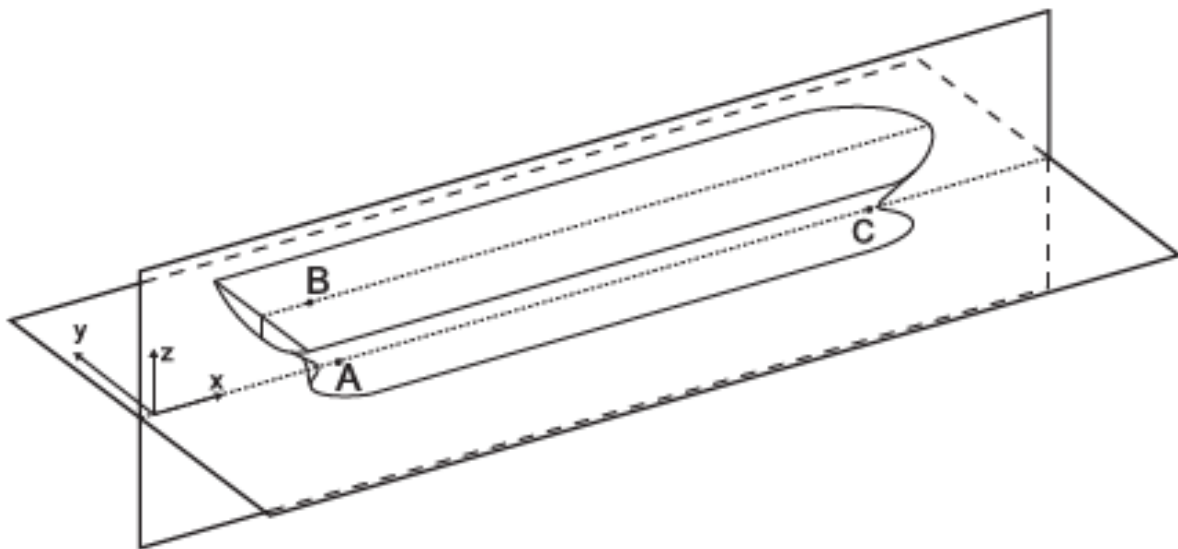


Figure 21. Boundary condition [7]

5.4. Structural Mesh Model

The finite element model representing the entire vessel includes all the structural components such as bulkheads, the girders, double bottom, side shell, cargo tanks, dome and other key structural connections of the vessel. In order to carry out fatigue screening analysis of knuckle joints identifying critical fatigue location, a global model with coarse mesh is used. Detailed analysis of critical knuckle joints is performed using local or sub model with fine mesh.

5.4.1. Global Model

For global fatigue screening, a region of the global model meshed with a mesh size of 1m which is equal to with stiffener spacing. A full-stochastic fatigue analysis using 12 wave directions and 25 wave periods results in 300 complex load cases. Hence the region of mesh density of 1m required to be restricted to reduce computation time. The spherical tanks and skirts are modelled sufficiently accurate and the transition of skirt towards the foundation deck modelled with substantially finer mesh. A coarse mesh is used at the aft and foreparts of the vessel. Figure 23 and Figure 26 shows global FE mesh of the vessel.

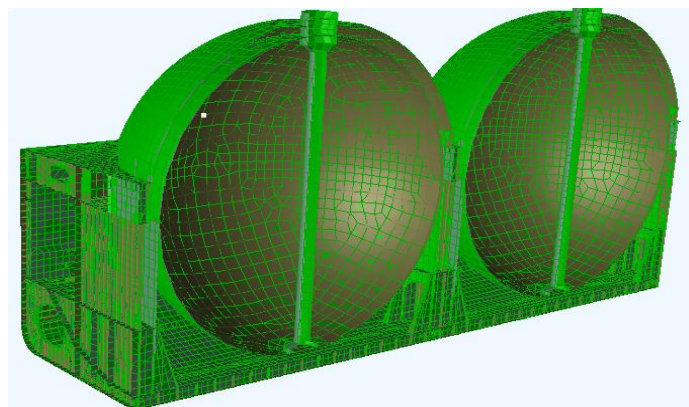


Figure 22. Midship FE mesh -Longitudinal section at the centre line.

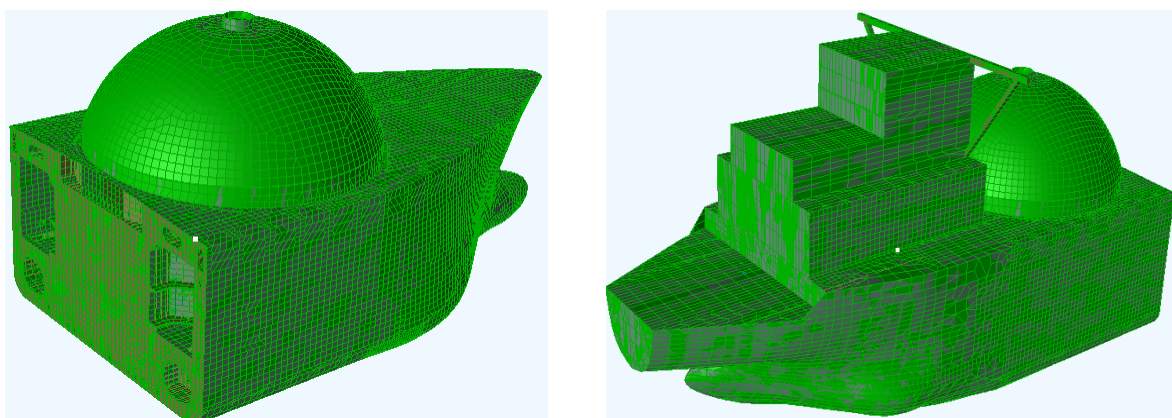


Figure 23. Fore and Aft Ship FE mesh.

5.4.2. Sub Model

The region under the fatigue analysis requires fine mesh compared to the global model with regular mesh type. The number of degrees of freedom will be increased due to the inclusion of dense mesh in the global model. Hence more computational time is required and the result output database is difficult to navigate. Local model i.e. sub model with finer mesh is used for fatigue study. Fatigue damage of hopper knuckle joints in the foundation deck situated around the liquid cargo tank 2 is reported in this thesis work. Local sub model for these knuckle joints on the starboard side is analyzed and checked for fatigue damage. Location of these 9 knuckle joints T2_k1 to T2_k9 is shown in Figure 24.

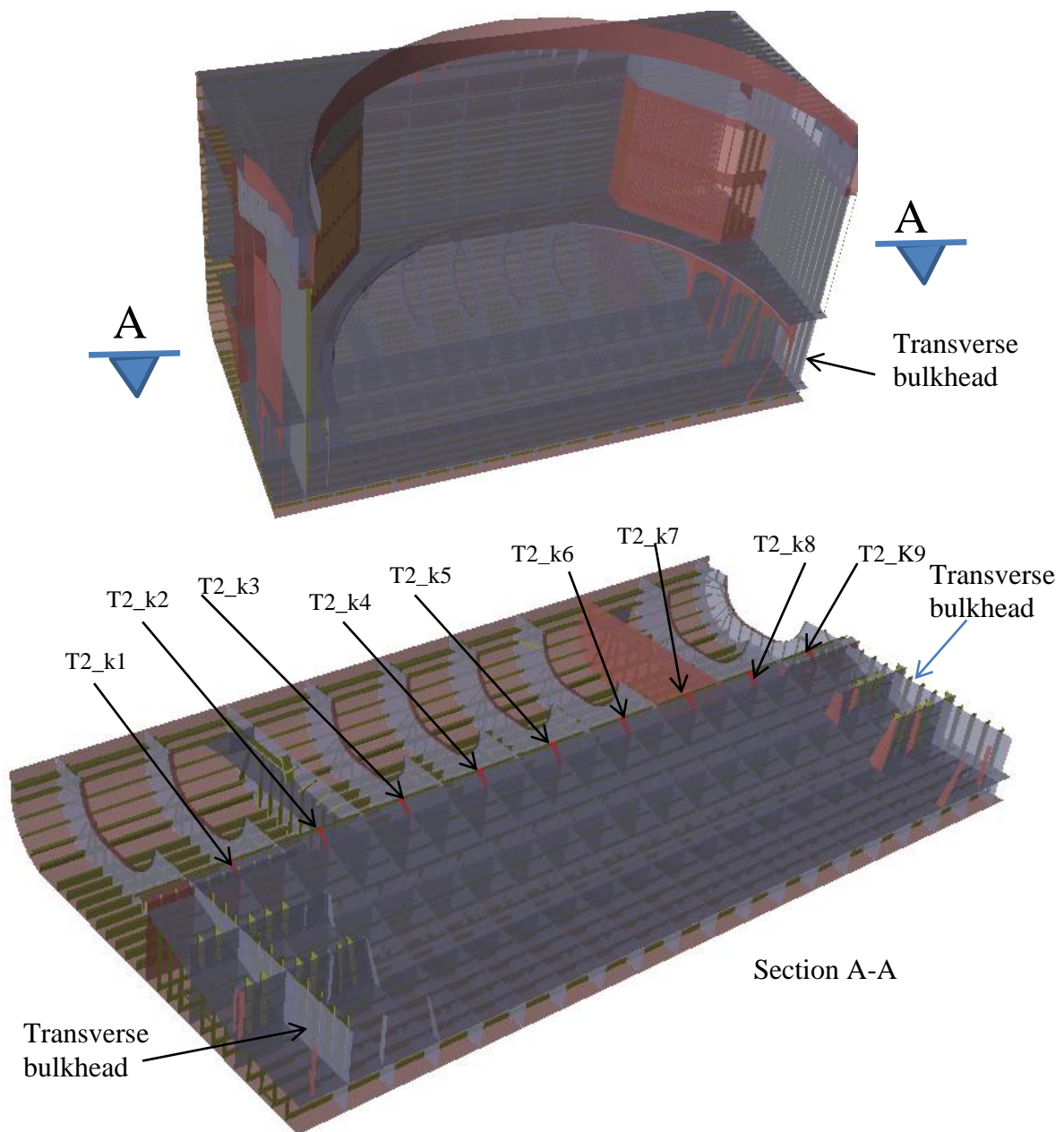


Figure 24. Locations of knuckle joints.

A portion of a global model corresponding to knuckle joint of the foundation deck is separated from the remaining part of the model, re-meshed and analyzed. The deformations from the global FE analysis are applied as boundary conditions on the borders of the sub model. The wave loads from the wave load analysis are also transferred to sub model. Typical global finite element model and sub model are shown in Figure 25. For sub model 8 node quadrilateral elements are used. The locations near the knuckle joints, mesh density of $t \times t$ is used, where t is the thickness of plate element.

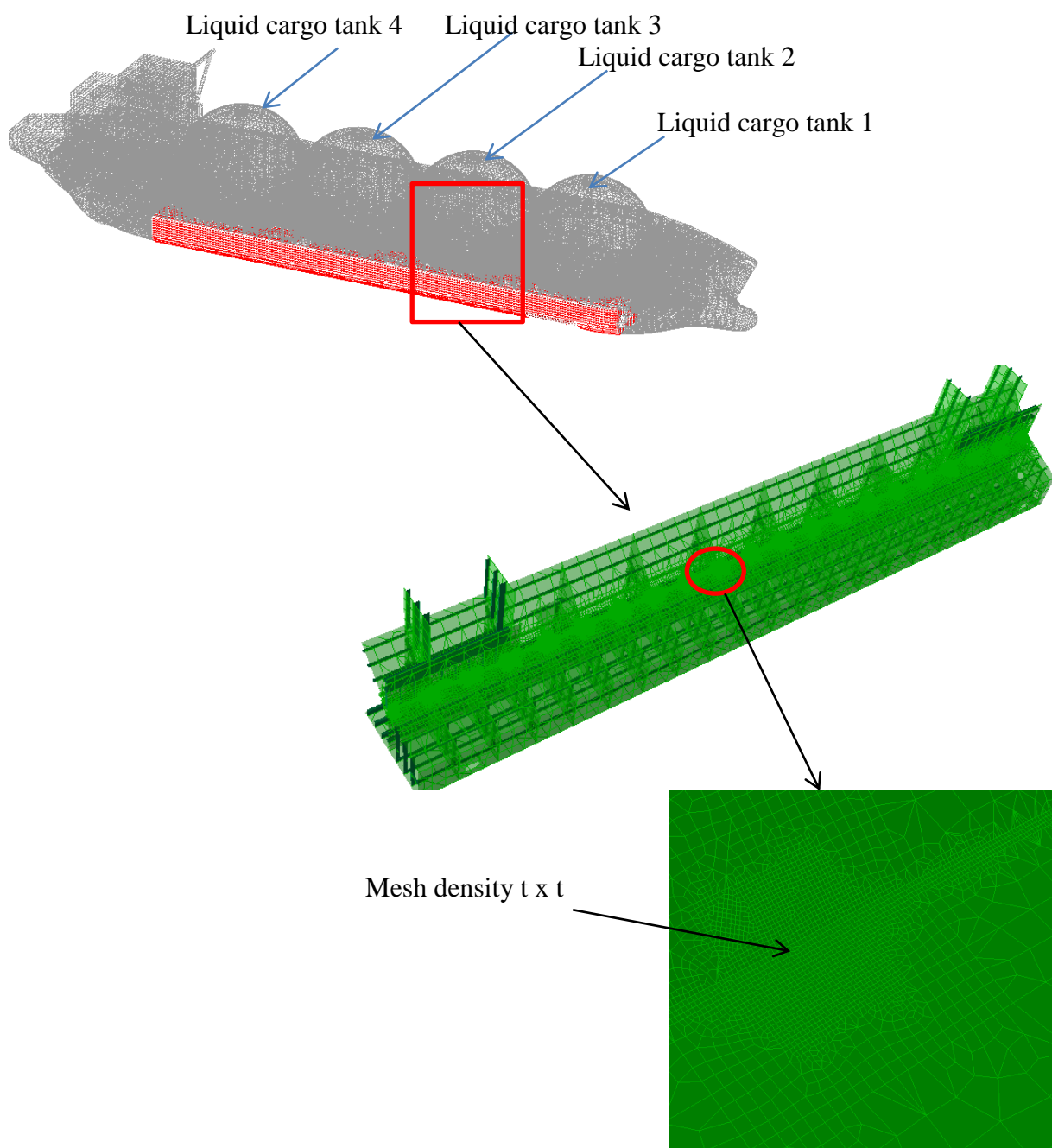


Figure 25. Sub model from the global FE model.

6. GLOBAL RESPONSE ANALYSIS

Hydrodynamic analysis of LNG carrier is carried out using the 3D potential theory program SESAM Hydro-D Wasim. A hydrodynamic analysis is carried out in the linear frequency domain for the full load and ballast condition. Wasim is a hydrodynamic analysis program for calculation of wave loading and wave induced responses of floating marine structures with forward speeds.

The hydrodynamic model of Moss type LNG carrier with spherical tanks is created in Hydro - D software as shown in Figure 26. To ensure transfer of wave load correctly to the structural FE model, the structural FE model used as a mass model.

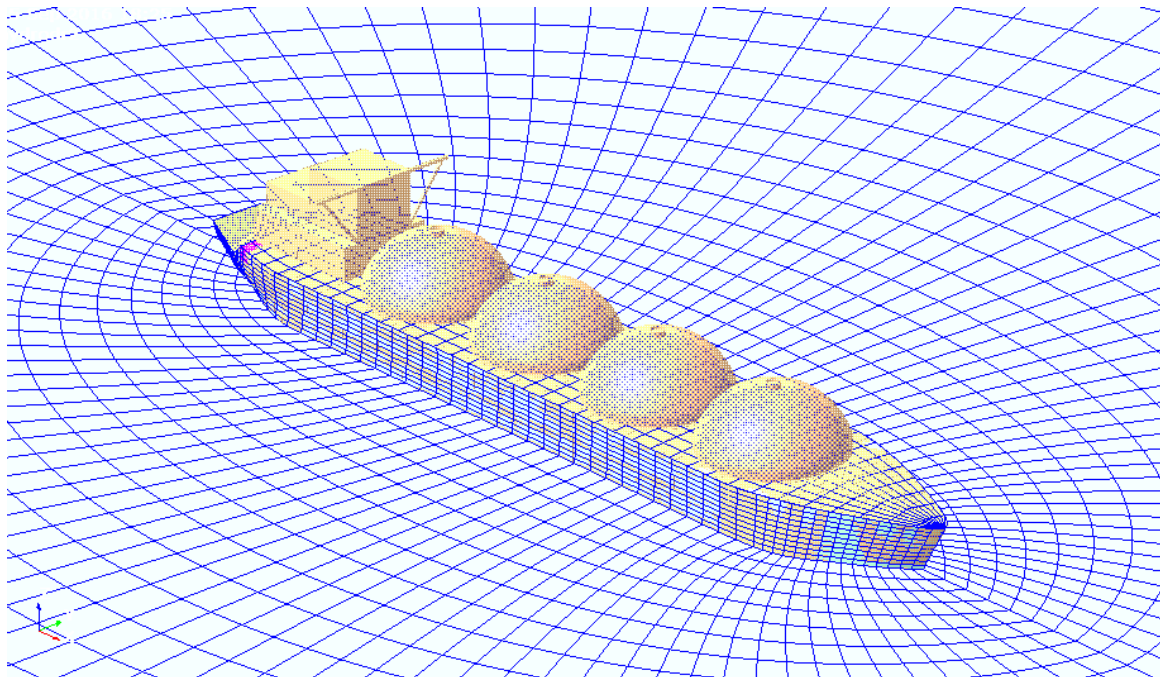


Figure 26. Hydrodynamic model.

6.1. Analysis Setup

For the hydrodynamic analysis, a coordinate system same as the global structural modelling discussed in Chapter 5 is adopted. To perform hydrodynamic analysis with 1m wave amplitude, wave periods from 5s to 30s with increments as shown in Table 3 and wave heading range from 0^0 to 360^0 with 30^0 increments are used. In the hydrodynamic analysis, the vessel's forward speed is assumed as $2/3$ of design speed i.e $2/3 \times 16$ knots equal to 5.49 m/s. The assumption of forward speed equal to $2/3$ of design speed approximates the average vessel speed over the entire lifetime of the vessel. The speed is assumed to be a constant.

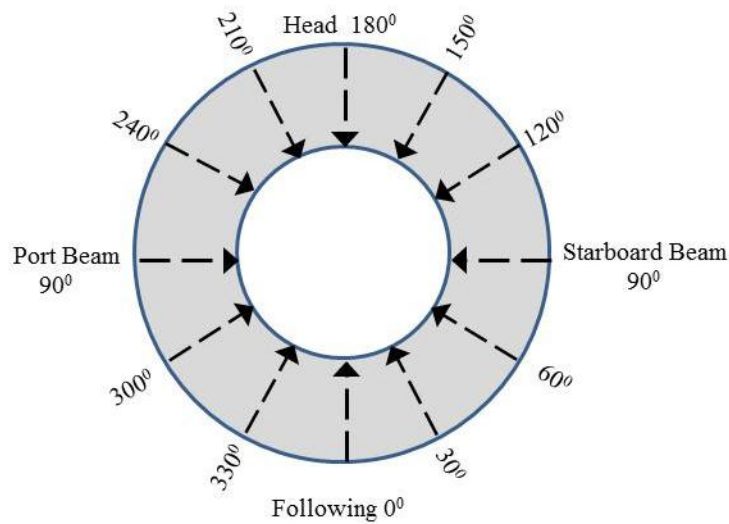


Figure 27. Wave heading direction for different load cases

Table 3. Wave periods.

Wave period (s)	5.0	5.25	5.5	5.75	6.0	6.25	6.5	6.75	7.0	7.5	8.0	9.0	10.0	11.0
	12.0	13.0	14.0	15.0	16.0	17.0	18.0	20.0	24.0	26.0	30.0			

6.1.1. Load cases

The LNG carrier experiences several different wave load cases, the most frequent load cases such as the full load condition and ballast condition are considered for the hydrodynamic wave load calculations. The tank arrangement and mass model properties of the hydrodynamic for the full load case with 11.9 m draught and ballast case with 6m draught are shown in Figure 28 to Figure 29 and Table 4 to Table 5.

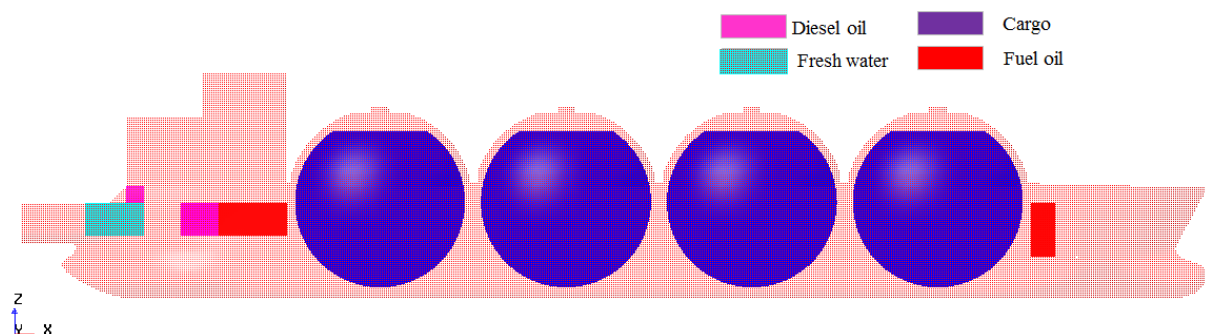


Figure 28. Tank arrangement for full load case- Longitudinal view

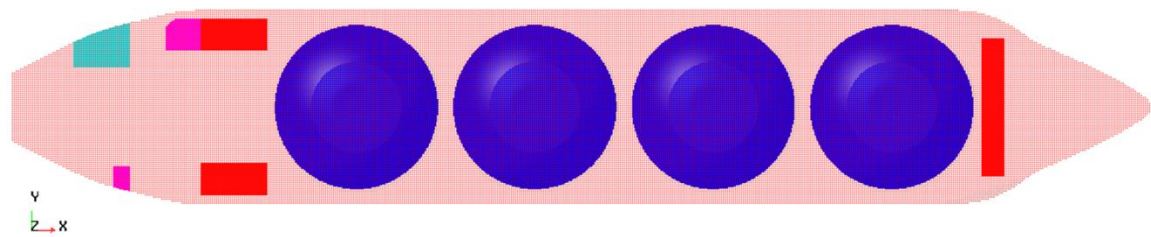


Figure 29. Tank arrangement for full load case- Plan view

Table 4. Mass Model – Full load case.

Property	Value	Units
Mass	1.088E+08	kg
Buoyancy Volume	1.362E+05	m ³
Centre of Buoyancy in coordinate (x,y,z)	(142.4,0,6.08)	m
Centre of Gravity in coordinate (x,y,z)	(149.7, 0.19, 21.27)	m
Radius of Gyration (x,y,z)	(11.49, 64.09, 64.31)	m

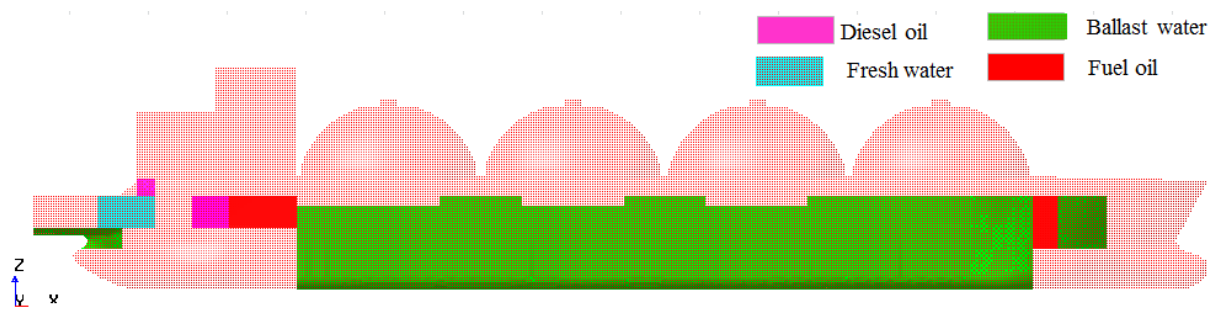


Figure 30. Tank arrangement for full ballast load case- Longitudinal view

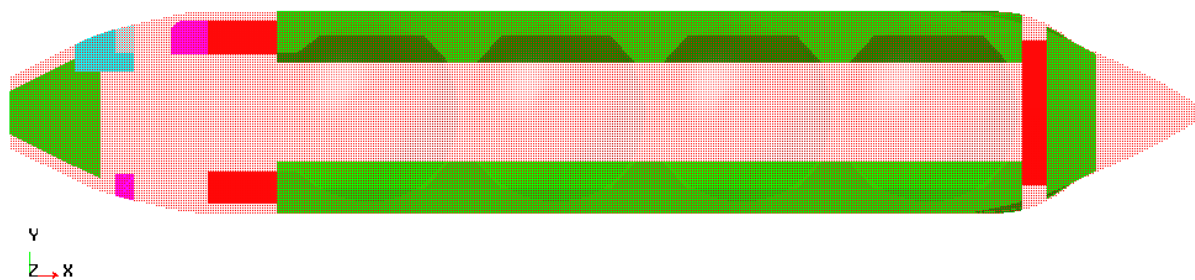


Figure 31. Tank arrangement for ballast load case- Plan view

Table 5. Mass Model – Ballast load case.

Property	Value	Units
Mass	1.015E+08	kg
Buoyancy Volume	6.3701E+04	m ³
Centre of Buoyancy in coordinate (x,y,z)	(143.5,0,3.09)	m
Centre of Gravity in coordinate (x,y,z)	(144.7, 0.433, 15.65)	m
Radius of Gyration (x,y,z)	(25.5, 92.19, 92.22)	m

6.2. Global Motion Responses

The results of the hydrodynamic analysis in the frequency domain are presented in the form of motion response of the vessel. The motion response of the vessel is expressed in terms of its Response Amplitude Operators (RAOs) for the 6 degrees of freedom. The translation motion Surge, Sway, Heave in x, y and z and rotational motion Roll, Pitch Yaw about x, y and z-direction, schematically shown in Figure 32.

For each wave frequency, the variations in motion responses are plotted in the form of the dimensional-less quantities. i.e. for translational motion in terms of (meters/meters) and rotational motion in terms of (deg-meters/meters).

The global motion responses of the vessel i.e. for translational motion and rotation motion are plotted for different wave headings and time period. Figure 33 and Figure 34 shows the global response motions for full load case and ballast load cases.

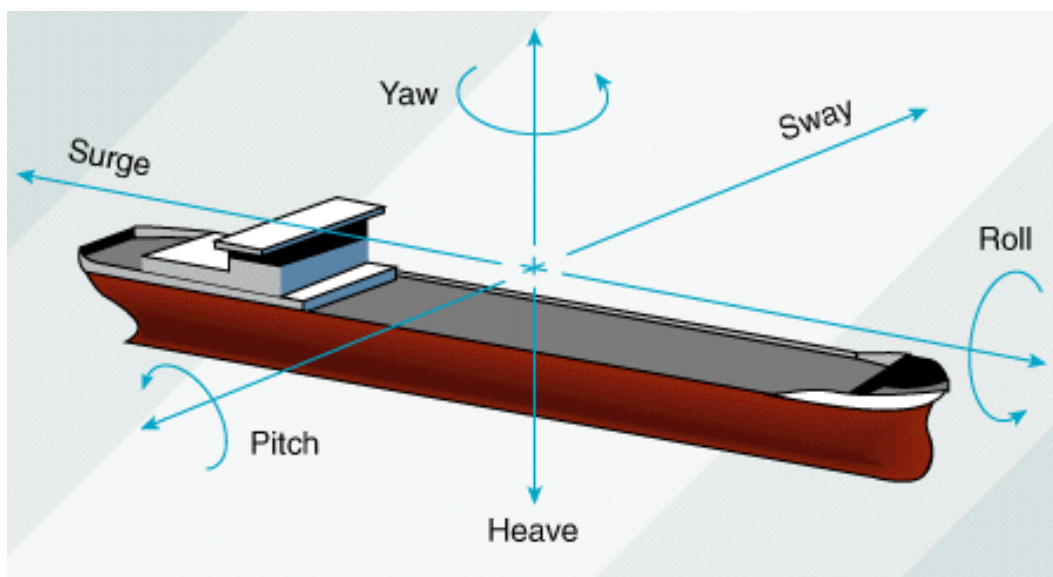


Figure 32. Wave heading direction for different load cases

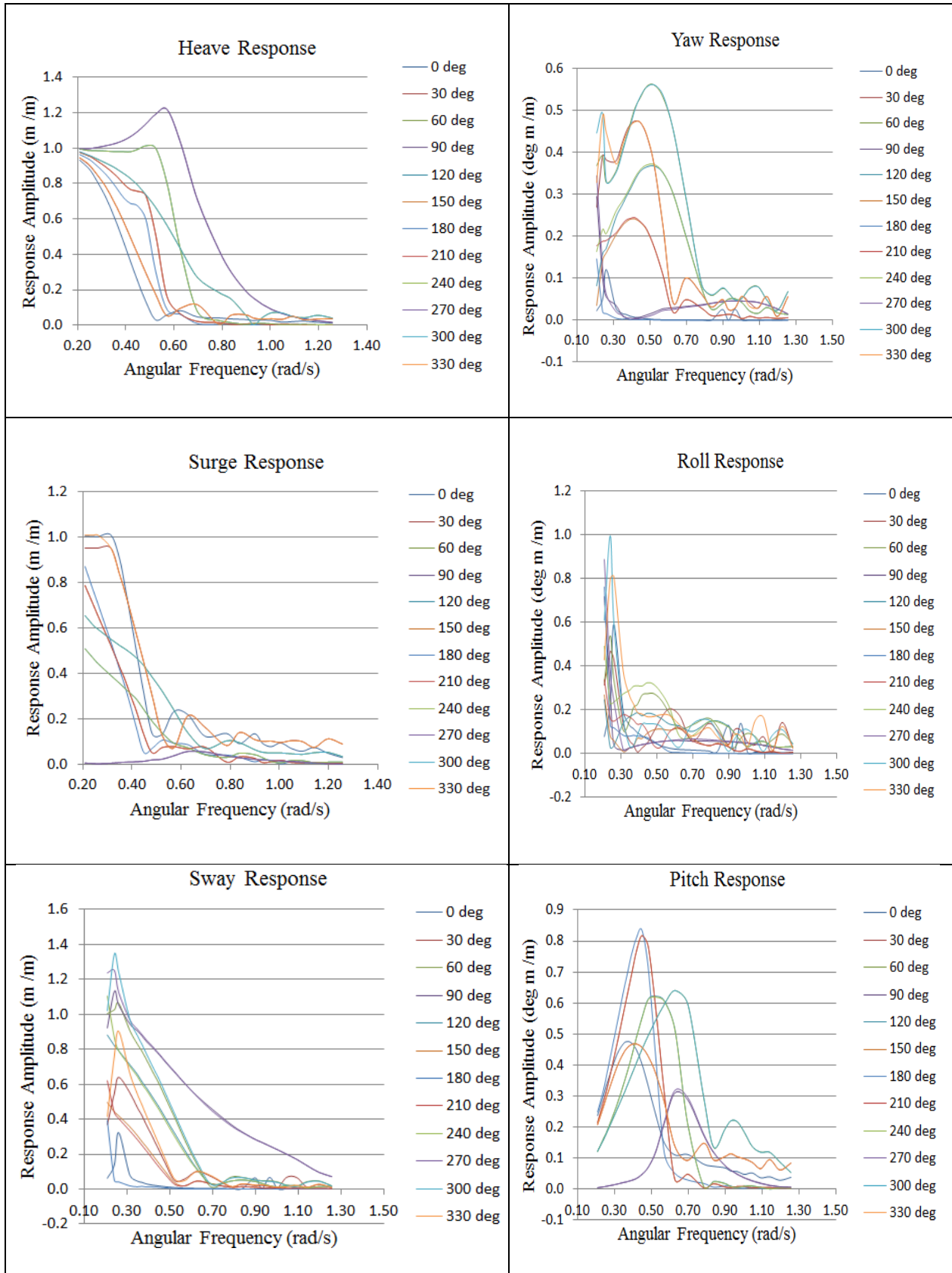


Figure 33. Global motions response –Full load case

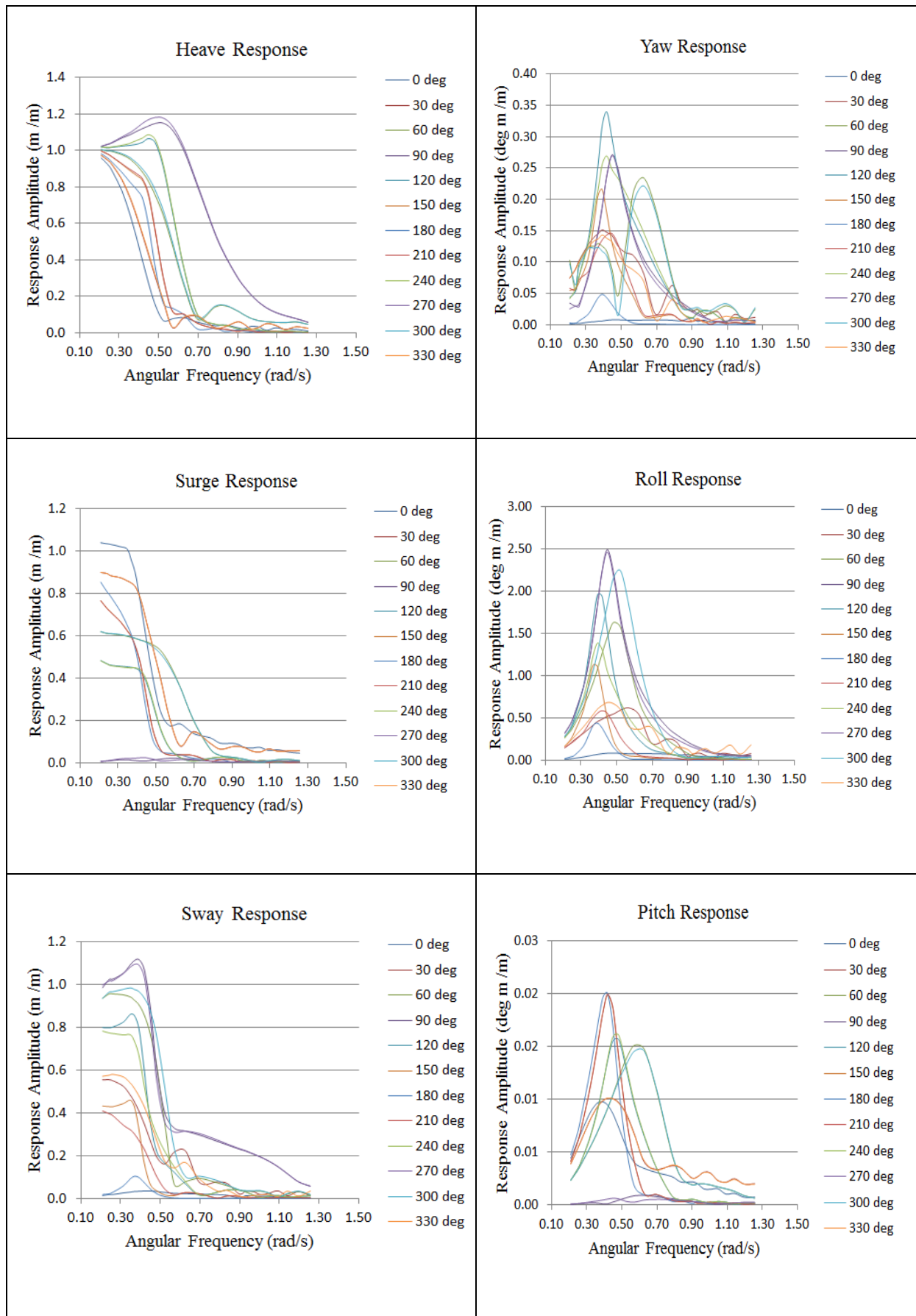


Figure 34. Global motions response – Ballast load case

7. GLOBAL STRUCTURAL ANALYSIS

To evaluate the fatigue damage, the linear structural analysis is performed by transferring hydrodynamic pressure loads obtained from the hydrodynamic analysis directly to the FE structural model. Figure 35 shows the hydrodynamic pressure on the hull for one of the wave direction. As mentioned in Chapter 5, the global structural FEA model of the ship is generated using the FE tool SESAM GeniE. The response of the structure due to wave loading is calculated by a linear FE-software, Sestra.

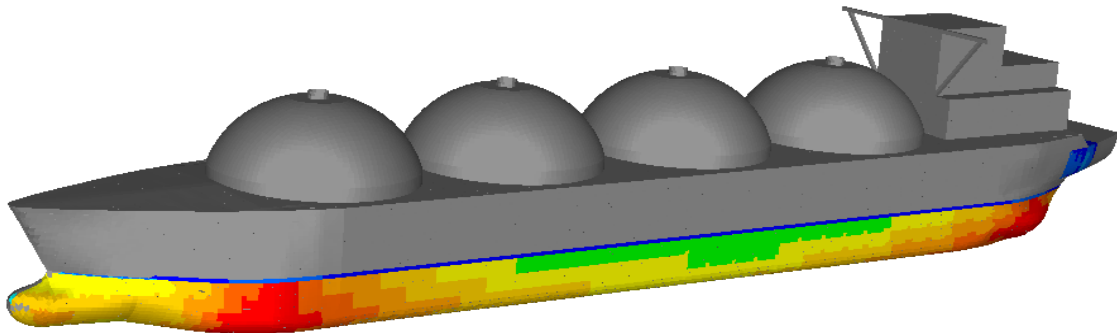


Figure 35. Wave load pressure on global model transferred from the hydrodynamic analysis.

7.1. Verification of load transfer

The inaccuracy in load transfer from hydrodynamics analysis to structural FE model is the main source of error in stochastic fatigue analysis. In order to check the accuracy of load transfer, the global structural response is compared between hydrodynamic model and structural model.

A global structural response such as moment and shear force from the structural analysis is compared with the results from the hydrodynamic analysis. Cutres software is employed to compute the bending moment and shear forces from structural analysis result. Structural responses from the hydrodynamic analysis are extracted from Hydro-D software.

20 sections are considered in order to establish a proper description of the bending moment and shear force distribution along the hull. Figure 36 and Figure 37 shows the comparison of global vertical bending moment and shear force between hydrodynamic analysis and structural analysis with the loads transferred from the hydrodynamic analysis.

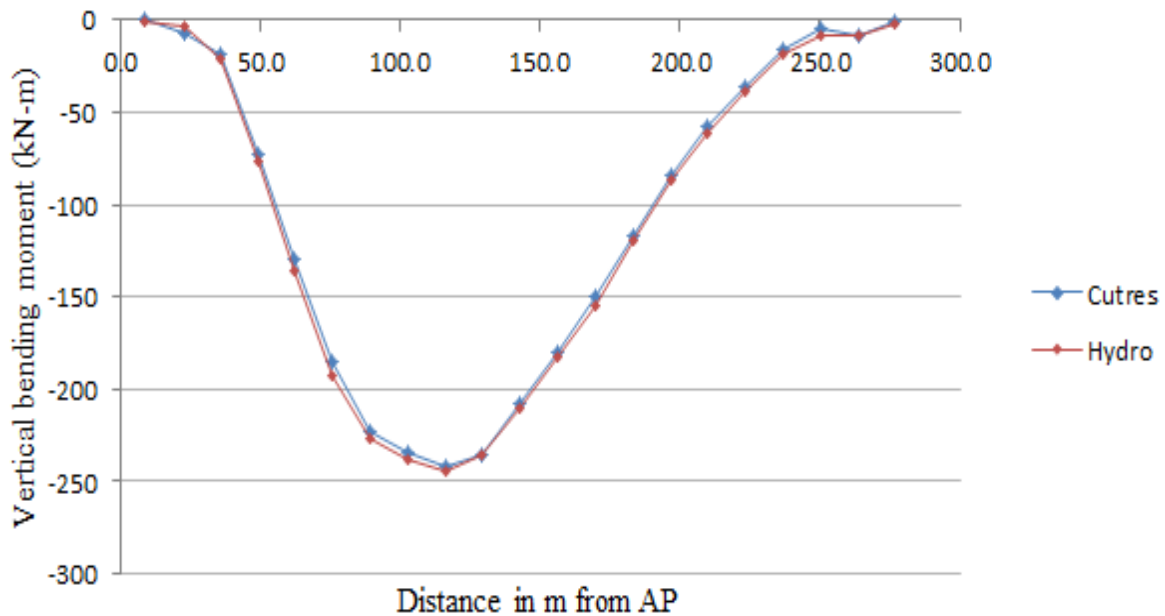


Figure 36. Vertical Bending Moment – 1m wave amplitude for a 90⁰ heading wave with period 24s.

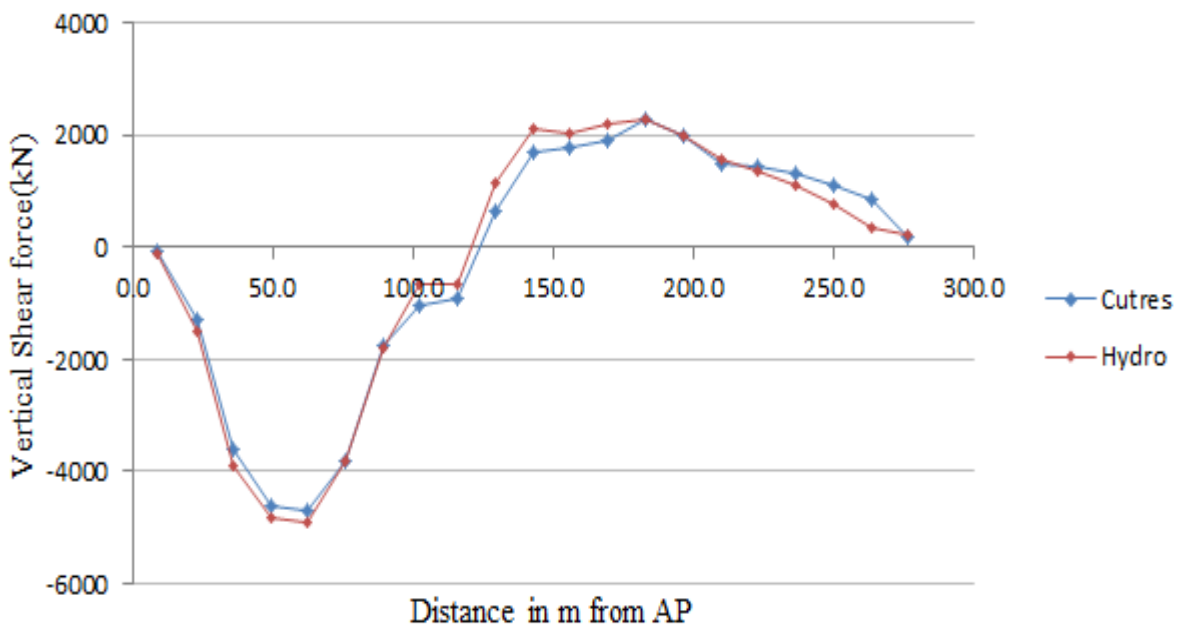


Figure 37. Vertical Shear Force – 1m wave amplitude for a 90⁰ heading wave with period 24s.

As mentioned in section 5.3, the structural model is supported at water line level at the aft and fore end. The reactions at these ends are close to zero values. As can be seen from the above Figure 36 and Figure 37, the bending moment and shear forces are in the acceptable range tending to zero.

7.2. Stress Transfer function

Maximum principal stress range is the basis for the fatigue damage calculation. Lower hopper knuckle joints with locations as described in section 5.4.2, exhibits maximum principal stress in ballast load case. Figure 38 shows the plot of maximum principal stress for the foundation deck including knuckle joints. Among the 9 knuckle joints, knuckle joint T2_k8 experiences a maximum principal stress of 42MPa. The principal stress transfer function for various wave frequencies are shown in Figure 39.

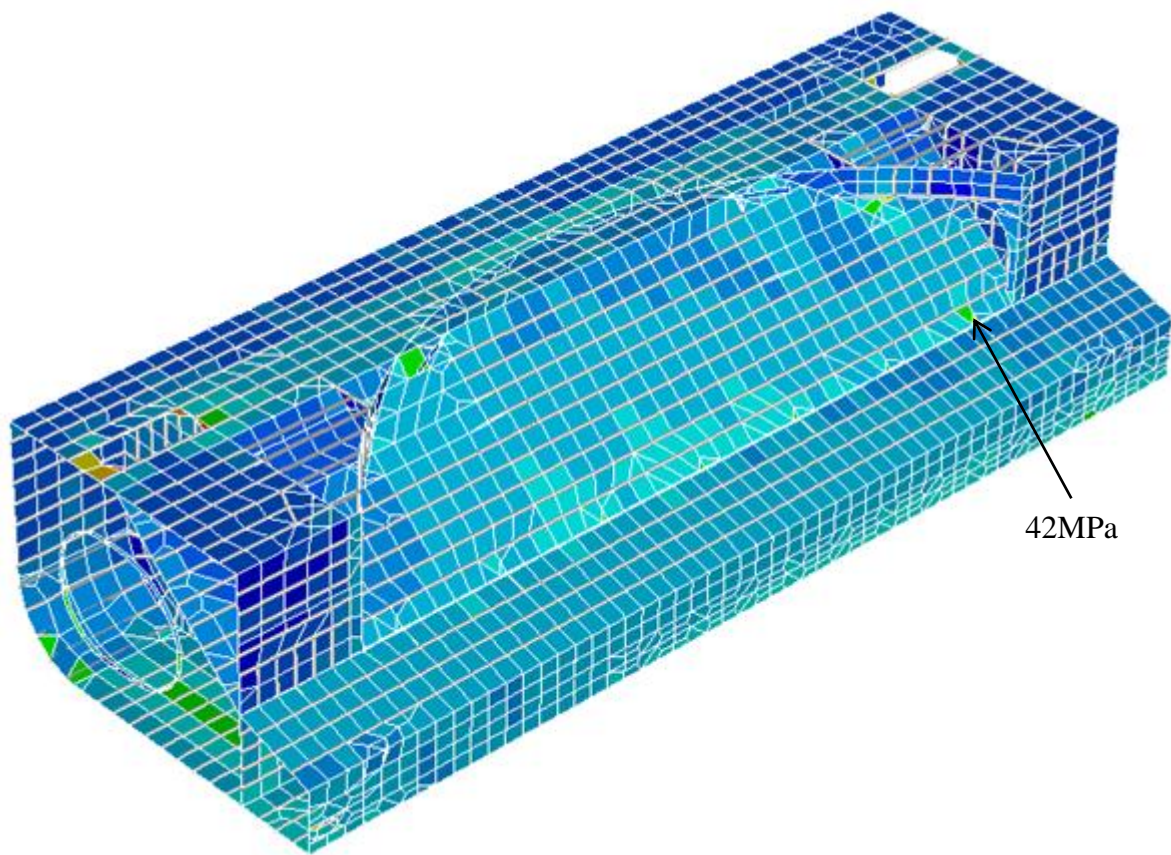


Figure 38. Maximum Principal stress-Ballast Load case

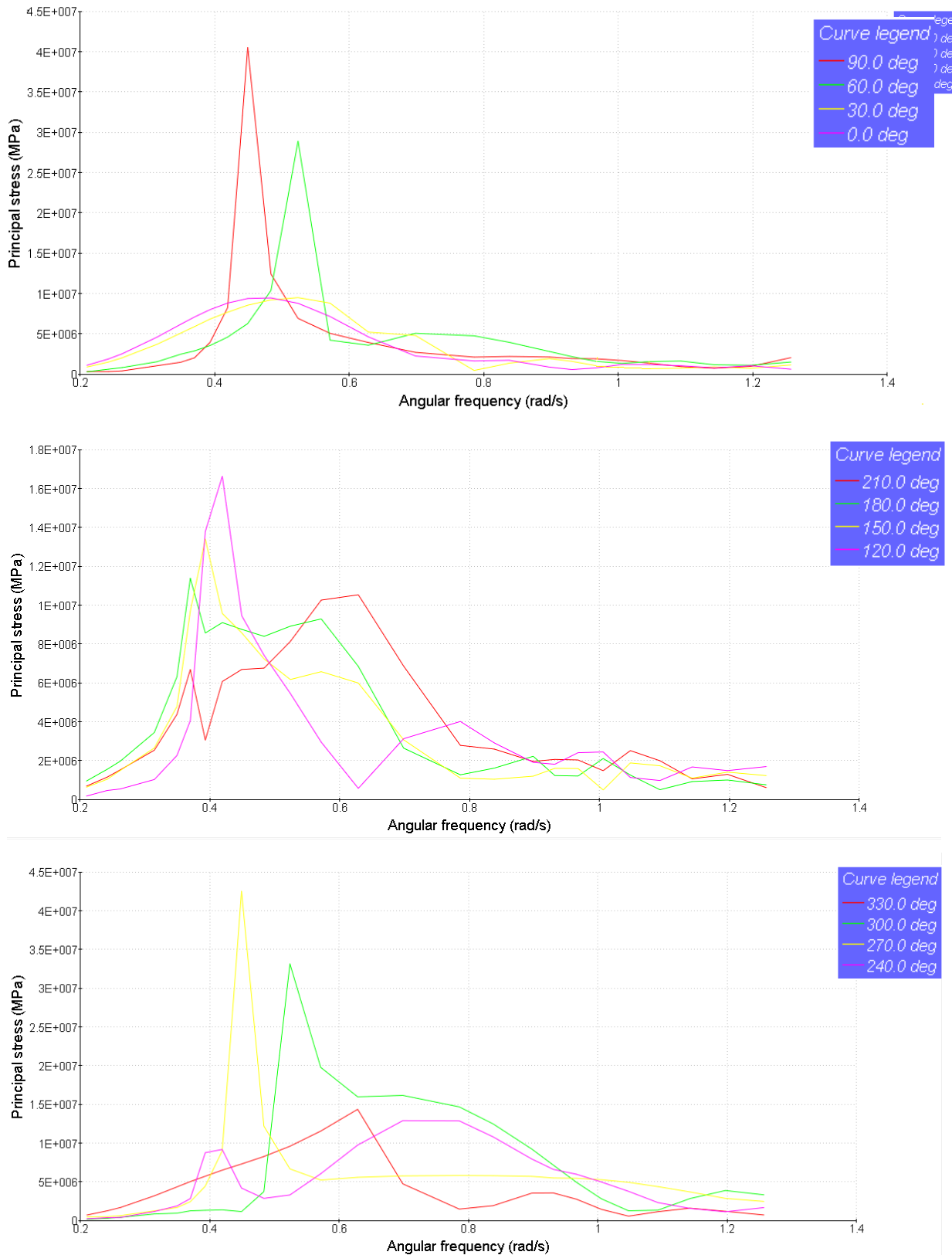


Figure 39. Principal Stress Transfer Function.-Ballast Load case

8. FATIGUE ANALYSIS

LNG carrier is considered as a kind of complex ship with advanced technology and usually designed for a life of 40 years. Stofat programme is used to perform spectral fatigue damage. As explained in the section 3.3.3, the spectral based fatigue calculation requires wave statistics, S-N curve, stress concentration factors and stresses from the structural analysis as input data.

Short term wave statistics are defined by a wave spectrum and short term wave direction distributions are defined by wave spreading. A Pierson-Moskowitz wave spectrum with cosine power 2 as a wave spreading function is used to represent short crested sea state. Figure 40 shows the wave energy spreading function with cosine exponent 2.

To ensure the structural integrity throughout the design life, maximum wave loads to be considered in the design. Probabilistic nature of the sea state over long term variability is represented by scatter diagram. The long-term probability of storm exceeding certain sea state is determined from scatter diagram. For the fatigue calculations presented in this thesis, the vessel is assumed to be trading in North Atlantic wave climate. Long-term wave statistics data in the North Atlantic Ocean is shown in Table 7 [15]. Furthermore, equal probability 8.33 % for all 12 direction headings is considered for fatigue evaluation.

The vessel is considered to be in operation for 85 per cent of its total design life [13]. Vessel fraction of time in full load and ballast load condition is taken as 50 percent of ship operation time [13]. The S-N i.e. Stress life curves approach is used in fatigue life damage calculation. In the current work, S-N curves are by ABS and DNV classification societies used in the calculation. For fatigue damage comparison, DNVC -I, DNVC-III, ABS C and ABS E are used. These curves are generally used to assess the fatigue damage of knuckle joints. S-N parameters for these curves [15],[8] are tabulated in Table 6 and S-N curves from DNV and ABS classification societies are presented in Figure 41 and Figure 42.

Table 6. S-N Curve Parameters.

SN-Curve	$N < 10^7$		$N > 10^7$	
	$\log \bar{a}$	m	$\log \bar{a}$	m
DNVC-I	12.164	3	15.606	5
DNVC-III	15.117	4	17.146	5
ABS C	13.626	3.5	17.412	5.5
ABS E	12.015	3	15.362	5

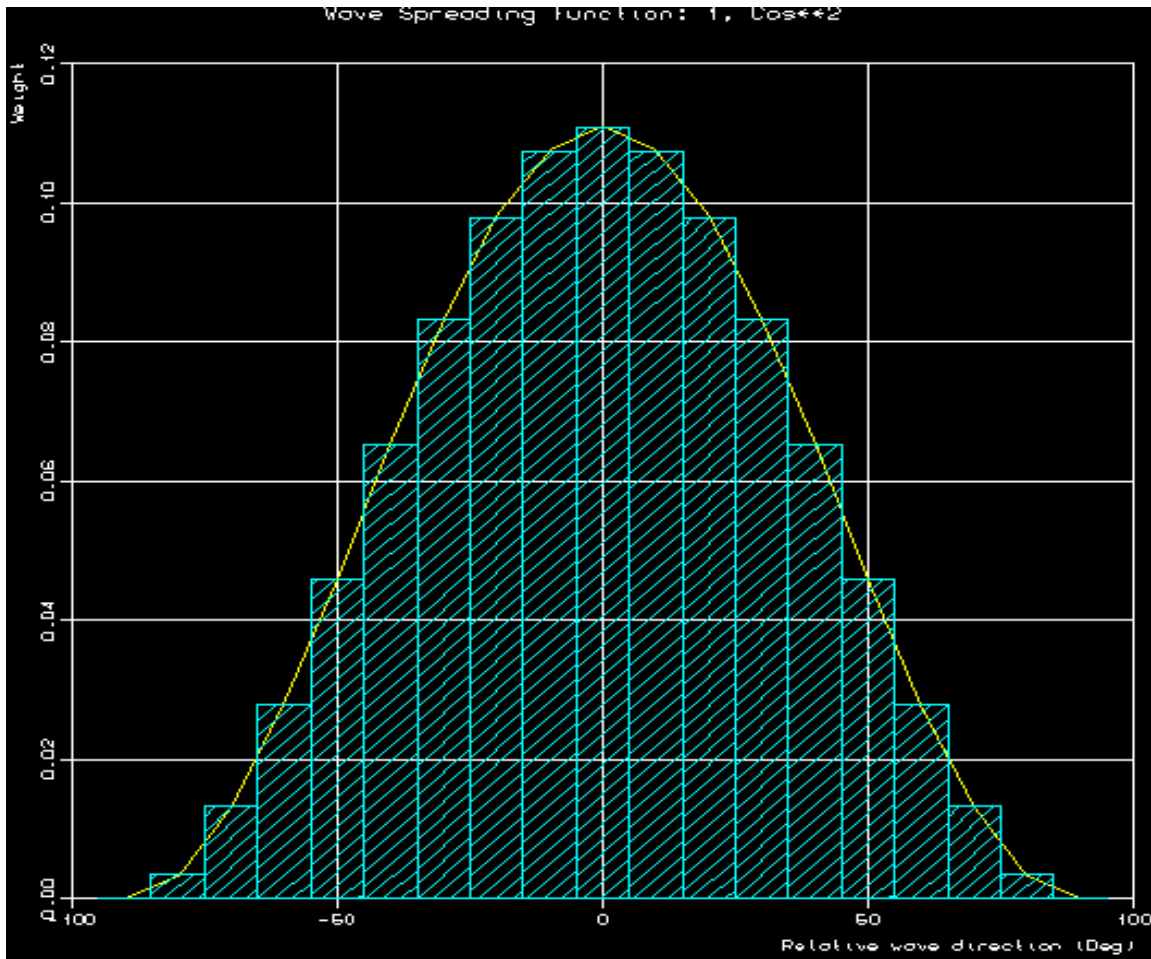


Figure 40. Wave spreading function for cosine power 2.

Table 7. Wave Scatter Data - North Atlantic.

Tz(s)	3.5	4.5	5.5	6.5	7.5	8.5	9.5	10.5	11.5	12.5	13.5	14.5	15.5	16.5	17.5	18.5	Sum
Hs (m)																	
0.5	1.3	133.7	865.6	1 186.0	634.2	186.3	36.9	5.6	0.7	0.1	0	0	0	0	0	0	3 050
1.5	0	29.3	986.0	4 976.0	7 738.0	5 569.7	2 375.7	703.5	160.7	30.5	5.1	0.8	0.1	0	0	0	22 575
2.5	0	2.2	197.5	2 158.8	6 230.0	7 449.5	4 860.4	2 066.0	644.5	160.2	33.7	6.3	1.1	0.2	0	0	23 810
3.5	0	0.2	34.9	695.5	3 226.5	5 675.0	5 099.1	2 838.0	1 114.4	337.7	84.3	18.2	3.5	0.6	0.1	0	19 128
4.5	0	0	6.0	196.1	1 354.3	3 288.5	3 857.5	2 685.5	1 275.2	455.1	130.9	31.9	6.9	1.3	0.2	0	13 289
5.5	0	0	1.0	51.0	498.4	1 602.9	2 372.7	2 008.3	1 126.0	463.6	150.9	41.0	9.7	2.1	0.4	0.1	8 328
6.5	0	0	0.2	12.6	167.0	690.3	1 257.9	1 268.6	825.9	386.8	140.8	42.2	10.9	2.5	0.5	0.1	4 806
7.5	0	0	0	3.0	52.1	270.1	594.4	703.2	524.9	276.7	111.7	36.7	10.2	2.5	0.6	0.1	2 586
8.5	0	0	0	0.7	15.4	97.9	255.9	350.6	296.9	174.6	77.6	27.7	8.4	2.2	0.5	0.1	1 309
9.5	0	0	0	0.2	4.3	33.2	101.9	159.9	152.2	99.2	48.3	18.7	6.1	1.7	0.4	0.1	626
10.5	0	0	0	0	1.2	10.7	37.9	67.5	71.7	51.5	27.3	11.4	4.0	1.2	0.3	0.1	285
11.5	0	0	0	0	0.3	3.3	13.3	26.6	31.4	24.7	14.2	6.4	2.4	0.7	0.2	0.1	124
12.5	0	0	0	0	0.1	1.0	4.4	9.9	12.8	11.0	6.8	3.3	1.3	0.4	0.1	0	51
13.5	0	0	0	0	0	0.3	1.4	3.5	5.0	4.6	3.1	1.6	0.7	0.2	0.1	0	21
14.5	0	0	0	0	0	0.1	0.4	1.2	1.8	1.8	1.3	0.7	0.3	0.1	0	0	8
15.5	0	0	0	0	0	0	0.1	0.4	0.6	0.7	0.5	0.3	0.1	0.1	0	0	3
16.5	0	0	0	0	0	0	0	0.1	0.2	0.2	0.2	0.1	0.1	0	0	0	1
Sum	1	165	2 091	9 280	19 922	24 879	20 870	12 898	6 245	2 479	837	247	66	16	3	1	100 000

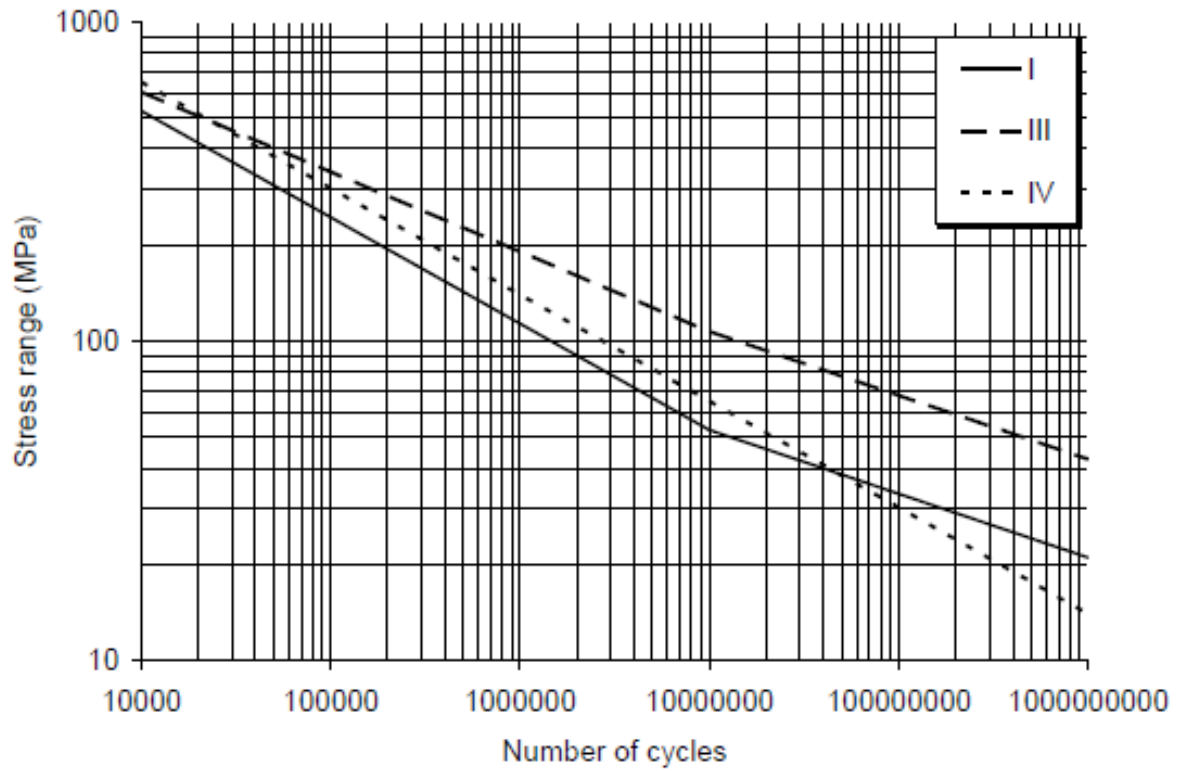


Figure 41. DNV-CN-30.7 2010 S-N curves [15].

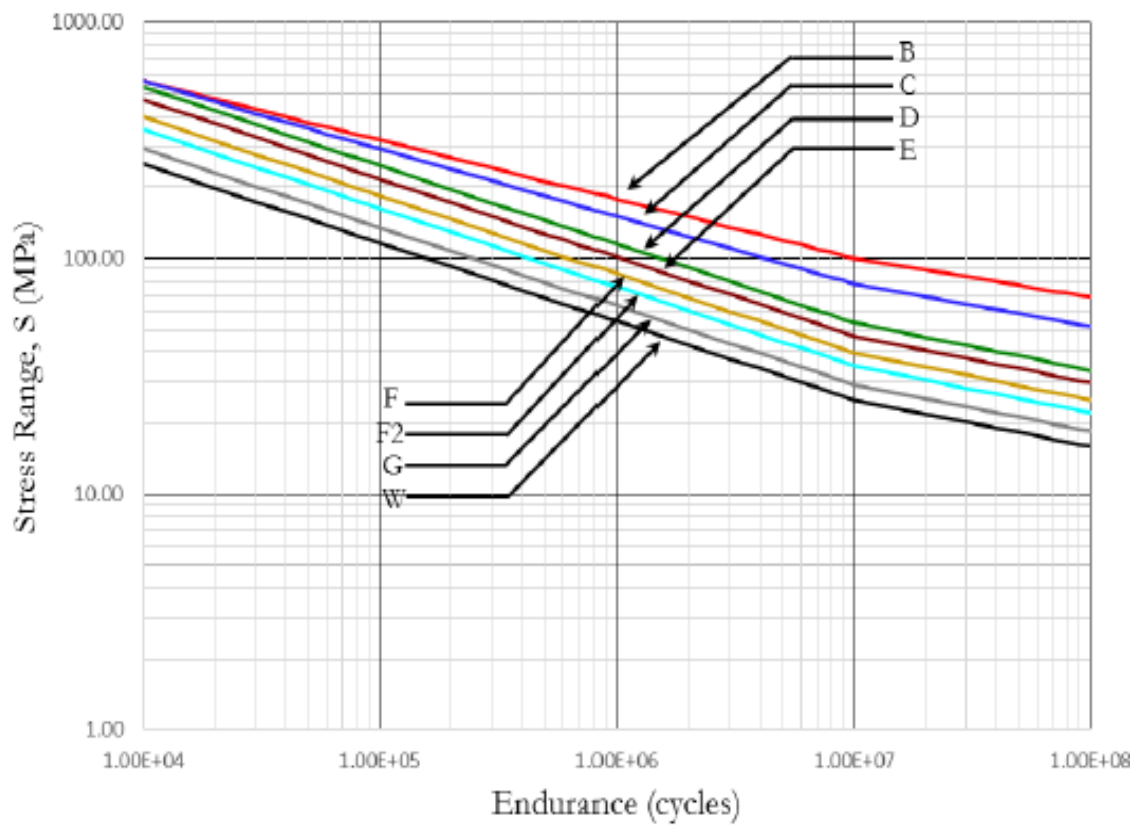
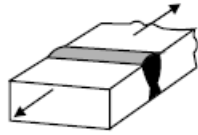
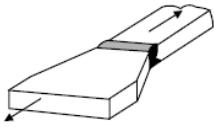
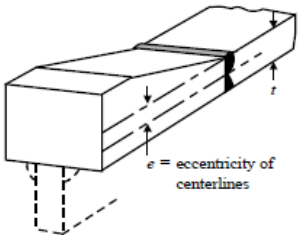


Figure 42. ABS S-N curves [8].

The S-N curve dictates the allowable stress limit based on the type of the weld and weld quality. Table 8 describe the stress limit and requirements for each type of S-N curve [9],[10], [12].

Table 8. Structural detail classification

SN-Curve	Requirements	Stress limit at 10^7 cycles (MPa)	Construction detail
DNVC-III	Rolled plates	106.97	-----
DNVC-I	<p>Welds made in flat position in shop.</p> <p>Weld run-off pieces to be used and subsequently removed.</p> <p>Plate edges to be ground flush in direction of stress.</p>	52.63	
ABS C	<p>With the weld overfill dressed flush with the surface and with the weld proved free from significant defects by non-destructive examination.</p> <p>The significance of defects should be determined with the aid of specialist advice and/or by the use of fracture mechanics analysis. The NDT technique must be selected with a view to ensuring the detection of such significant defects.</p>	78.16	 
ABS E	The corners of the cross-section of the stressed element at the weld toes should be dressed to a smooth profile.	47	

For the fatigue damage calculation, DNV GL rule specifies the 10^{-2} as the load probability level of exceedance whereas ABS rule recommends 10^{-4} as the load probability level of exceedance.

For a quick assessment of fatigue damage variation among the 9 knuckle joints as shown in section 5.4.2, element fatigue check option in Stofat is used. The geometric and eccentric stress concentration factor is taken as 1.0 in the calculation whereas weld stress concentration factor is assumed as 1.5. Damage is calculated for the ballast load and full load cases. The summary of calculation is attached in Appendix A. Results of total damage based on element fatigue check for various knuckle joints are compiled in Table 9.

Table 9. Total Fatigue Damage at knuckle joints for various S-N Curve.

Knuckle joint	Distance in m from AFT Perpendicular	DNVC-I	DNVC-III	ABS-C	ABS-E
T2_k1	193.96	0.004	0.002	0.002	0.043
T2_k2	188.92	0.014	0.006	0.009	0.129
T2_k3	183.88	0.031	0.013	0.022	0.268
T2_k4	178.84	0.043	0.018	0.031	0.362
T2_k5	173.8	0.048	0.020	0.036	0.397
T2_k6	168.76	0.047	0.020	0.035	0.391
T2_k7	163.72	0.065	0.028	0.050	0.514
T2_k8	158.68	0.087	0.037	0.068	0.678
T2_k9	153.64	0.024	0.010	0.016	0.225

Ballast load case is the governing load case and it contributes around 80 to 90 percent to the total damage. As illustrated in Figure 18, Figure 19 and Figure 24, the load transfer points i.e skirt foundation of liquid cargo tank situated away from the knuckle joints and majority of the liquid cargo is transferred to the upper knuckle joints.

The comparison of total fatigue for the various S-N curve is presented in Figure 43. As can be seen from the Figure 43, among the 9 knuckle joints, knuckle joint T2_k8 undergoes maximum damage. It should be noted that the fatigue damage is very sensitive to the fatigue stress range and fatigue damage is proportional to the inverse slope of the S-N curve.

Among the 4 S-N curves, S-N curve ABS- E yields a maximum damage of 0.68 due to a lower limit on the allowable stress on the weld whereas joint with DNVC-I curve exhibits better performance in fatigue damage due to increased allowable stress limit. Fatigue life of bent knuckle plate which is represented by DNVC-I S-N curve is 7 times higher than welded knuckle joint confirming to ABS-E curve.

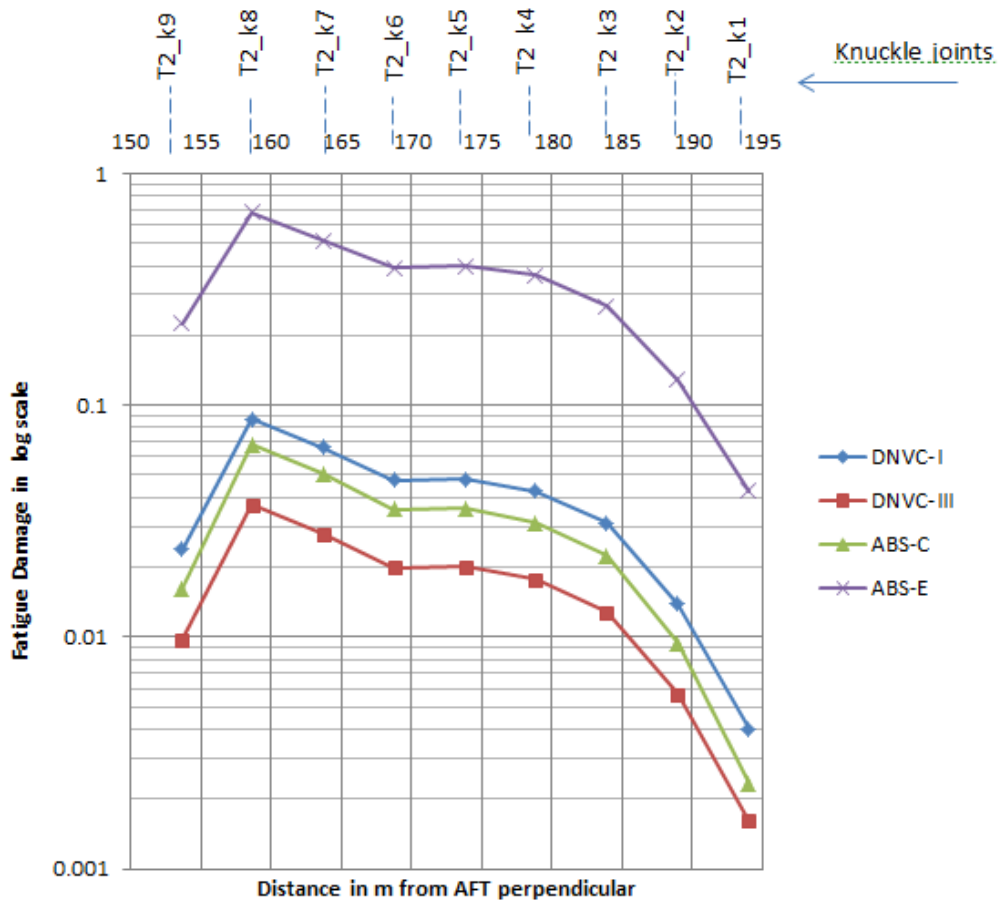


Figure 43. Fatigue damage at different position of knuckle joints around tank2.

For the knuckle joint T2_k8 which experiences maximum damage, hot spot fatigue is calculated for different S-N curves.

Hot-spot stresses are calculated with no fabrication-related misalignment and welds are not considered in the FE model. For each full load and ballast loading condition, principal stresses at 0.5 t and 1.5 t from hot spot are read out and linearly extrapolated to the intersection line to obtain a hot spot.

The fatigue damages are calculated for 5 elements in the hotspot region corresponding knuckle joint T2_k8. These elements are shown in Figure 44. The hotspot values for ballast and full load cases are computed and the summary of damages for each load cases are presented in appendix B. The total damage based on hotspot are presented in Table 10.

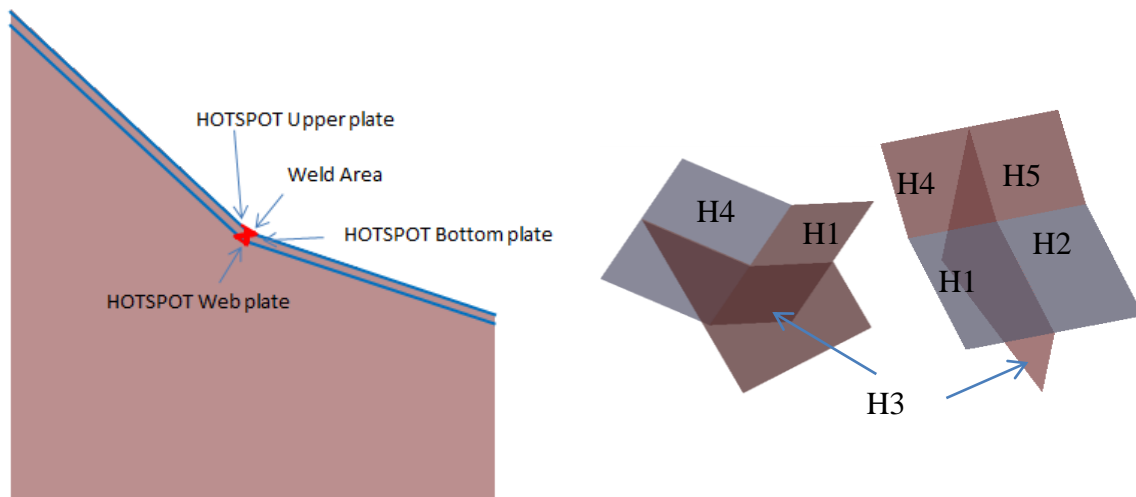


Figure 44. Hotspot of Hopper knuckle joint.

Table 10. Fatigue Damage for various S-N Curve.

S-N Curve	H1	H2	H3	H4	H5
DNVC-I	0.0826	0.0377	0.0317	0.0651	0.0456
DNVC-III	0.0352	0.0156	0.0131	0.0274	0.0190
ABS-C	0.0640	0.0271	0.0229	0.0490	0.0336
ABS-E	0.6435	0.3271	0.2731	0.5299	0.3804

Figure 45 shows the fatigue damage ratio distribution of each wave heading. The plot provides directional influence information of wave headings on the damage. The damage is based on fatigue analysis with equal probability for all wave directions.

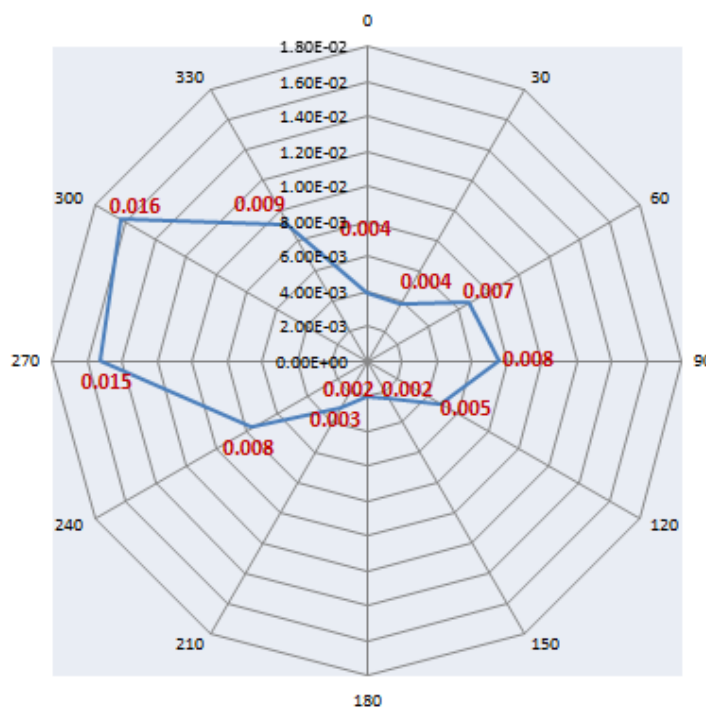


Figure 45. Polar Plot of Total Fatigue Damage.

As can be seen from the polar plot, the majority of the total damage is scattered between 240° to 330° wave headings which correspond to 50% of the total damage. The wave heading 270° and 300° contribute around 20% each to the total damage.

The results of the hot spot calculation by Stofat are presented in Appendix C present the elements with the maximum usage factors for different wave directions and the calculated fatigue life for these elements.

9. CONCLUSIONS AND RECOMMENDATIONS

North Atlantic Ocean is known for its harsh environment and the vessels operating in this region requires strict design requirement in order to have good fatigue strength. Hopper knuckle joints are the most critical joints susceptibility to fatigue failure due to high stress concentration. Due to cargo containment system, the area is inaccessible for inspection and repair. Knuckle joints exposed to a more complex stress response, full stochastic fatigue calculations based on using direct wave load analysis significantly increase the reliability of the results. The detailed computational procedures of a stochastic spectral approach for calculating fatigue damage ratios are illustrated in this thesis, and the method has been applied in predicting the fatigue life of hopper knuckle joint in a Moss type spherical tank LNG carrier.

A linear structural FE-analysis of the entire vessel is performed by transferring hydrodynamic loads directly onto the global model. Local or sub model with fine mesh for critical knuckle joint is analyzed with boundary displacements from global model and followed by a fatigue analysis using hotspot approach. The predicted fatigue damage ratio based on hot spot stress is compared using different S-N curves DNVC-I, DNVC-III, ABS-C and ABS-E. The following salient conclusions are drawn from the thesis work:

1. Influence of different wave directions related to stress transfer function from FE structural analysis is studied to find the most critical wave direction. This study reveals that the magnitude of the stress transfer function varies depending on the wave direction. For the hopper knuckle joints considered in this study, maximum stress transfer function occurs at 270^0 and the magnitude of maximum principal stress is around 42 MPa.
2. Furthermore, for the hopper knuckle joints studied in this thesis, ballast load case contributes around 85 to 90 % to the total fatigue damage. The contribution from full load case is around 10 to 15 % depending on the location of knuckle joints. This is due to the location load transfer points i.e., skirt foundation which transfer loads from liquid cargo to tank foundation is located away from the knuckle joints under study.
3. The majority of the total damage is scattered between 240^0 to 330^0 wave headings which correspond to 50% of the total damage. The wave heading 270^0 and 300^0 contribute around 20% each to the total damage.

4. Fatigue damage ratio comparison among different S-N curves shows joint with the S-N curve having highest allowable stress range exhibits better fatigue life i.e., low fatigue damage ratio. For the joints under current study, results reveal that the bent knuckle joint from rolled plate shows better fatigue life in comparison with welded joint. Fatigue life of bent knuckle plate is 7 times higher than welded knuckle joint confirming to ABS-E curve requirements.
5. The fatigue calculation involves variables such as S-N curve, wave scatter data, and wave spectrum. One of the design variable i.e., the S-N curve is used for the parametric study and the damage ratio result reflects the fatigue life which has a direct consequence on the weld preparation quality and inspection category. Higher weld quality and stringent inspection type results in increased fatigue life.

Due to the limited time, the fatigue damage study focused only on direct calculation method based on the linear FE analysis. However, the following points are recommended for the future work:

1. Though the fatigue damage assessment by stochastic spectral fatigue yields reliable results but involves time-consuming computational procedures. The equivalent design wave method may be used to assess the fatigue damage at the preliminary design stages. The comparison of damages against the spectral fatigue gives the factor of safety embedded in the equivalent design approach. However, the DNV GL classification society requires fatigue limit state on a critical area such as hopper knuckle joints should be assessed by directly calculated loads. The equivalent design wave approach at the preliminary design stage of the project can be used to identify the critical fatigue locations in the vessel.
2. Welds are ignored in the current fatigue analysis and the effect of the weld can be considered to account for tensile residual stresses from welding which will further decrease the fatigue life.
3. The variables involved in the fatigue design subjected to significant uncertainty and hence the resulting fatigue damage assessment is also associated with large uncertainties. The calculated loads on the vessel are uncertain due to the stochastic nature of the wave loads and uncertainties in the sailing route. Furthermore, uncertainties associated in FE

modelling, the evaluation of stress concentration, local weld geometry, initial imperfections will attribute to the uncertainties in the calculated fatigue life of a structural detail. A reliability-based fatigue assessment should be carried out directly through a stochastic modelling of these uncertain variables.

ACKNOWLEDGEMENTS

First of all, I would like to thank Prof. Philippe Rigo from University de Liege (ULg) as coordinator of the EMSHIP program and Prof. Maciej Taczala from West Pomeranian University of Technology Szczecin (ZUT), as local coordinators of EMSHIP program in Poland. I thank them for their technical guidance and help on academic and administrative issues. I would like also to mention that I would be grateful for the guidance and feedback from Prof Maciej Taczala from ZUT as my master thesis supervisor.

As this master thesis was partly developed in Westcon Design Poland office in Szczecin (Poland), I would like to pass on my sincere regards to Dr Jazukiewicz Alfred for furnishing technical details. I would also like to mention a word of gratitude for Dr. Lech Tamborski for his valuable advice on hydrodynamic analysis.

This thesis was developed in the frame of the European Master Course in “Integrated Advanced Ship Design” named “EMSHIP” for “European Education in Advanced Ship Design”, Ref.: 159652-1-2009-1-BE-ERA MUNDUS-EMMC.

REFERENCES

- [1] S. Valsgård, T. K. Østvold, O. Rognebakke, E. Byklum, and H. O. Sele, 2006. Gas carrier development for an expanding market. ICSOT 2006: Design, Construction & Operation of Natural Gas Carriers & Offshore Systems, Korea.
- [2] Central Commission for the Navigation of the Rhine and Oil Companies International Marine Forum, 2010. International Safety Guide for Inland Navigation Tank-barges and Terminals. Strasbourg Cedex: Central Commission for the Navigation of the Rhine.
- [3] A. Almar Naes, 1985. Fatigue Handbook: offshore steel structures. Trondheim, Norway: Tapir Publishers.
- [4] N.E. Dowling, 2007. Mechanical Behaviour of Materials. Third edition, Pearson: Prentice Hall.
- [5] [Dr. Dominique Beghin](#), 2006. Fatigue of Ship structural details. SNAME Technical and research bulletin 2-31.
- [6] DNVGL-Rules for classification: Ships, 2016. Part5 Ship types, Chapter 7 Liquefied gas tankers
- [7] DNVGL-CG-0127, 2016. Class guideline- Finite element analysis
- [8] ABS,2016. Guide for spectral-based fatigue analysis for vessels.
- [9] ABS,2016. Rules for Building and classification-Steel vessels, Part 5C Specific Vessel Types
- [10] ABS,2014. Guide for Fatigue Assessment of Offshore Structures
- [11] DNVGL-CG-0129, 2015 . Class guideline- Fatigue assessment of ship structures.
- [12] DNVGL-RP-0005,2014. Recommended practice, Fatigue design of offshore steel structures.
- [13] DNVGL- Rules for classification, 2016. Part 3 Hull, Chapter 9 Fatigue.
- [14] DNV Classification Notes - No. 34.1, 2013. CSA - Direct Analysis of Ship Structures
- [15] DNV Classification Notes - No. 30.7, 2014. Fatigue Assessment of Ship Structures
- [16] DNV 2014. SESAM User Manual Genie: Concept design and analysis of offshore structures. Version 6.9.
- [17] DNV 2013. SESAM User Manual Sestra: Superelement Structure Analysis. Version 8.3.
- [18] DNV GL SESAM Hydro-D user manual Wasim: Wave Loads on vessels with Forward Speed. Version 5.3.
- [19] DNV 2011.V SESAM Xtract user manual: Postprocessor for Presentation, Animation and Reporting of Results. Version 3.0.

- [20] DNV GL 2016.SESAM Submod user manual: Transfer Displacements from Global Model to Sub-Model. Version 3.0.
- [21] DNV 1994. SESAM Cutres user manual: Presentation of Sectional Results, Version 1.2.
- [22] DNV GL 2016.SESAM Stofat user manual: Fatigue Damage Calculation of Welded Plates and Shells. Version 3.7-05.
- [23] <http://shipmind.net/gas-carriers-> Pictures for tank types

APPENDICES

Appendix A: Summary of Element Fatigue damage Calculation

Table 11. Fatigue Damage at knuckle joints for various S-N Curve –Ballast Load case.

Knuckle joint	Distance in m from AFT Perpendicular	DNVC-I	DNVC-III	ABS-C	ABS-E
T2_k1	193.96	0.004	0.001	0.002	0.037
T2_k2	188.92	0.013	0.005	0.009	0.122
T2_k3	183.88	0.029	0.012	0.021	0.244
T2_k4	178.84	0.040	0.017	0.030	0.336
T2_k5	173.8	0.046	0.019	0.035	0.375
T2_k6	168.76	0.046	0.019	0.035	0.374
T2_k7	163.72	0.063	0.027	0.049	0.490
T2_k8	158.68	0.081	0.035	0.064	0.609
T2_k9	153.64	0.021	0.008	0.014	0.188

Table 12. Fatigue Damage at knuckle joints for various S-N Curve –Ballast Load case.

Knuckle joint	Distance in m from AFT Perpendicular	DNVC-I	DNVC-III	ABS-C	ABS-E
T2_k1	193.96	0.000	0.000	0.000	0.005
T2_k2	188.92	0.001	0.000	0.000	0.007
T2_k3	183.88	0.002	0.001	0.001	0.024
T2_k4	178.84	0.002	0.001	0.001	0.027
T2_k5	173.8	0.002	0.001	0.001	0.022
T2_k6	168.76	0.002	0.001	0.001	0.017
T2_k7	163.72	0.002	0.001	0.001	0.024
T2_k8	158.68	0.007	0.003	0.004	0.068
T2_k9	153.64	0.003	0.001	0.002	0.036

Appendix B: Summary of Hot Spot Fatigue damage Calculation

Table 13. Fatigue Damage for various S-N Curve –Ballast Load case.

S-N Curve	H1	H2	H3	H4	H5
DNVC-I	0.0775	0.0348	0.0304	0.0592	0.0435
DNVC-III	0.0331	0.0144	0.0126	0.025	0.0182
ABS-C	0.0609	0.0254	0.0222	0.0454	0.0325
ABS-E	0.5903	0.2960	0.2590	0.4690	0.3580

Table 14. Fatigue Damage for various S-N Curve –Full Load case.

S-N Curve	H1	H2	H3	H4	H5
DNVC-I	0.0051	0.0029	0.0013	0.0059	0.0021
DNVC-III	0.0021	0.0012	0.0005	0.0024	0.0008
ABS-C	0.0031	0.0017	0.0007	0.0036	0.0011
ABS-E	0.0532	0.0311	0.0141	0.0609	0.0224

Appendix C : Fatigue Calculation Result

Hotspot with S-N curve DNVC-I -----Ballast Load Case

```

Hotspot name           : H1
Description of hotspot :
Coordinate reference system : Current superelement
Hotspot name           : H2
Description of hotspot :
Coordinate reference system : Current superelement
Hotspot name           : H3
Description of hotspot :
Coordinate reference system : Current superelement
Hotspot name           : H4
Description of hotspot :
Coordinate reference system : Current superelement
Hotspot name           : H5
Description of hotspot :
Coordinate reference system : Current superelement

Status on failure      : *FAIL* when UsageFactor > 1.0
Design fatigue life    : 40.0 years
Fatigue calculation based on : Spectraof maximum principal stresses
Wave spectrum          : Pierson Moskowitz
    
```

HotName	FatPnt atNode	Stat	UsageFac	Element EleType atSide	AccFatLif X-coord. AxialScf ElThick WeiScale	StrCycle Y-coord. BendScf RefSyst WeiShape	SNCurve Z-coordinate ShearScf DistanceToHot StressRange
H1	HotS 54665	PASS	7.75E-02	25245 SCQS28 MidPlane	5.16E+02 1.59E+02 0.6375 0.016	1.13E+08 -1.21E+01 0.3825 CurrSupE	DNVC-I 4.0069E+00 0.6375 0.0000E+00
H1	t1/2	PASS	4.84E-02	25245 SCQS28 MidPlane	8.26E+02 1.59E+02 0.6375 0.016	1.13E+08 -1.20E+01 0.3825 CurrSupE	DNVC-I 1.7777E+08 0.6375 1.0247E-02
H1	t3/2	PASS	1.70E-02	25246 SCQS28 MidPlane	2.36E+03 1.59E+02 0.6375 0.016	1.14E+08 -1.20E+01 0.3825 CurrSupE	DNVC-I 3.9992E+00 0.6375 2.5304E-02
H2	HotS 54665	PASS	3.48E-02	19242 SCQS28 MidPlane	1.15E+03 1.59E+02 0.6375 0.016	1.14E+08 -1.21E+01 0.3825 CurrSupE	DNVC-I 4.0069E+00 0.6375 0.0000E+00
H2	t1/2	PASS	2.58E-02	19242 SCQS28 MidPlane	8.51E+06 1.55E+03 0.6375 0.016	9.51E-01 1.14E+08 -1.20E+01 0.3825 CurrSupE	DNVC-I 1.4909E+08 0.6375 1.0236E-02
H2	t3/2	PASS	1.10E-02	19563 SCTS26 MidPlane	3.65E+03 1.59E+02 0.6375 0.016	1.14E+08 -1.20E+01 0.3825 CurrSupE	DNVC-I 3.9992E+00 0.6375 2.4333E-02
					6.61E+06	9.45E-01	1.1836E+08

HotName	FatPnt atNode	Stat	UsageFac	Element EleType atSide	AccFatLif X-coord. AxialScf ElThick WeiScale	StrCycle Y-coord. BendScf RefSyst WeiShape	SNCurve Z-coordinate ShearScf DistanceToHot StressRange
H3	HotS 54665	PASS	3.04E-02	22333 SCQS28 MidPlane	1.32E+03 1.59E+02 0.6375 0.016 7.94E+06	1.12E+08 -1.21E+01 0.3825 CurrSupE 9.28E-01	DNVC-I 4.0069E+00 0.6375 0.0000E+00 1.5130E+08
H3	t1/2 64214	PASS	1.73E-02	22333 SCQS28 MidPlane	2.32E+03 1.59E+02 0.6375 0.016 7.06E+06	1.12E+08 -1.21E+01 0.3825 CurrSupE 9.29E-01	DNVC-I 4.0016E+00 0.6375 6.3713E-03 1.3412E+08
H3	t3/2 64364	PASS	4.24E-03	22408 SCQS28 MidPlane	9.44E+03 1.59E+02 0.6375 0.016 5.32E+06	1.12E+08 -1.21E+01 0.3825 CurrSupE 9.31E-01	DNVC-I 3.9897E+00 0.6375 2.0372E-02 1.0023E+08

HotName	FatPnt atNode	Stat	UsageFac	Element EleType atSide	AccFatLif X-coord. AxialScf ElThick WeiScale	StrCycle Y-coord. BendScf RefSyst WeiShape	SNCurve Z-coordinate ShearScf DistanceToHot StressRange
H4	HotS 54665	PASS	5.92E-02	23168 SCQS28 MidPlane	6.75E+02 1.59E+02 0.6375 0.016 9.52E+06	1.13E+08 -1.21E+01 0.3825 CurrSupE 9.49E-01	DNVC-I 4.0069E+00 0.6375 0.0000E+00 1.6790E+08
H4	t1/2	PASS	4.28E-02	23168 SCQS28 MidPlane	9.34E+02 1.59E+02 0.6375 0.016 8.86E+06	1.13E+08 -1.21E+01 0.3825 CurrSupE 9.49E-01	DNVC-I 4.0123E+00 0.6375 1.1319E-02 1.5652E+08
H4	t3/2	PASS	2.44E-02	23167 SCQS28 MidPlane	1.64E+03 1.59E+02 0.6375 0.016 7.86E+06	1.14E+08 -1.21E+01 0.3825 CurrSupE 9.49E-01	DNVC-I 4.0232E+00 0.6375 2.5301E-02 1.3895E+08

HotName	FatPnt atNode	Stat	UsageFac	Element EleType atSide	AccFatLif X-coord. AxialScf ElThick WeiScale	StrCycle Y-coord. BendScf RefSyst WeiShape	SNCurve Z-coordinate ShearScf DistanceToHot StressRange
H5	HotS 54665	PASS	4.35E-02	20813 SCQS28 MidPlane	9.20E+02 1.59E+02 0.6375 0.016 8.82E+06	1.13E+08 -1.21E+01 0.3825 CurrSupE 9.45E-01	DNVC-I 4.0069E+00 0.6375 0.0000E+00 1.5796E+08
H5	t1/2	PASS	2.86E-02	20813 SCQS28 MidPlane	1.40E+03 1.59E+02 0.6375 0.016 8.08E+06	1.13E+08 -1.21E+01 0.3825 CurrSupE 9.45E-01	DNVC-I 4.0123E+00 0.6375 1.1309E-02 1.4457E+08
H5	t3/2	PASS	1.43E-02	20814 SCQS28 MidPlane	2.79E+03 1.59E+02 0.6375 0.016 6.97E+06	1.14E+08 -1.21E+01 0.3825 CurrSupE 9.44E-01	DNVC-I 4.0232E+00 0.6375 2.5296E-02 1.2529E+08

Number of hotspots printed : 5
 Number of hotspots failed : 0
 Number of interpolation points failed: 0

Hotspot with S-N curve DNVC-III -----Ballast Load Case

```

Hotspot name           : H1
Description of hotspot :
Coordinate reference system : Current superelement
Hotspot name           : H2
Description of hotspot :
Coordinate reference system : Current superelement
Hotspot name           : H3
Description of hotspot :
Coordinate reference system : Current superelement
Hotspot name           : H4
Description of hotspot :
Coordinate reference system : Current superelement
Hotspot name           : H5
Description of hotspot :
Coordinate reference system : Current superelement

Status on failure      : *FAIL* when UsageFactor > 1.0
Design fatigue life    : 40.0 years
Fatigue calculation based on : Spectraof maximum principal stresses
Wave spectrum          : Pierson Moskowitz
    
```

HotName	FatPnt atNode	Stat	UsageFac	Element EleType atSide	AccFatLif X-coord. AxialScf ElThick WeiScale	StrCycle Y-coord. BendScf RefSyst WeiShape	SNCurve Z-coordinate ShearScf DistanceToHot StressRange
H1	HotS 54665	PASS	3.31E-02	25245 SCQS28 MidPlane	1.21E+03 1.59E+02 0.6375 0.016	1.13E+08 -1.21E+01 0.3825 CurrSupE	DNVC-III 4.0069E+00 0.6375 0.0000E+00
H1	t1/2	PASS	2.03E-02	25245 SCQS28 MidPlane	1.97E+03 1.59E+02 0.6375 0.016	1.13E+08 -1.20E+01 0.3825 CurrSupE	DNVC-III 4.0043E+00 0.6375 1.0247E-02
H1	t3/2	PASS	6.90E-03	25246 SCQS28 MidPlane	5.80E+03 1.59E+02 0.6375 0.016	1.14E+08 -1.20E+01 0.3825 CurrSupE	DNVC-III 3.9992E+00 0.6375 2.5304E-02

HotName	FatPnt atNode	Stat	UsageFac	Element EleType atSide	AccFatLif X-coord. AxialScf ElThick WeiScale	StrCycle Y-coord. BendScf RefSyst WeiShape	SNCurve Z-coordinate ShearScf DistanceToHot StressRange
H2	HotS 54665	PASS	1.44E-02	19242 SCQS28 MidPlane	2.78E+03 1.59E+02 0.6375 0.016	1.14E+08 -1.21E+01 0.3825 CurrSupE	DNVC-III 4.0069E+00 0.6375 0.0000E+00
H2	t1/2	PASS	1.06E-02	19242 SCQS28 MidPlane	3.79E+03 1.59E+02 0.6375 0.016	1.14E+08 -1.20E+01 0.3825 CurrSupE	DNVC-III 4.0043E+00 0.6375 1.0236E-02
H2	t3/2	PASS	4.42E-03	19563 SCTS26 MidPlane	9.05E+03 1.59E+02 0.6375 0.016	1.14E+08 -1.20E+01 0.3825 CurrSupE	DNVC-III 3.9992E+00 0.6375 2.4333E-02

HotName	FatPnt atNode	Stat	UsageFac	Element EleType atSide	AccFatLif X-coord. AxialScf ElThick WeiScale	StrCycle Y-coord. BendScf RefSyst WeiShape	SNCurve Z-coordinate ShearScf DistanceToHot StressRange
H3	HotS 54665	PASS	1.26E-02	22333 SCQS28 MidPlane	3.18E+03 1.59E+02 0.6375 0.016 7.94E+06	1.12E+08 -1.21E+01 0.3825 CurrSupE 9.28E-01	DNVC-III 4.0069E+00 0.6375 0.0000E+00 1.5130E+08
H3	t1/2 64214	PASS	7.04E-03	22333 SCQS28 MidPlane	5.68E+03 1.59E+02 0.6375 0.016 7.06E+06	1.12E+08 -1.21E+01 0.3825 CurrSupE 9.29E-01	DNVC-III 4.0016E+00 0.6375 6.3713E-03 1.3412E+08
H3	t3/2 64364	PASS	1.70E-03	22408 SCQS28 MidPlane	2.36E+04 1.59E+02 0.6375 0.016 5.32E+06	1.12E+08 -1.21E+01 0.3825 CurrSupE 9.31E-01	DNVC-III 3.9897E+00 0.6375 2.0372E-02 1.0023E+08

HotName	FatPnt atNode	Stat	UsageFac	Element EleType atSide	AccFatLif X-coord. AxialScf ElThick WeiScale	StrCycle Y-coord. BendScf RefSyst WeiShape	SNCurve Z-coordinate ShearScf DistanceToHot StressRange
H4	HotS 54665	PASS	2.50E-02	23168 SCQS28 MidPlane	1.60E+03 1.59E+02 0.6375 0.016 9.52E+06	1.13E+08 -1.21E+01 0.3825 CurrSupE 9.49E-01	DNVC-III 4.0069E+00 0.6375 0.0000E+00 1.6790E+08
H4	t1/2	PASS	1.79E-02	23168 SCQS28 MidPlane	2.24E+03 1.59E+02 0.6375 0.016 8.86E+06	1.13E+08 -1.21E+01 0.3825 CurrSupE 9.49E-01	DNVC-III 4.0123E+00 0.6375 1.1319E-02 1.5652E+08
H4	t3/2	PASS	1.00E-02	23167 SCQS28 MidPlane	4.00E+03 1.59E+02 0.6375 0.016 7.86E+06	1.14E+08 -1.21E+01 0.3825 CurrSupE 9.49E-01	DNVC-III 4.0232E+00 0.6375 2.5301E-02 1.3895E+08

HotName	FatPnt atNode	Stat	UsageFac	Element EleType atSide	AccFatLif X-coord. AxialScf ElThick WeiScale	StrCycle Y-coord. BendScf RefSyst WeiShape	SNCurve Z-coordinate ShearScf DistanceToHot StressRange
H5	HotS 54665	PASS	1.82E-02	20813 SCQS28 MidPlane	2.20E+03 1.59E+02 0.6375 0.016 8.82E+06	1.13E+08 -1.21E+01 0.3825 CurrSupE 9.45E-01	DNVC-III 4.0069E+00 0.6375 0.0000E+00 1.5796E+08
H5	t1/2	PASS	1.18E-02	20813 SCQS28 MidPlane	3.39E+03 1.59E+02 0.6375 0.016 8.08E+06	1.13E+08 -1.21E+01 0.3825 CurrSupE 9.45E-01	DNVC-III 4.0123E+00 0.6375 1.1309E-02 1.4457E+08
H5	t3/2	PASS	5.80E-03	20814 SCQS28 MidPlane	6.89E+03 1.59E+02 0.6375 0.016 6.97E+06	1.14E+08 -1.21E+01 0.3825 CurrSupE 9.44E-01	DNVC-III 4.0232E+00 0.6375 2.5296E-02 1.2529E+08

Number of hotspots printed : 5
 Number of hotspots failed : 0
 Number of interpolation points failed: 0

Hotspot with S-N curve ABS-C -----Ballast Load Case

```

Hotspot name           : H1
Description of hotspot :
Coordinate reference system : Current superelement
Hotspot name           : H2
Description of hotspot :
Coordinate reference system : Current superelement
Hotspot name           : H3
Description of hotspot :
Coordinate reference system : Current superelement
Hotspot name           : H4
Description of hotspot :
Coordinate reference system : Current superelement
Hotspot name           : H5
Description of hotspot :
Coordinate reference system : Current superelement

Status on failure      : *FAIL* when UsageFactor > 1.0
Design fatigue life    : 40.0 years
Fatigue calculation based on : Spectraof maximum principal stresses
Wave spectrum          : Pierson Moskowitz
    
```

HotName	FatPnt	Stat	UsageFac	Element	AccFatLif	StrCycle	SNCurve
atNode				EleType	X-coord.	Y-coord.	Z-coordinate
				atSide	AxialScf	BendScf	ShearScf
					ElThick	RefSyst	DistanceToHot
					WeiScale	WeiShape	StressRange
H1	HotS	PASS	6.09E-02	25245	6.56E+02	1.13E+08	ABS-C-A
	54665			SCQS28	1.59E+02	-1.21E+01	4.0069E+00
				MidPlane	0.6375	0.3825	0.6375
					0.016	CurrSupE	0.0000E+00
					1.01E+07	9.51E-01	1.7757E+08
H1	t1/2	PASS	3.65E-02	25245	1.10E+03	1.13E+08	ABS-C-A
				SCQS28	1.59E+02	-1.20E+01	4.0043E+00
				MidPlane	0.6375	0.3825	0.6375
					0.016	CurrSupE	1.0247E-02
					9.11E+06	9.51E-01	1.6014E+08
H1	t3/2	PASS	1.16E-02	25246	3.45E+03	1.14E+08	ABS-C-A
				SCQS28	1.59E+02	-1.20E+01	3.9992E+00
				MidPlane	0.6375	0.3825	0.6375
					0.016	CurrSupE	2.5304E-02
					7.29E+06	9.49E-01	1.2861E+08

HotName	FatPnt	Stat	UsageFac	Element	AccFatLif	StrCycle	SNCurve
atNode				EleType	X-coord.	Y-coord.	Z-coordinate
				atSide	AxialScf	BendScf	ShearScf
					ElThick	RefSyst	DistanceToHot
					WeiScale	WeiShape	StressRange
H2	HotS	PASS	2.54E-02	19242	1.58E+03	1.14E+08	ABS-C-A
	54665			SCQS28	1.59E+02	-1.21E+01	4.0069E+00
				MidPlane	0.6375	0.3825	0.6375
					0.016	CurrSupE	0.0000E+00
					8.49E+06	9.51E-01	1.4892E+08
H2	t1/2	PASS	1.83E-02	19242	2.19E+03	1.14E+08	ABS-C-A
				SCQS28	1.59E+02	-1.20E+01	4.0043E+00
				MidPlane	0.6375	0.3825	0.6375
					0.016	CurrSupE	1.0236E-02
					7.96E+06	9.50E-01	1.4007E+08
H2	t3/2	PASS	7.19E-03	19563	5.56E+03	1.14E+08	ABS-C-A
				SCTS26	1.59E+02	-1.20E+01	3.9992E+00
				MidPlane	0.6375	0.3825	0.6375
					0.016	CurrSupE	2.4333E-02
					6.61E+06	9.45E-01	1.1823E+08

HotName	FatPnt atNode	Stat	UsageFac	Element EleType atSide	AccFatLif X-coord. AxialScf ElThick WeiScale	StrCycle Y-coord. BendScf RefSyst WeiShape	SNCurve Z-coordinate ShearScf DistanceToHot StressRange
H3	HotS 54665	PASS	2.22E-02	22333 SCQS28 MidPlane	1.80E+03 1.59E+02 0.6375 0.016 7.93E+06	1.12E+08 -1.21E+01 0.3825 CurrSupE 9.28E-01	ABS-C-A 4.0069E+00 0.6375 0.0000E+00 1.5113E+08
H3	t1/2 64214	PASS	1.19E-02	22333 SCQS28 MidPlane	3.35E+03 1.59E+02 0.6375 0.016 7.05E+06	1.12E+08 -1.21E+01 0.3825 CurrSupE 9.29E-01	ABS-C-A 4.0016E+00 0.6375 6.3713E-03 1.3397E+08
H3	t3/2 64364	PASS	2.56E-03	22408 SCQS28 MidPlane	1.56E+04 1.59E+02 0.6375 0.016 5.32E+06	1.12E+08 -1.21E+01 0.3825 CurrSupE 9.32E-01	ABS-C-A 3.9897E+00 0.6375 2.0372E-02 1.0011E+08

HotName	FatPnt atNode	Stat	UsageFac	Element EleType atSide	AccFatLif X-coord. AxialScf ElThick WeiScale	StrCycle Y-coord. BendScf RefSyst WeiShape	SNCurve Z-coordinate ShearScf DistanceToHot StressRange
H4	HotS 54665	PASS	4.54E-02	23168 SCQS28 MidPlane	8.80E+02 1.59E+02 0.6375 0.016 9.50E+06	1.13E+08 -1.21E+01 0.3825 CurrSupE 9.49E-01	ABS-C-A 4.0069E+00 0.6375 0.0000E+00 1.6771E+08
H4	t1/2	PASS	3.19E-02	23168 SCQS28 MidPlane	1.25E+03 1.59E+02 0.6375 0.016 8.85E+06	1.13E+08 -1.21E+01 0.3825 CurrSupE 9.49E-01	ABS-C-A 4.0123E+00 0.6375 1.1319E-02 1.5634E+08
H4	t3/2	PASS	1.72E-02	23167 SCQS28 MidPlane	2.32E+03 1.59E+02 0.6375 0.016 7.86E+06	1.14E+08 -1.21E+01 0.3825 CurrSupE 9.49E-01	ABS-C-A 4.0232E+00 0.6375 2.5301E-02 1.3879E+08

HotName	FatPnt atNode	Stat	UsageFac	Element EleType atSide	AccFatLif X-coord. AxialScf ElThick WeiScale	StrCycle Y-coord. BendScf RefSyst WeiShape	SNCurve Z-coordinate ShearScf DistanceToHot StressRange
H5	HotS 54665	PASS	3.25E-02	20813 SCQS28 MidPlane	1.23E+03 1.59E+02 0.6375 0.016 8.83E+06	1.13E+08 -1.21E+01 0.3825 CurrSupE 9.45E-01	ABS-C-A 4.0069E+00 0.6375 0.0000E+00 1.5778E+08
H5	t1/2	PASS	2.06E-02	20813 SCQS28 MidPlane	1.94E+03 1.59E+02 0.6375 0.016 8.07E+06	1.13E+08 -1.21E+01 0.3825 CurrSupE 9.45E-01	ABS-C-A 4.0123E+00 0.6375 1.1309E-02 1.4440E+08
H5	t3/2	PASS	9.65E-03	20814 SCQS28 MidPlane	4.14E+03 1.59E+02 0.6375 0.016 6.98E+06	1.14E+08 -1.21E+01 0.3825 CurrSupE 9.45E-01	ABS-C-A 4.0232E+00 0.6375 2.5296E-02 1.2515E+08

Number of hotspots printed : 5

Number of hotspots failed : 0

Number of interpolation points failed: 0

Hotspot with S-N curve ABS-E -----Ballast Load Case

```

Hotspot name           : H1
Description of hotspot :
Coordinate reference system : Current superelement
Hotspot name           : H2
Description of hotspot :
Coordinate reference system : Current superelement
Hotspot name           : H3
Description of hotspot :
Coordinate reference system : Current superelement
Hotspot name           : H4
Description of hotspot :
Coordinate reference system : Current superelement
Hotspot name           : H5
Description of hotspot :
Coordinate reference system : Current superelement

Status on failure      : *FAIL* when UsageFactor > 1.0
Design fatigue life    : 40.0 years
Fatigue calculation based on : Spectraof maximum principal stresses
Wave spectrum          : Pierson Moskowitz
    
```

HotName	FatPnt	Stat	UsageFac	Element	AccFatLif	StrCycle	SNCurve
atNode				EleType	X-coord.	Y-coord.	Z-coordinate
				atSide	AxialScf	BendScf	ShearScf
					ElThick	RefSyst	DistanceToHot
					WeiScale	WeiShape	StressRange
H1	HotS	PASS	5.90E-01	25245	6.78E+01	1.13E+08	ABS-E-A
	54665			SCQS28	1.59E+02	-1.21E+01	4.0069E+00
				MidPlane	0.6375	0.3825	0.6375
					0.016	CurrSupE	0.0000E+00
					1.01E+07	9.51E-01	1.7757E+08
H1	t1/2	PASS	3.94E-01	25245	1.01E+02	1.13E+08	ABS-E-A
				SCQS28	1.59E+02	-1.20E+01	4.0043E+00
				MidPlane	0.6375	0.3825	0.6375
					0.016	CurrSupE	1.0247E-02
					9.11E+06	9.51E-01	1.6014E+08
H1	t3/2	PASS	1.58E-01	25246	2.54E+02	1.14E+08	ABS-E-A
				SCQS28	1.59E+02	-1.20E+01	3.9992E+00
				MidPlane	0.6375	0.3825	0.6375
					0.016	CurrSupE	2.5304E-02
					7.29E+06	9.49E-01	1.2861E+08

HotName	FatPnt	Stat	UsageFac	Element	AccFatLif	StrCycle	SNCurve
atNode				EleType	X-coord.	Y-coord.	Z-coordinate
				atSide	AxialScf	BendScf	ShearScf
					ElThick	RefSyst	DistanceToHot
					WeiScale	WeiShape	StressRange
H2	HotS	PASS	2.96E-01	19242	1.35E+02	1.14E+08	ABS-E-A
	54665			SCQS28	1.59E+02	-1.21E+01	4.0069E+00
				MidPlane	0.6375	0.3825	0.6375
					0.016	CurrSupE	0.0000E+00
					8.49E+06	9.51E-01	1.4892E+08
H2	t1/2	PASS	2.28E-01	19242	1.76E+02	1.14E+08	ABS-E-A
				SCQS28	1.59E+02	-1.20E+01	4.0043E+00
				MidPlane	0.6375	0.3825	0.6375
					0.016	CurrSupE	1.0236E-02
					7.96E+06	9.50E-01	1.4007E+08
H2	t3/2	PASS	1.06E-01	19563	3.77E+02	1.14E+08	ABS-E-A
				SCTS26	1.59E+02	-1.20E+01	3.9992E+00
				MidPlane	0.6375	0.3825	0.6375
					0.016	CurrSupE	2.4333E-02
					6.61E+06	9.45E-01	1.1823E+08

HotName	FatPnt atNode	Stat	UsageFac	Element EleType atSide	AccFatLif X-coord. AxialScf ElThick WeiScale	StrCycle Y-coord. BendScf RefSyst WeiShape	SNCurve Z-coordinate ShearScf DistanceToHot StressRange
H3	HotS 54665	PASS	2.59E-01	22333 SCQS28 MidPlane	1.55E+02 1.59E+02 0.6375 0.016 7.93E+06	1.12E+08 -1.21E+01 0.3825 CurrSupE 9.28E-01	ABS-E-A 4.0069E+00 0.6375 0.0000E+00 1.5113E+08
H3	t1/2 64214	PASS	1.58E-01	22333 SCQS28 MidPlane	2.54E+02 1.59E+02 0.6375 0.016 7.05E+06	1.12E+08 -1.21E+01 0.3825 CurrSupE 9.29E-01	ABS-E-A 4.0016E+00 0.6375 6.3713E-03 1.3397E+08
H3	t3/2 64364	PASS	4.41E-02	22408 SCQS28 MidPlane	9.08E+02 1.59E+02 0.6375 0.016 5.32E+06	1.12E+08 -1.21E+01 0.3825 CurrSupE 9.32E-01	ABS-E-A 3.9897E+00 0.6375 2.0372E-02 1.0011E+08

HotName	FatPnt atNode	Stat	UsageFac	Element EleType atSide	AccFatLif X-coord. AxialScf ElThick WeiScale	StrCycle Y-coord. BendScf RefSyst WeiShape	SNCurve Z-coordinate ShearScf DistanceToHot StressRange
H4	HotS 54665	PASS	4.69E-01	23168 SCQS28 MidPlane	8.54E+01 1.59E+02 0.6375 0.016 9.50E+06	1.13E+08 -1.21E+01 0.3825 CurrSupE 9.49E-01	ABS-E-A 4.0069E+00 0.6375 0.0000E+00 1.6771E+08
H4	t1/2	PASS	3.55E-01	23168 SCQS28 MidPlane	1.13E+02 1.59E+02 0.6375 0.016 8.85E+06	1.13E+08 -1.21E+01 0.3825 CurrSupE 9.49E-01	ABS-E-A 4.0123E+00 0.6375 1.1319E-02 1.5634E+08
H4	t3/2	PASS	2.17E-01	23167 SCQS28 MidPlane	1.84E+02 1.59E+02 0.6375 0.016 7.86E+06	1.14E+08 -1.21E+01 0.3825 CurrSupE 9.49E-01	ABS-E-A 4.0232E+00 0.6375 2.5301E-02 1.3879E+08

HotName	FatPnt atNode	Stat	UsageFac	Element EleType atSide	AccFatLif X-coord. AxialScf ElThick WeiScale	StrCycle Y-coord. BendScf RefSyst WeiShape	SNCurve Z-coordinate ShearScf DistanceToHot StressRange
H5	HotS 54665	PASS	3.58E-01	20813 SCQS28 MidPlane	1.12E+02 1.59E+02 0.6375 0.016 8.83E+06	1.13E+08 -1.21E+01 0.3825 CurrSupE 9.45E-01	ABS-E-A 4.0069E+00 0.6375 0.0000E+00 1.5778E+08
H5	t1/2	PASS	2.49E-01	20813 SCQS28 MidPlane	1.61E+02 1.59E+02 0.6375 0.016 8.07E+06	1.13E+08 -1.21E+01 0.3825 CurrSupE 9.45E-01	ABS-E-A 4.0123E+00 0.6375 1.1309E-02 1.4440E+08
H5	t3/2	PASS	1.35E-01	20814 SCQS28 MidPlane	2.96E+02 1.59E+02 0.6375 0.016 6.98E+06	1.14E+08 -1.21E+01 0.3825 CurrSupE 9.45E-01	ABS-E-A 4.0232E+00 0.6375 2.5296E-02 1.2515E+08

Number of hotspots printed : 5

Number of hotspots failed : 0

Number of interpolation points failed: 0

Hotspot with S-N curve DNVC-I -----Full Load Case

```

Hotspot name           : H1
Description of hotspot :
Coordinate reference system : Current superelement
Hotspot name           : H2
Description of hotspot :
Coordinate reference system : Current superelement
Hotspot name           : H3
Description of hotspot :
Coordinate reference system : Current superelement
Hotspot name           : H4
Description of hotspot :
Coordinate reference system : Current superelement
Hotspot name           : H5
Description of hotspot :
Coordinate reference system : Current superelement

Status on failure      : *FAIL* when UsageFactor > 1.0
Design fatigue life    : 40.0 years
Fatigue calculation based on : Spectraof maximum principal stresses
Wave spectrum          : Pierson Moskowitz
    
```

HotName	FatPnt atNode	Stat	UsageFac	Element EleType atSide	AccFatLif X-coord. AxialScf ElThick WeiScale	StrCycle Y-coord. BendScf RefSyst WeiShape	SNCurve Z-coordinate ShearScf DistanceToHot StressRange
H1	HotS 162724	PASS	5.12E-03	183552 FQUS24 MidPlane	7.82E+03 1.59E+02 0.6375 0.016 5.84E+06	1.16E+08 -1.21E+01 0.3825 CurrSupE 9.62E-01	DNVC-I 4.0069E+00 0.6375 0.0000E+00 9.7401E+07
H1	t1/2	PASS	3.97E-03	183552 FQUS24 MidPlane	1.01E+04 1.59E+02 0.6375 0.016 5.56E+06	1.16E+08 -1.20E+01 0.3825 CurrSupE 9.64E-01	DNVC-I 4.0043E+00 0.6375 1.0247E-02 9.2298E+07
H1	t3/2	PASS	2.19E-03	183553 FQUS24 MidPlane	1.83E+04 1.59E+02 0.6375 0.016 4.96E+06	1.16E+08 -1.20E+01 0.3825 CurrSupE 9.66E-01	DNVC-I 3.9992E+00 0.6375 2.5304E-02 8.1342E+07

HotName	FatPnt atNode	Stat	UsageFac	Element EleType atSide	AccFatLif X-coord. AxialScf ElThick WeiScale	StrCycle Y-coord. BendScf RefSyst WeiShape	SNCurve Z-coordinate ShearScf DistanceToHot StressRange
H2	HotS 162724	PASS	2.89E-03	177549 FQUS24 MidPlane	1.38E+04 1.59E+02 0.6375 0.016 5.10E+06	1.17E+08 -1.21E+01 0.3825 CurrSupE 9.53E-01	DNVC-I 4.0069E+00 0.6375 0.0000E+00 8.9563E+07
H2	t1/2	PASS	1.87E-03	177549 FQUS24 MidPlane	2.14E+04 1.59E+02 0.6375 0.016 4.68E+06	1.17E+08 -1.20E+01 0.3825 CurrSupE 9.54E-01	DNVC-I 4.0043E+00 0.6375 1.0236E-02 8.1858E+07
H2	t3/2	PASS	4.07E-04	177870 FTRS25 MidPlane	4.00E+04 1.59E+02 0.6375 0.016 3.49E+06	1.17E+08 -1.20E+01 0.3825 CurrSupE 9.59E-01	DNVC-I 3.9992E+00 0.6375 2.4333E-02 5.9842E+07

HotName	FatPnt atNode	Stat	UsageFac	Element EleType atSide	AccFatLif X-coord. AxialScf ElThick WeiScale	StrCycle Y-coord. BendScf RefSyst WeiShape	SNCurve Z-coordinate ShearScf DistanceToHot StressRange
H3	HotS 162724	PASS	1.27E-03	180640 FQUS24 MidPlane	3.15E+04 1.59E+02 0.6375 0.016 4.42E+06	1.17E+08 -1.21E+01 0.3825 CurrSupE 9.64E-01	DNVC-I 4.0069E+00 0.6375 0.0000E+00 7.4574E+07
H3	t1/2	PASS	7.45E-04	180640 FQUS24 MidPlane	4.00E+04 1.59E+02 0.6375 0.016 3.99E+06	1.17E+08 -1.21E+01 0.3825 CurrSupE 9.66E-01	DNVC-I 4.0010E+00 0.6375 7.9998E-03 6.6618E+07
H3	t3/2	PASS	2.17E-04	180715 FQUS24 MidPlane	4.00E+04 1.59E+02 0.6375 0.016 3.15E+06	1.17E+08 -1.21E+01 0.3825 CurrSupE 9.71E-01	DNVC-I 3.9893E+00 0.6375 2.4000E-02 5.1179E+07

HotName	FatPnt atNode	Stat	UsageFac	Element EleType atSide	AccFatLif X-coord. AxialScf ElThick WeiScale	StrCycle Y-coord. BendScf RefSyst WeiShape	SNCurve Z-coordinate ShearScf DistanceToHot StressRange
H4	HotS 162724	PASS	5.91E-03	181475 FQUS24 MidPlane	6.77E+03 1.59E+02 0.6375 0.016 6.03E+06	1.16E+08 -1.21E+01 0.3825 CurrSupE 9.63E-01	DNVC-I 4.0069E+00 0.6375 0.0000E+00 1.0013E+08
H4	t1/2	PASS	4.46E-03	181475 FQUS24 MidPlane	8.97E+03 1.59E+02 0.6375 0.016 5.70E+06	1.16E+08 -1.21E+01 0.3825 CurrSupE 9.64E-01	DNVC-I 4.0123E+00 0.6375 1.1319E-02 9.4496E+07
H4	t3/2	PASS	2.71E-03	181474 FQUS24 MidPlane	1.48E+04 1.59E+02 0.6375 0.016 5.16E+06	1.16E+08 -1.21E+01 0.3825 CurrSupE 9.65E-01	DNVC-I 4.0232E+00 0.6375 2.5301E-02 8.5309E+07

HotName	FatPnt atNode	Stat	UsageFac	Element EleType atSide	AccFatLif X-coord. AxialScf ElThick WeiScale	StrCycle Y-coord. BendScf RefSyst WeiShape	SNCurve Z-coordinate ShearScf DistanceToHot StressRange
H5	HotS 162724	PASS	2.05E-03	179120 FQUS24 MidPlane	1.95E+04 1.59E+02 0.6375 0.016 4.77E+06	1.17E+08 -1.21E+01 0.3825 CurrSupE 9.55E-01	DNVC-I 4.0069E+00 0.6375 0.0000E+00 8.3274E+07
H5	t1/2	PASS	1.69E-03	179120 FQUS24 MidPlane	2.36E+04 1.59E+02 0.6375 0.016 4.61E+06	1.18E+08 -1.21E+01 0.3825 CurrSupE 9.56E-01	DNVC-I 4.0123E+00 0.6375 1.1309E-02 7.9976E+07
H5	t3/2	PASS	1.22E-03	179121 FQUS24 MidPlane	3.27E+04 1.59E+02 0.6375 0.016 4.34E+06	1.18E+08 -1.21E+01 0.3825 CurrSupE 9.58E-01	DNVC-I 4.0232E+00 0.6375 2.5296E-02 7.4625E+07

Number of hotspots printed : 5
 Number of hotspots failed : 0
 Number of interpolation points failed: 0

Hotspot with S-N curve DNVC-III -----Full Load Case

```

Hotspot name           : H1
Description of hotspot :
Coordinate reference system : Current superelement
Hotspot name           : H2
Description of hotspot :
Coordinate reference system : Current superelement
Hotspot name           : H3
Description of hotspot :
Coordinate reference system : Current superelement
Hotspot name           : H4
Description of hotspot :
Coordinate reference system : Current superelement
Hotspot name           : H5
Description of hotspot :
Coordinate reference system : Current superelement

Status on failure      : *FAIL* when UsageFactor > 1.0
Design fatigue life    : 40.0 years
Fatigue calculation based on : Spectraof maximum principal stresses
Wave spectrum          : Pierson Moskowitz
    
```

HotName	FatPnt atNode	Stat	UsageFac	Element EleType atSide	AccFatLif X-coord. AxialScf ElThick WeiScale	StrCycle Y-coord. BendScf RefSyst WeiShape	SNCurve Z-coordinate ShearScf DistanceToHot StressRange
H1	HotS 162724	PASS	2.05E-03	183552 FQUS24 MidPlane	1.96E+04 1.59E+02 0.6375 0.016 5.84E+06	1.16E+08 -1.21E+01 0.3825 CurrSupE 9.62E-01	DNVC-III 4.0069E+00 0.6375 0.0000E+00 9.7401E+07
H1	t1/2	PASS	1.58E-03	183552 FQUS24 MidPlane	2.53E+04 1.59E+02 0.6375 0.016 5.56E+06	1.16E+08 -1.20E+01 0.3825 CurrSupE 9.64E-01	DNVC-III 4.0043E+00 0.6375 1.0247E-02 9.2298E+07
H1	t3/2	PASS	8.71E-04	183553 FQUS24 MidPlane	4.00E+04 1.59E+02 0.6375 0.016 4.96E+06	1.16E+08 -1.20E+01 0.3825 CurrSupE 9.66E-01	DNVC-III 3.9992E+00 0.6375 2.5304E-02 8.1342E+07
H2	HotS 162724	PASS	1.15E-03	177549 FQUS24 MidPlane	3.47E+04 1.59E+02 0.6375 0.016 5.10E+06	1.17E+08 -1.21E+01 0.3825 CurrSupE 9.53E-01	DNVC-III 4.0069E+00 0.6375 0.0000E+00 8.9563E+07
H2	t1/2	PASS	7.43E-04	177549 FQUS24 MidPlane	4.00E+04 1.59E+02 0.6375 0.016 4.68E+06	1.17E+08 -1.20E+01 0.3825 CurrSupE 9.54E-01	DNVC-III 4.0043E+00 0.6375 1.0236E-02 8.1858E+07
H2	t3/2	PASS	1.62E-04	177870 FTRS25 MidPlane	4.00E+04 1.59E+02 0.6375 0.016 3.49E+06	1.17E+08 -1.20E+01 0.3825 CurrSupE 9.59E-01	DNVC-III 3.9992E+00 0.6375 2.4333E-02 5.9842E+07

HotName	FatPnt atNode	Stat	UsageFac	Element EleType atSide	AccFatLif X-coord. AxialScf ElThick WeiScale	StrCycle Y-coord. BendScf RefSyst WeiShape	SNCurve Z-coordinate ShearScf DistanceToHot StressRange
H3	HotS 162724	PASS	5.06E-04	180640 FQUS24 MidPlane	4.00E+04 1.59E+02 0.6375 0.016 4.42E+06	1.17E+08 -1.21E+01 0.3825 CurrSupE 9.64E-01	DNVC-III 4.0069E+00 0.6375 0.0000E+00 7.4574E+07
H3	t1/2	PASS	2.97E-04	180640 FQUS24 MidPlane	4.00E+04 1.59E+02 0.6375 0.016 3.99E+06	1.17E+08 -1.21E+01 0.3825 CurrSupE 9.66E-01	DNVC-III 4.0010E+00 0.6375 7.9998E-03 6.6618E+07
H3	t3/2	PASS	8.66E-05	180715 FQUS24 MidPlane	4.00E+04 1.59E+02 0.6375 0.016 3.15E+06	1.17E+08 -1.21E+01 0.3825 CurrSupE 9.71E-01	DNVC-III 3.9893E+00 0.6375 2.4000E-02 5.1179E+07

HotName	FatPnt atNode	Stat	UsageFac	Element EleType atSide	AccFatLif X-coord. AxialScf ElThick WeiScale	StrCycle Y-coord. BendScf RefSyst WeiShape	SNCurve Z-coordinate ShearScf DistanceToHot StressRange
H4	HotS 162724	PASS	2.37E-03	181475 FQUS24 MidPlane	1.69E+04 1.59E+02 0.6375 0.016 6.03E+06	1.16E+08 -1.21E+01 0.3825 CurrSupE 9.63E-01	DNVC-III 4.0069E+00 0.6375 0.0000E+00 1.0013E+08
H4	t1/2	PASS	1.78E-03	181475 FQUS24 MidPlane	2.24E+04 1.59E+02 0.6375 0.016 5.70E+06	1.16E+08 -1.21E+01 0.3825 CurrSupE 9.64E-01	DNVC-III 4.0123E+00 0.6375 1.1319E-02 9.4496E+07
H4	t3/2	PASS	1.08E-03	181474 FQUS24 MidPlane	3.70E+04 1.59E+02 0.6375 0.016 5.16E+06	1.16E+08 -1.21E+01 0.3825 CurrSupE 9.65E-01	DNVC-III 4.0232E+00 0.6375 2.5301E-02 8.5309E+07

HotName	FatPnt atNode	Stat	UsageFac	Element EleType atSide	AccFatLif X-coord. AxialScf ElThick WeiScale	StrCycle Y-coord. BendScf RefSyst WeiShape	SNCurve Z-coordinate ShearScf DistanceToHot StressRange
H5	HotS 162724	PASS	8.19E-04	179120 FQUS24 MidPlane	4.00E+04 1.59E+02 0.6375 0.016 4.77E+06	1.17E+08 -1.21E+01 0.3825 CurrSupE 9.55E-01	DNVC-III 4.0069E+00 0.6375 0.0000E+00 8.3274E+07
H5	t1/2	PASS	6.75E-04	179120 FQUS24 MidPlane	4.00E+04 1.59E+02 0.6375 0.016 4.61E+06	1.18E+08 -1.21E+01 0.3825 CurrSupE 9.56E-01	DNVC-III 4.0123E+00 0.6375 1.1309E-02 7.9976E+07
H5	t3/2	PASS	4.88E-04	179121 FQUS24 MidPlane	4.00E+04 1.59E+02 0.6375 0.016 4.34E+06	1.18E+08 -1.21E+01 0.3825 CurrSupE 9.58E-01	DNVC-III 4.0232E+00 0.6375 2.5296E-02 7.4625E+07

Number of hotspots printed : 5

Number of hotspots failed : 0

Number of interpolation points failed: 0

Hotspot with S-N curve ABS-C -----Full Load Case

```

Hotspot name           : H1
Description of hotspot :
Coordinate reference system : Current superelement
Hotspot name           : H2
Description of hotspot :
Coordinate reference system : Current superelement
Hotspot name           : H3
Description of hotspot :
Coordinate reference system : Current superelement
Hotspot name           : H4
Description of hotspot :
Coordinate reference system : Current superelement
Hotspot name           : H5
Description of hotspot :
Coordinate reference system : Current superelement

Status on failure      : *FAIL* when UsageFactor > 1.0
Design fatigue life    : 40.0 years
Fatigue calculation based on : Spectraof maximum principal stresses
Wave spectrum          : Pierson Moskowitz
    
```

HotName	FatPnt atNode	Stat	UsageFac	Element EleType atSide	AccFatLif X-coord. AxialScf ElThick WeiScale	StrCycle Y-coord. BendScf RefSyst WeiShape	SNCurve Z-coordinate ShearScf DistanceToHot StressRange
---------	------------------	------	----------	------------------------------	--	--	---

H1	HotS 162724	PASS	3.10E-03	183552 FQUS24 MidPlane	1.29E+04 1.59E+02 0.6375 0.016 5.84E+06	1.16E+08 -1.21E+01 0.3825 CurrSupE 9.63E-01	ABS-C-A 4.0069E+00 0.6375 0.0000E+00 9.7290E+07
H1	t1/2	PASS	2.34E-03	183552 FQUS24 MidPlane	1.71E+04 1.59E+02 0.6375 0.016 5.55E+06	1.16E+08 -1.20E+01 0.3825 CurrSupE 9.63E-01	ABS-C-A 4.0043E+00 0.6375 1.0247E-02 9.2193E+07
H1	t3/2	PASS	1.21E-03	183553 FQUS24 MidPlane	3.30E+04 1.59E+02 0.6375 0.016 4.96E+06	1.16E+08 -1.20E+01 0.3825 CurrSupE 9.67E-01	ABS-C-A 3.9992E+00 0.6375 2.5304E-02 8.1250E+07

HotName	FatPnt atNode	Stat	UsageFac	Element EleType atSide	AccFatLif X-coord. AxialScf ElThick WeiScale	StrCycle Y-coord. BendScf RefSyst WeiShape	SNCurve Z-coordinate ShearScf DistanceToHot StressRange
---------	------------------	------	----------	------------------------------	--	--	---

H2	HotS 162724	PASS	1.66E-03	177549 FQUS24 MidPlane	2.41E+04 1.59E+02 0.6375 0.016 5.10E+06	1.17E+08 -1.21E+01 0.3825 CurrSupE 9.53E-01	ABS-C-A 4.0069E+00 0.6375 0.0000E+00 8.9461E+07
H2	t1/2	PASS	1.02E-03	177549 FQUS24 MidPlane	3.91E+04 1.59E+02 0.6375 0.016 4.67E+06	1.17E+08 -1.20E+01 0.3825 CurrSupE 9.54E-01	ABS-C-A 4.0043E+00 0.6375 1.0236E-02 8.1765E+07
H2	t3/2	PASS	1.91E-04	177870 FTRS25 MidPlane	4.00E+04 1.59E+02 0.6375 0.016 3.48E+06	1.17E+08 -1.20E+01 0.3825 CurrSupE 9.59E-01	ABS-C-A 3.9992E+00 0.6375 2.4333E-02 5.9774E+07

HotName	FatPnt atNode	Stat	UsageFac	Element EleType atSide	AccFatLif X-coord. AxialScf ElThick WeiScale	StrCycle Y-coord. BendScf RefSyst WeiShape	SNCurve Z-coordinate ShearScf DistanceToHot StressRange
H3	HotS 162724	PASS	6.68E-04	180640 FQUS24 MidPlane	4.00E+04 1.59E+02 0.6375 0.016 4.41E+06	1.17E+08 -1.21E+01 0.3825 CurrSupE 9.64E-01	ABS-C-A 4.0069E+00 0.6375 0.0000E+00 7.4489E+07
H3	t1/2	PASS	3.71E-04	180640 FQUS24 MidPlane	4.00E+04 1.59E+02 0.6375 0.016 3.99E+06	1.17E+08 -1.21E+01 0.3825 CurrSupE 9.66E-01	ABS-C-A 4.0010E+00 0.6375 7.9998E-03 6.6542E+07
H3	t3/2	PASS	9.57E-05	180715 FQUS24 MidPlane	4.00E+04 1.59E+02 0.6375 0.016 3.14E+06	1.17E+08 -1.21E+01 0.3825 CurrSupE 9.71E-01	ABS-C-A 3.9893E+00 0.6375 2.4000E-02 5.1120E+07

HotName	FatPnt atNode	Stat	UsageFac	Element EleType atSide	AccFatLif X-coord. AxialScf ElThick WeiScale	StrCycle Y-coord. BendScf RefSyst WeiShape	SNCurve Z-coordinate ShearScf DistanceToHot StressRange
H4	HotS 162724	PASS	3.63E-03	181475 FQUS24 MidPlane	1.10E+04 1.59E+02 0.6375 0.016 6.01E+06	1.16E+08 -1.21E+01 0.3825 CurrSupE 9.63E-01	ABS-C-A 4.0069E+00 0.6375 0.0000E+00 1.0001E+08
H4	t1/2	PASS	2.66E-03	181475 FQUS24 MidPlane	1.50E+04 1.59E+02 0.6375 0.016 5.69E+06	1.16E+08 -1.21E+01 0.3825 CurrSupE 9.63E-01	ABS-C-A 4.0123E+00 0.6375 1.1319E-02 9.4389E+07
H4	t3/2	PASS	1.54E-03	181474 FQUS24 MidPlane	2.60E+04 1.59E+02 0.6375 0.016 5.16E+06	1.16E+08 -1.21E+01 0.3825 CurrSupE 9.65E-01	ABS-C-A 4.0232E+00 0.6375 2.5301E-02 8.5212E+07

HotName	FatPnt atNode	Stat	UsageFac	Element EleType atSide	AccFatLif X-coord. AxialScf ElThick WeiScale	StrCycle Y-coord. BendScf RefSyst WeiShape	SNCurve Z-coordinate ShearScf DistanceToHot StressRange
H5	HotS 162724	PASS	1.14E-03	179120 FQUS24 MidPlane	3.52E+04 1.59E+02 0.6375 0.016 4.77E+06	1.17E+08 -1.21E+01 0.3825 CurrSupE 9.55E-01	ABS-C-A 4.0069E+00 0.6375 0.0000E+00 8.3179E+07
H5	t1/2	PASS	9.19E-04	179120 FQUS24 MidPlane	4.00E+04 1.59E+02 0.6375 0.016 4.60E+06	1.18E+08 -1.21E+01 0.3825 CurrSupE 9.57E-01	ABS-C-A 4.0123E+00 0.6375 1.1309E-02 7.9884E+07
H5	t3/2	PASS	6.42E-04	179121 FQUS24 MidPlane	4.00E+04 1.59E+02 0.6375 0.016 4.33E+06	1.18E+08 -1.21E+01 0.3825 CurrSupE 9.59E-01	ABS-C-A 4.0232E+00 0.6375 2.5296E-02 7.4540E+07

Number of hotspots printed : 5

Number of hotspots failed : 0

Number of interpolation points failed: 0

Hotspot with S-N curve ABS-E -----Full Load Case

```

Hotspot name           : H1
Description of hotspot :
Coordinate reference system : Current superelement
Hotspot name           : H2
Description of hotspot :
Coordinate reference system : Current superelement
Hotspot name           : H3
Description of hotspot :
Coordinate reference system : Current superelement
Hotspot name           : H4
Description of hotspot :
Coordinate reference system : Current superelement
Hotspot name           : H5
Description of hotspot :
Coordinate reference system : Current superelement

Status on failure      : *FAIL* when UsageFactor > 1.0
Design fatigue life    : 40.0 years
Fatigue calculation based on : Spectraof maximum principal stresses
Wave spectrum          : Pierson Moskowitz
    
```

HotName	FatPnt	Stat	UsageFac	Element	AccFatLif	StrCycle	SNCurve
atNode				EleType	X-coord.	Y-coord.	Z-coordinate
				atSide	AxialScf	BendScf	ShearScf
					ElThick	RefSyst	DistanceToHot
					WeiScale	WeiShape	StressRange
H1	HotS	PASS	5.32E-02	183552	7.52E+02	1.16E+08	ABS-E-A
	162724			FQUS24	1.59E+02	-1.21E+01	4.0069E+00
				MidPlane	0.6375	0.3825	0.6375
					0.016	CurrSupE	0.0000E+00
					5.84E+06	9.63E-01	9.7290E+07
H1	t1/2	PASS	4.19E-02	183552	9.54E+02	1.16E+08	ABS-E-A
				FQUS24	1.59E+02	-1.20E+01	4.0043E+00
				MidPlane	0.6375	0.3825	0.6375
					0.016	CurrSupE	1.0247E-02
					5.55E+06	9.63E-01	9.2193E+07
H1	t3/2	PASS	2.38E-02	183553	1.68E+03	1.16E+08	ABS-E-A
				FQUS24	1.59E+02	-1.20E+01	3.9992E+00
				MidPlane	0.6375	0.3825	0.6375
					0.016	CurrSupE	2.5304E-02
					4.96E+06	9.67E-01	8.1250E+07

HotName	FatPnt	Stat	UsageFac	Element	AccFatLif	StrCycle	SNCurve
atNode				EleType	X-coord.	Y-coord.	Z-coordinate
				atSide	AxialScf	BendScf	ShearScf
					ElThick	RefSyst	DistanceToHot
					WeiScale	WeiShape	StressRange
H2	HotS	PASS	3.11E-02	177549	1.29E+03	1.17E+08	ABS-E-A
	162724			FQUS24	1.59E+02	-1.21E+01	4.0069E+00
				MidPlane	0.6375	0.3825	0.6375
					0.016	CurrSupE	0.0000E+00
					5.10E+06	9.53E-01	8.9461E+07
H2	t1/2	PASS	2.04E-02	177549	1.96E+03	1.17E+08	ABS-E-A
				FQUS24	1.59E+02	-1.20E+01	4.0043E+00
				MidPlane	0.6375	0.3825	0.6375
					0.016	CurrSupE	1.0236E-02
					4.67E+06	9.54E-01	8.1765E+07
H2	t3/2	PASS	4.58E-03	177870	8.73E+03	1.17E+08	ABS-E-A
				FTRS25	1.59E+02	-1.20E+01	3.9992E+00
				MidPlane	0.6375	0.3825	0.6375
					0.016	CurrSupE	2.4333E-02
					3.48E+06	9.59E-01	5.9774E+07

HotName	FatPnt atNode	Stat	UsageFac	Element EleType atSide	AccFatLif X-coord. AxialScf ElThick WeiScale	StrCycle Y-coord. BendScf RefSyst WeiShape	SNCurve Z-coordinate ShearScf DistanceToHot StressRange
H3	HotS 162724	PASS	1.41E-02	180640 FQUS24 MidPlane	2.84E+03 1.59E+02 0.6375 0.016 4.41E+06	1.17E+08 -1.21E+01 0.3825 CurrSupE 9.64E-01	ABS-E-A 4.0069E+00 0.6375 0.0000E+00 7.4489E+07
H3	t1/2	PASS	8.34E-03	180640 FQUS24 MidPlane	4.79E+03 1.59E+02 0.6375 0.016 3.99E+06	1.17E+08 -1.21E+01 0.3825 CurrSupE 9.66E-01	ABS-E-A 4.0010E+00 0.6375 7.9998E-03 6.6542E+07
H3	t3/2	PASS	2.46E-03	180715 FQUS24 MidPlane	1.63E+04 1.59E+02 0.6375 0.016 3.14E+06	1.17E+08 -1.21E+01 0.3825 CurrSupE 9.71E-01	ABS-E-A 3.9893E+00 0.6375 2.4000E-02 5.1120E+07

HotName	FatPnt atNode	Stat	UsageFac	Element EleType atSide	AccFatLif X-coord. AxialScf ElThick WeiScale	StrCycle Y-coord. BendScf RefSyst WeiShape	SNCurve Z-coordinate ShearScf DistanceToHot StressRange
H4	HotS 162724	PASS	6.09E-02	181475 FQUS24 MidPlane	6.57E+02 1.59E+02 0.6375 0.016 6.01E+06	1.16E+08 -1.21E+01 0.3825 CurrSupE 9.63E-01	ABS-E-A 4.0069E+00 0.6375 0.0000E+00 1.0001E+08
H4	t1/2	PASS	4.68E-02	181475 FQUS24 MidPlane	8.54E+02 1.59E+02 0.6375 0.016 5.69E+06	1.16E+08 -1.21E+01 0.3825 CurrSupE 9.63E-01	ABS-E-A 4.0123E+00 0.6375 1.1319E-02 9.4389E+07
H4	t3/2	PASS	2.93E-02	181474 FQUS24 MidPlane	1.37E+03 1.59E+02 0.6375 0.016 5.16E+06	1.16E+08 -1.21E+01 0.3825 CurrSupE 9.65E-01	ABS-E-A 4.0232E+00 0.6375 2.5301E-02 8.5212E+07

HotName	FatPnt atNode	Stat	UsageFac	Element EleType atSide	AccFatLif X-coord. AxialScf ElThick WeiScale	StrCycle Y-coord. BendScf RefSyst WeiShape	SNCurve Z-coordinate ShearScf DistanceToHot StressRange
H5	HotS 162724	PASS	2.24E-02	179120 FQUS24 MidPlane	1.79E+03 1.59E+02 0.6375 0.016 4.77E+06	1.17E+08 -1.21E+01 0.3825 CurrSupE 9.55E-01	ABS-E-A 4.0069E+00 0.6375 0.0000E+00 8.3179E+07
H5	t1/2	PASS	1.86E-02	179120 FQUS24 MidPlane	2.15E+03 1.59E+02 0.6375 0.016 4.60E+06	1.18E+08 -1.21E+01 0.3825 CurrSupE 9.57E-01	ABS-E-A 4.0123E+00 0.6375 1.1309E-02 7.9884E+07
H5	t3/2	PASS	1.36E-02	179121 FQUS24 MidPlane	2.95E+03 1.59E+02 0.6375 0.016 4.33E+06	1.18E+08 -1.21E+01 0.3825 CurrSupE 9.59E-01	ABS-E-A 4.0232E+00 0.6375 2.5296E-02 7.4540E+07

Number of hotspots printed : 5

Number of hotspots failed : 0

Number of interpolation points failed: 0
